THESIS

AN INVESTIGATION INTO BEAVER-INDUCED HOLOCENE SEDIMENTATION USING GROUND PENETRATING RADAR AND SEISMIC REFRACTION: BEAVER MEADOWS, ROCKY MOUNTAIN NATIONAL PARK, COLORADO

Submitted by

Natalie Kramer

Department of Geosciences

In partial fulfillment of the requirements

For the degree of Master of Science

Colorado State University

Fort Collins, Colorado

Summer 2011

Master's Committee:

Advisor: Ellen Wohl
Co-Advisor: Dennis Harry

Paul Meiman

ABSTRACT

AN INVESTIGATION INTO BEAVER-INDUCED HOLOCENE SEDIMENTATION USING GROUND PENETRATING RADAR AND SEISMIC REFRACTION: BEAVER MEADOWS, ROCKY MOUNTAIN NATIONAL PARK, COLORADO

This study used ~1 km of near-surface seismic refraction (SSR) data and ~6 km of ground penetrating radar (GPR) data to infer the impact of Holocene beaver activity on sediment aggradation in Beaver Meadows, Rocky Mountain National Park. GPR data were used to uniquely identify radar packages of genetically related strata corresponding to glacial, non-glacial, and beaver-induced sedimentation. The radar package relating to glacial deposition was wedge-shaped and predominantly composed of a diffraction-rich, chaotic facie. The radar package relating to alluvium was draped over the glacial deposits and was characterized by multiple facies, but in general contained complex, slightly continuous reflectors interfingered with continuous, horizontal to subhorizontal reflectors. The radar package related to beaver-induced sedimentation was characterized by a laterally continuous parallel facie, interpreted to be ponded sediment, that abruptly truncated into a zone of chaotic reflectors, interpreted to be a beaver dam. In order to determine the relative magnitude of post-glacial deposition, the bedrock contact was determined using seismic refraction, GPR, auger data, and previous seismic and drilling studies. This study concludes that beaver damming is an important aggradational process trapping sediments within the Holocene, but did not cause significant amounts of aggradation. Beaver-induced sediments constituted ~50 percent of the alluvium, but the alluvium only constituted ~15% of the total valley fill, with a mean depth of ~1.3 m. The thin veneer of Holocene sediment implies that Beaver Meadows is not a site of continuous sediment deposition, but rather one characterized by episodic temporal and spatial aggradation, punctuated by incision, re-working and exhumation.

ACKNOWLEDGEMENTS

I would like to send a big thank you to my advisors, Ellen Wohl and Dennis Harry, and to my co-researcher, Lina Polvi, for their patience, availability, feedback, encouragement and general support throughout this entire project. I would also like to thank Paul Meiman for representation on my graduate committee and for opening up my mind toward the importance of riparian corridors and wetland areas for ecosystem function. Funding was primarily through the Warner Graduate Research Grant, the American Chemical Society Petroleum Research Fund Grant PRF #45939, and a teaching assistantship, provided by the Department of Geosciences, Colorado State University. Additional funding was provided by the Colorado Scientific Society, Hill Memorial Scholarship, and NSF's Research Experience for Undergraduates program. I would especially like to thank the Rocky Mountain Park Research staff, in particular Judy Visty and Cheri Yost for their logistical support and tolerance of nagging scientists as well as Judy Barnes for supplying me with crucial historical documents. I could not have accomplished this research without the tireless effort of my field assistants: Benton Line and Ben Mayer, and to all those who helped me out in the field: Phil Eskamani, Brent Barker, Zan Rubin, Tyler Houghton, Bryan Crisswell, and Kyle Basler-Reeder. A final thank you goes to Leif Anderson for helping me keep my sanity by making me take breaks to go kayaking. And of course, this thesis would not have been possible without the work of the industrious beaver.

TABLE OF CONTENTS

LIST OF TABLES

LIST OF FIGURES

1 INTRODUCTION

1.1 Context and Research Hypotheses

Historic range of variability (HRV) describes the background variability in natural systems in the absence of intensive human impacts (Veblen and Donnegan, 2005; Dillon et al., 2005; Millar and Woolfenden, 1999). In this thesis, I focus on the HRV of a geomorphic system. Landscape managers working on restoration efforts are often interested in knowing the HRV of a site so they can restore and manage areas to a 'natural' state prior to human impact. HRV provides essential information on the natural dynamic range of a geomorphic system and how it responds to changes in climate, vegetation and population fluxes of key species. The study of past responses of a system gives insight into what changes can occur with or without the managed reduction of human impact. Thus, managers can use information gained from HRV to recognize a range of possibilities for conservation.

Intensive and extensive human land use in the Rocky Mountain region began in the early 1800s and included mining, timber harvest, tie drives, beaver trapping, water diversions, roads, grazing and recreation (Wohl, 2001). Thus it is often difficult to characterize 'natural' conditions devoid of human impact since 'natural' analog sites in the region are almost non-existent. However, the HRV can be inferred from a thorough analysis of depositional features (grain-size distribution, stratigraphy, depositional environment) within sedimentary basins where alluvial records of past landscape dynamics are likely to be preserved. Within the vicinity of Rocky Mountain National Park (RMNP), low gradient wet meadows have minimal terrace development and relatively undissected alluvial fill, which suggests that incision due to base level lowering has not occurred. Consequently, the alluvial record may be fairly complete and investigations of the sediment therein will lead to insight into sediment dynamics throughout the Holocene.

A specific concern within RMNP is the current drying of wet meadows and how it may be related to the eradication of beavers within the park. Prior to re-introducing beaver as a management strategy to retain wetland ecosystems, it would be useful to know the magnitude of influence of beaver activity on sedimentation and on the preservation of wet meadows throughout the Holocene. If beavers were key agents in creating and maintaining the wet meadow ecosystem in the past (Ruede-

mann and Schoonmaker, 1938; Ives, 1942; McKinstry et al., 2001; Westbrook, 2005; Westbrook et al., 2010), then without their presence wet meadow ecosystems within the mountains will likely deteriorate. The loss of wet meadows is a concern for ecologists because wet meadows have been shown to support higher biodiversity than adjacent drier ecosystems (Nilsson, 2002).

Qualitative studies from the first half of the 20th century suggest that beavers are important agents for the creation and maintenance of fertile meadows (beaver-meadow complexes). Writing of wet meadows in New York, Ruedemann and Schoonmaker (1938) stated:

> "Having been active for many thousands of years, [beavers] have accomplished an enormous amount of aggrading work and are important physiographic agents."

Closer to RMNP, Ives (1942) stated:

> "It is apparent that the work of the beaver, in the glaciated parts of the Rocky Mountain region at least, is a very important factor in the production and maintenance of the extensive wet meadows [the beaver meadow complex], commonly attributed to the filling of glacial lakes."

Although Modern sedimentation rates and the maintenance of extensive wet meadows by beaver has been studied extensively (Butler and Malanson, 1995; Cooper et al., 2006; Westbrook, 2005; Gurnell, 1998; Olson and Hubert, 1994; Rosell et al., 2005), a quantitative assessment of beaver-induced aggradation through the Holocene has not been conducted until recently. Work by Persico and Meyer (2009) in Yellowstone suggests that the cumulative effect of beaver sedimentation behind dams during the Holocene may not be as great as qualitative assessments suggest. In contrast, recent observations and measurements of modern beaver pond sedimentation on floodplains as well as terraces in RMNP imply that the beaver activity has broader impacts beyond the dam (Westbrook et al., 2010).

This thesis uses two non-invasive geophysical techniques, ground penetrating radar (GPR) and near-surface seismic refraction (SSR), to investigate and provide quantitative data regarding the relative magnitude of beaver-induced sedimentation in the Holocene; the main hypotheses (H1 and H2) being:

- $H1_o$: Alluvium does not constitute a substantial portion of valley fill (<25%).
- $H1_a$: Alluvium constitutes a substantial portion of valley fill (>25%).

and

- $H2_o$: Beaver-induced sedimentation does not constitute a substantial portion of alluvium (<25%).
- $H2_a$: Beaver-induced sedimentation constitutes a substantial portion of alluvium (>25%).

The terms valley fill and alluvium in these hypotheses have specific meanings within this thesis.

Valley fill refers to all sediments, glacial and non-glacial, deposited above bedrock.

Alluvium refers to all non-glacial sediments stratigraphically above glacial deposits.

I use 25% as an arbitrary threshold for substantial aggradation. H1 tests whether aggradation of alluvium in the Holocene was minimal compared to pre-Holocene deposition. H2 tests whether beavers were important contributors to alluviation. If both null hypotheses are rejected, then it is likely that beavers were important agents in aggrading and expanding the meadow during the Holocene. If $H1_o$ is not rejected but $H2_o$ is rejected, the story becomes more complicated. This scenario implies that the contribution of sedimentation from beaver damming is an important process for aggradation. However, since the proportion of aggradation is not great compared to total valley fill, beaver-induced aggradation is not responsible for substantial amounts of aggradation in the Holocene. These hypotheses do not address whether beavers played a substantial role in maintaining wet meadows. Even if beavers are not important agents aiding sediment retention and aggradation, they are still integral to maintaining a wet meadow and its associated biodiversity (Westbrook et al., 2010, 2006; Nilsson, 2002).

GPR and SSR are appropriate near-surface geophysical techniques to obtain data to test these hypotheses. GPR profiles provide information regarding primary depositional structure and SSR is very useful in identifying boundaries between layers of markedly different lithologies (Reynolds, 1997; Neal, 2004). This study uses GPR to identify depth to bedrock, till, alluvium and buried beaver pond deposits and SSR to identify depth to bedrock when bedrock was too deep to image with the GPR.

In addition to examining the relative importance of ponded sediments in total valley fill in Beaver Meadows, an important outcome of this study is the creation of GPR type facies for glacial till, alluvium and beaver pond sediments in the Colorado Front Range. The dense GPR array and extensive field verification of facies interpretations in Beaver Meadows will allow researchers to more

quickly interpret and analyze GPR data in similar wet meadows using less dense arrays of GPR data and fewer field verifications. It is important to note that although GPR has been used effectively to image subsurface stratigraphy of fluvial, fluvioglacial and glacial deposits (Neal, 2004; Schrott and Sass, 2008; Bersezio et al., 2007; Kostic and Aigner, 2007), this may be the first study to use GPR to recognize buried beaver dams and associated ponded sediment.

1.2 Background Information

This section describes the location, geomorphology, hydrology, geology, vegetation, climate, sedimentation and historic land use of Beaver Meadows; it is concluded by an annotated bibliography of previous studies conducted within the meadows. Although this thesis is focused on beavers, I do not discuss beavers again until the sedimentation and historic land use sub-sections.

1.2.1 Study area

This study was conducted in Upper Beaver Meadows, a montane valley at ~2530 m above sea level, which is located on the Front Range within Rocky Mountain National Park (RMNP), Colorado (Figure 1.1). The study site is officially named Upper Beaver Meadows but will henceforth be referred to as Beaver Meadows. Within this study, Beaver Meadows is broken up into three separate study areas, West Beaver Meadows (WBM), East Beaver Meadows (EBM), and North Beaver Meadows (NBM) (Figure 1.1).

Figure 1.2 delineates the watershed boundaries for each of these four study areas as well as for the upper catchments of NBM and WBM. Table 1.1 summarizes the contributing watershed area, elevation and gradient along the stream channel for each watershed delineated in Figure 1.2. Figure 1.3 graphs the longitudinal profiles from the western drainage divide and the northern drainage divide to the eastern boundary of the study area where the road crosses Beaver Brook. Beaver Meadows was broken up into three distinct study areas since each area has distinctly different geology and gradient. NBM has the steepest gradient (0.056 m/m) and was never glaciated. Although WBM and EBM have similar gradients (0.024 m/m and 0.025 m/m, respectively), WBM is bordered by bedrock to the north and Pleistocene till to the south, while EBM is surrounded by Pleistocene till. A bedrock map and explanation of glaciation are presented in section 1.2.2.

Climate patterns in RMNP are controlled by elevation and the north-south trending continental divide. Weather typically comes from the west and most of the moisture is released on the western slope. Grand Lake (western slope, elevation ~2550 m) receives about 51 cm (20 in) of precipitation per year while Estes Park (eastern slope, elevation ~2290 m) receives about 33 cm (13 in) of precipitation per year (www.nps.gov, accessed Oct 2008). Beaver Meadows is about 7 km to the west of Estes Park and thus precipitation is probably similar. Mean annual precipitation in Beaver Meadows includes rain from frequent summer convective storms as well as snow during the winter. The upper watershed develops a persistent snow pack, but the meadow only has transient coverage immediately following winter and spring snow storms. Graf (1997) measured ~14 cm and ~25 cm of rain for Beaver Meadows from May through September for 1994 and 1995, respectively. Assuming Graf's values represent total rainfall during a year and that ~33 cm is a good average yearly estimate for total precipitation, Beaver Meadows probably receives somewhere between 8-19 cm of snow per year.

The hydrology of Beaver Meadows is primarily driven by melting snow pack from higher elevations. Runoff peaks in the late spring and early summer. Flash floods from convective summer rainstorms do not occur at elevations above 2300 m (Jarrett, 1990) and thus do not affect Beaver Meadows. Prehistoric stream flows reconstructed using tree-ring chronologies for Boulder Creek suggest notable multi-year low flow periods during the 1840s and 1880s (Woodhouse and Lukas, 2006).

Beaver Brook is ungaged, but discharge on Beaver Brook was measured by Graf (1997) in 1994 and 1995 between May and November. Graf found: 1) Baseflow of 0.003-0.0035 m^3/s was reached in early August in 1994 and in early September in 1995. 2) Peak flows in 1994 were between 0.05-0.06 m^3/s, while peak flows in 1995 were 4-6 times this value. 3) Peak flows increased downstream due to significant groundwater inflow and inflow from the northern tributary (NBM). 4) Convective summer rainstorms do not appear to increase runoff for more than a few days. The values reported are from a gage upstream of a diversion that was in operation during almost the entire 20^{th} century. Beaver Brook has a bedload of cobbles, gravels, and felsic-rich sands, and the water remains clear throughout the run-off season, suggesting minimal suspended load.

Vegetation within RMNP varies by elevation and is classified into three zones: montane (~1830-2740 m), subalpine (~2740-3400 m), and alpine (>3400 m). Beaver Meadows is within the montane zone, which is characterized on the east side of the divide by shrubs mixed with ponderosa pines (*Pi-*

nus ponderosa C.Lawson) on the south-facing slopes and a mixture of ponderosa pine and Douglas-fir (*Pseudotsuga menziesii* Franco) on the north-facing slopes (Salas et al., 2005). Figure 1.4 shows the distribution of vegetation communities in Beaver Meadows simplified from the classification by the USGS-NPS (2010) Vegetation Mapping Program. The valley bottom is mainly dominated by herbaceous wetland and herbaceous upland species with a smattering of willows (*Salix* spp.) and cottonwoods (*Populus* spp.) along the riparian corridor, although both the willows and cottonwoods are almost non-existent outside of elk exclosures. In wetter portions of the meadow the vegetation is predominantly sedges (*Carex* spp.), mountain rush (*Juncus balticus* Willd.) and bluejoint (*Calamagrostis canadensis* P.Beauv). Due to the current drying of the Meadow, there is an invasion of xeric, upland herbaceous and shrub species such as sage (*Artemisia frigida* Willd.), cinquefoil (*Potentilla fruticosa* Rydb.), wild rose (*Rosa woodsii* Lindl.), and invasive Canada thistle (*Cirsium arvense* Scop.).

Table 1.1: Landscape characteristics of each study area. Watershed boundaries and stream channels are delineated on Figure 1.2 and the longitudinal profiles of both Beaver Brook and the northern tributary are drawn on Figure 1.3.

Study Area[1]	Watershed Area[2] (km^2)	Max/Min Elevation[3] (m)	Relief (m)	Stream Gradient[4] (m/m)
EBM	14	2525/2494	31	0.024
NBM	3.3	2615/2536	79	0.056
WBM	13	2570/2525	45	0.025
UC_NBM	0.67	2762/2615	147	0.119
UC_WBM	46.1	3134/2570	564	0.144

1. EBM is East Beaver Meadows, NBM is North Beaver Meadows, WBM is West Beaver Meadows. UC_WBM is the upper catchment of WBM and UC_NBP is the upper catchment for NBM.
2. Watershed area was calculated using the streamstats GIS server (USGS, 2010)
3. Max/Min elevations for the study areas refer to the maximum and minimum elevations within each study area along the stream channel. Maximum relief for the entire watershed is 962 m.
4. Stream gradients were calculated for lengths of streams within the study area. The stream gradients for the upper catchments were calculated as if the stream extended to the top of the divide. Since the channel is straight in these catchments, the stream gradient closely approximates valley gradient.

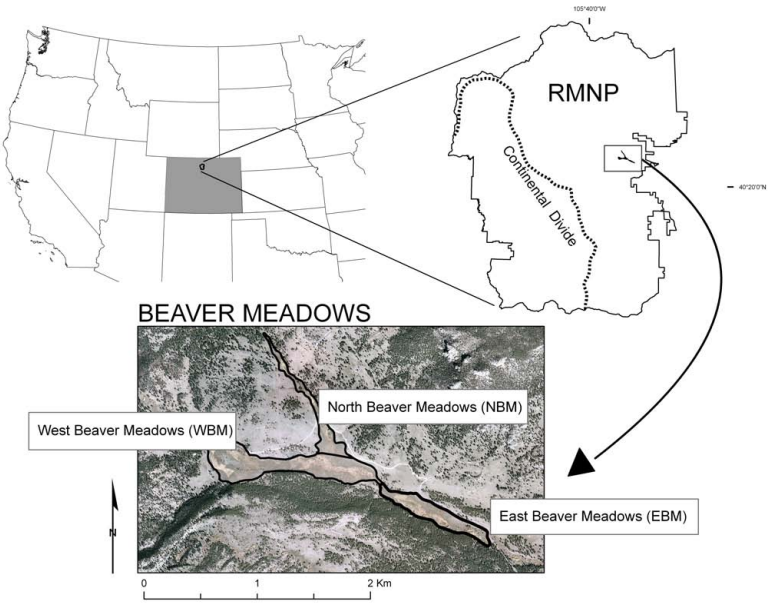

Figure 1.1: Site location map and study areas within Beaver Meadows

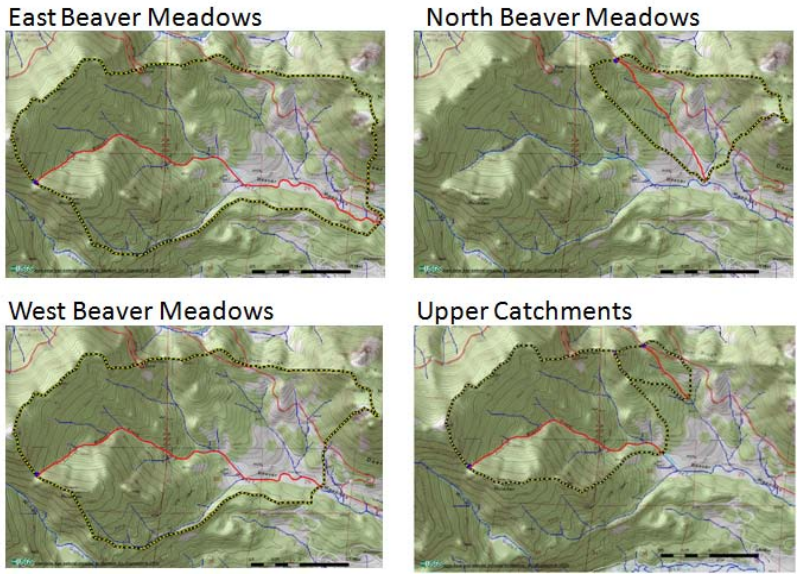

Figure 1.2: Contributing watershed areas. Watershed areas are delineated by the yellow and black dashed line for each study area and for the upper catchments. Contributing areas were delineated from the drainage outlets using Streamstats GIS server (USGS, 2010). The red lines represent the main channel and are extended up to the watershed divides. Long profiles along the marked channels are shown in Figure 1.3.

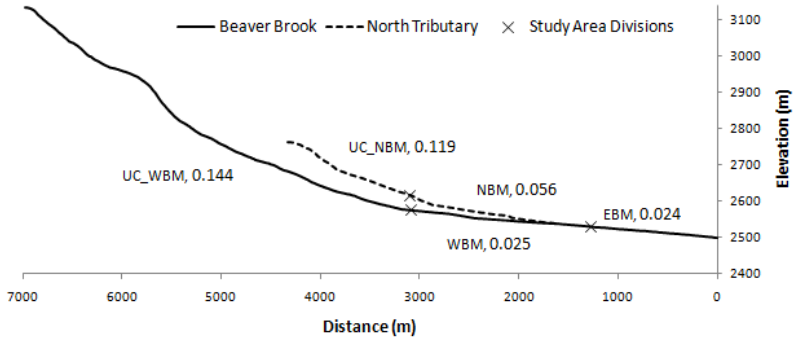

Figure 1.3: Long profile of Beaver Brook and the main northern tributary. Gradients for each study area and the upper catchments are shown. Streams were extended up to the divide. See Figure 1.2 for a planview.

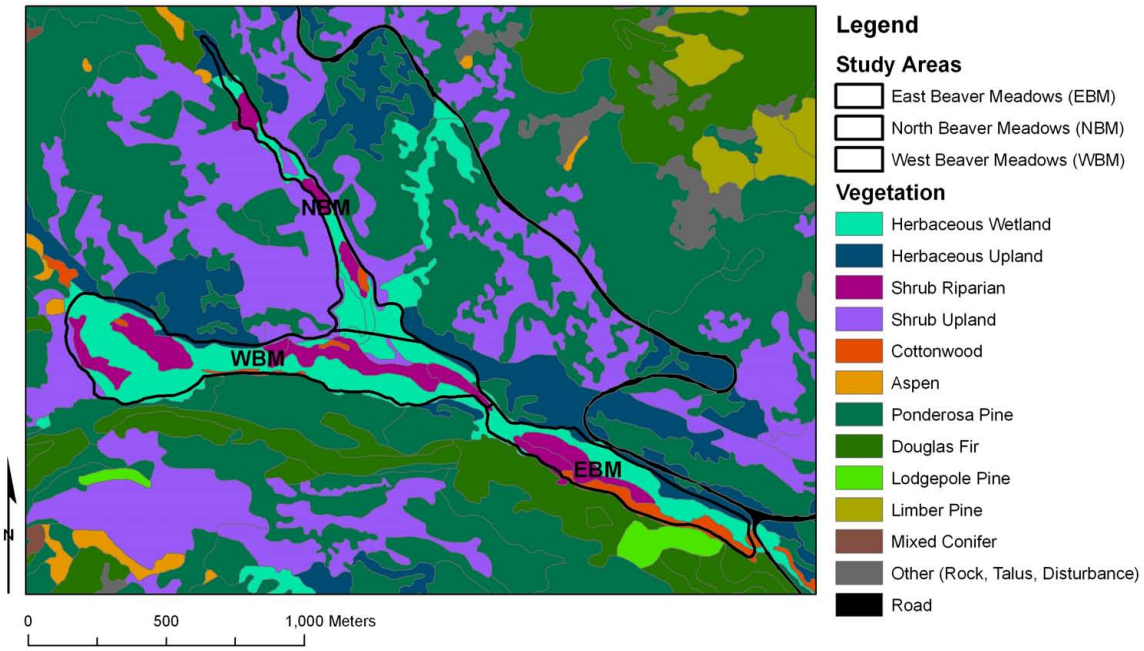

Figure 1.4: Vegetation. Polygons from USGS-NPS (2010). Vegetation classification simplified from original for ease of viewing.

1.2.2 Geologic and glacial history

A map of the geology in the vicinity of Beaver Meadows is shown in Figure 1.5. The basement rock outcrops along the northern edge of the meadow and is a combination of Proterozoic Silver Plume granite and biotite schist and gneiss that was exposed following regional uplift in the late Cretaceous and early Tertiary (Braddock and Cole, 1990). Subsequent erosion degraded the Southern Rocky Mountains, producing low relief topography (Anderson et al., 2006). Cenozoic exhumation of the adjacent sedimentary basin by the South Platte River rejuvenated the relief of the Rocky Mountains and fluvial erosion was responsible for carving the deep canyons and valleys that we see today (Anderson et al., 2006; Madole et al., 1998; Lee, 1917). Mountain glaciers were superimposed upon this pre-existing landscape during the Pleistocene. Glacial erosion significantly increased local relief along the spine of the mountain range (Anderson et al., 2006), creating the glacial landscape of majestic cirques, spires and headwalls so characteristic of RMNP. Exhumation of the range-bounding basin continues today and fluvial erosion has increased the overall relief.

At their furthest extent, most glaciers terminated at elevations between 2700 to 2500 m, 70-40 km west of the mountain front (Madole et al., 1998). The Thompson glacier, as shown in Figure 1.6, flowed through Beaver Meadows and Moraine Park and terminated at roughly 2400 m elevation. (Braddock and Cole, 1990). It is important to note that mountain glaciers flow through pre-existing valleys bounded by bedrock and thus the land surface is not continuously glaciated above the elevation of maximum glacial extent. Although Beaver Meadows was glaciated during the Pleistocene (glacial advances during the Holocene were relatively small and did not reach Beaver Meadows), most of its upper catchment was not.

Three ages of tills near the lower limit of glaciations can be differentiated in RMNP based on relative degrees of weathering and their areal, stratigraphic and topographic expression (Madole et al., 1998). Figure 1.7 places the three tills: Pinedale (10-31 ka), Bull-Lake (130-300 ka) and Pre-Bull Lake (300-1800 ka), within a geologic time-frame and illustrates the stratigraphic and topographic expression between the three glacial deposits (Madole et al., 1998; Madole, 1980; Madole et al., 2010).

Pinedale moraines have steep crested morainal topography while Bull Lake moraines have a more subdued topographic expression (Madole et al., 1998). Pre-Bull Lake deposits are generally sheet-like and do not have any noticeable topographic expression. It is easy to differentiate Pinedale tills from

older tills based solely on soil profiles and weathering. Pinedale tills have weak soil development and thin weathering rinds on clasts. Both Bull Lake and Pre-Bull Lake tills have strong soil development with increased clay content, making them hard to distinguish from each other based only on soil profiles (Madole et al., 1998; Dethier et al., 2003).

My surficial mapping of Pinedale, Bull Lake and Pre-Bull Lake tills surrounding Beaver Meadows (Figure 1.5) does not agree with the widely referenced geologic map of Rocky Mountain National Park and vicinity by Braddock and Cole (1990). On that map, the Bull Lake till does not border the southern boundary of Beaver Meadows and only outcrops along the northern boundary of EBM. I have mapped Bull Lake till inset to the Pinedale till and bordering the southern boundary of both EBM and WBM. The mapping presented here, which is at a finer spatial resolution than the regional map, more accurately portrays the glacial geology. Contacts were drawn based on personal communication with Richard Madole (October, 2010), interpretation of air photos and field observations. The lateral moraine between Beaver Meadows and Moraine Park to the south is capped with Pinedale till but, due to the thickness of the moraine, it is believed that this lateral moraine is actually composed of multiple tills of different ages stacked on top of one another, similar to the schematic shown in Figure 1.7.

Bull Lake till probably dammed the valley at the border between WBM and EBM (Figure 1.5). The dam may have existed for a short time, impounding meltwater behind it. When the dam was overtopped and the Bull Lake terminal moraine breached, erosion through the Bull lake terminal moraine created a spillway for glacial meltwater. It is likely that stream power was not great enough to transport large boulders as it eroded through the moraine and thus large glacial boulders were left as a lag. Deposition of outwash and reworking by Bull Lake meltwater, and possibly again by Pinedale meltwater, may have stratified glacial deposits in the spillway. Subsequent infilling by alluvium buried most of the glacially deposited boulders and outwash, leaving behind a valley bottom characterized by scattered boulder protrusions (Figure 1.8).

The damming of the Beaver Brook valley by the Bull Lake terminal moraine could have impounded glaciofluvial sediment (outwash) and stratified drift from meltwater behind it. Madole et al. (1998) notes that "stratified drift is common in end moraines near the down valley limit of glaciations." Mapped glaciofluvial deposits predominantly consist of pebbles and cobbles (Madole et al., 1998), but as meltwater receded and stream power decreased, layers of sorted sands could have been deposited.

In addition to altering the Pinedale/Bull Lake boundary, I mapped a small pre-Bull lake deposit that was previously unmapped. This deposit was recognized in the field by Richard Madole. It contains small boulders, cobbles and gravel that are incongruent with the surrounding bedrock, and it lies outside the extent of the Bull Lake glacial deposits. The sheet-like nature and lack of topographic expression is consistent with pre-Bull Lake deposits mapped elsewhere (Richmond, 1960).

Beaver Meadows is located near the terminus of glaciations and thus was a deposition zone, not an erosion zone. Near the terminus of glaciers, ice sheets are thrust upward on top of basal layers and little to no work is performed by the ice on the bedrock boundary. For this reason, I do not expect to see a u-shaped profile cut into the bedrock on the north side of the valley, but rather the continuation of the bedrock slope exposed at the surface. In addition, paleo-soils and alluvium from the interglacial period between the Pinedale and Bull Lake glaciations may be preserved.

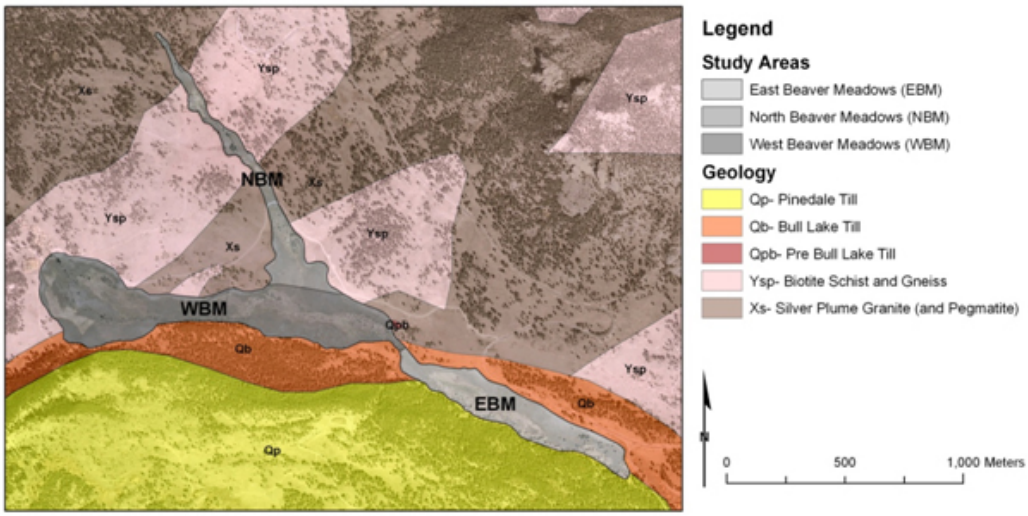

Figure 1.5: Surficial geology. Geologic mapping of basement rock by Braddock and Cole (1990). Geologic mapping of till deposits is based on field observations and personal communication with Richard Madole, October 2010. Note the small Pre-Bull Lake till deposit near the boundary between EBM and WBM.

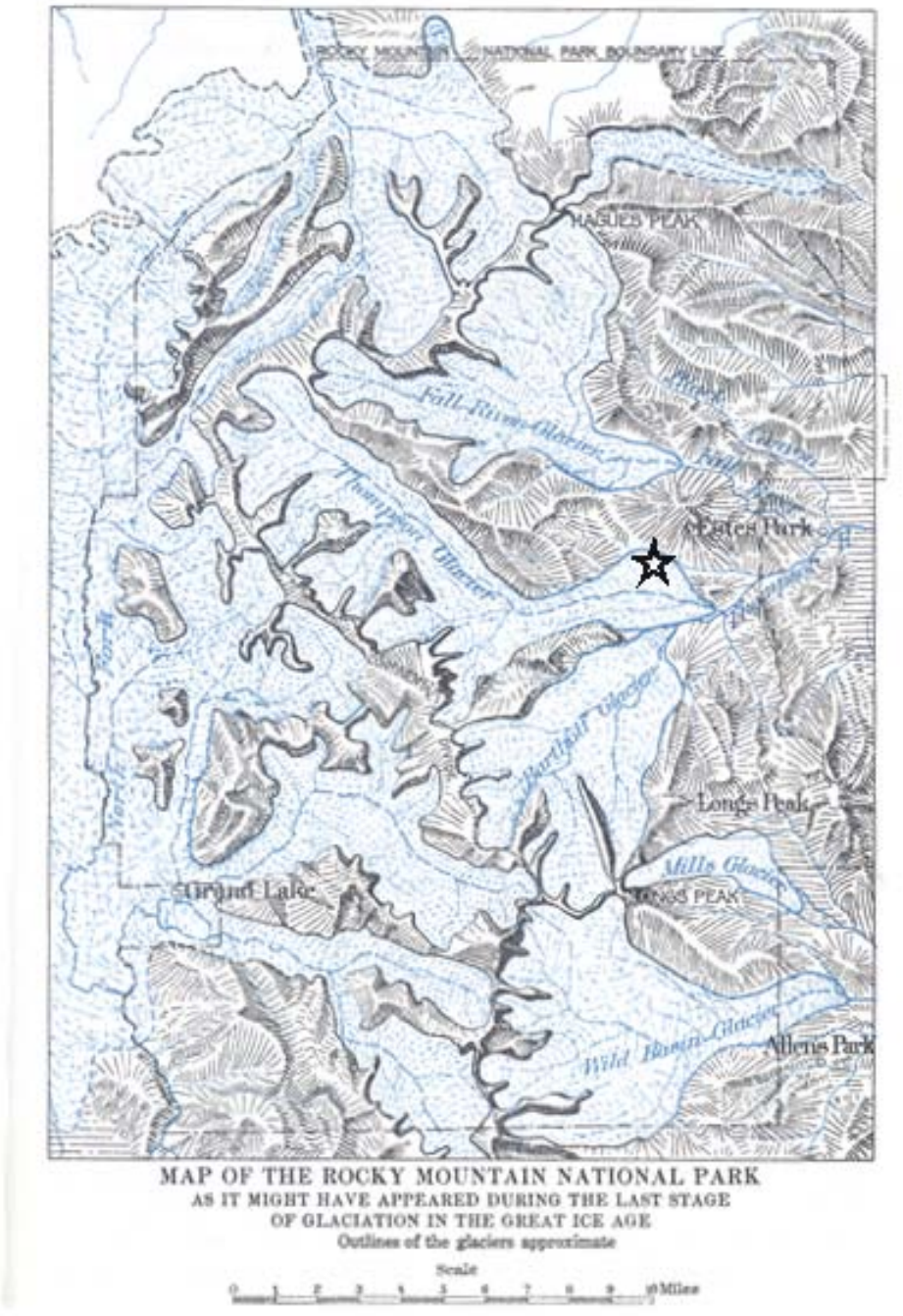

Figure 1.6: Maximum glacial extent. Figure adapted from Lee (1917). Star marks the location of Beaver Meadows near the terminus of the Thompson glacier.

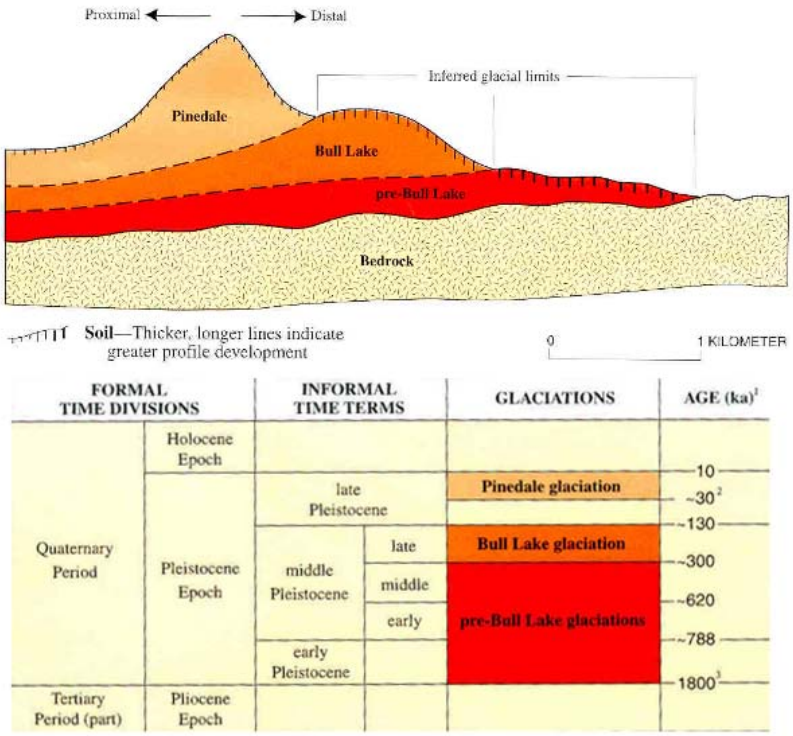

Figure 1.7: Till stratigraphy. Schematic by Madole et al. (1998) showing morphologic and soil differences between tills of different ages in RMNP. Pinedale glaciation began to recede from its terminal moraines 13,000-14,000 BP (Madole, 1980). Recent carbon dates suggest Pinedale glaciation is older than 31,000 BP (Madole et al., 2010).

Figure 1.8: Alluvium draped glacial deposits. Infilling by alluvium in EBM buried most of the glacially deposited boulders and outwash, leaving behind a valley bottom characterized by scattered boulder protrusions. Car for scale.

1.2.3 Holocene climate

Following recession of the Pinedale glaciers from their terminal moraines ~13000-14000 BP (years before present) (Madole, 1980), the climate remained cooler than it is today until the retreat of the smaller Holocene Satanta Peak glaciation prior to ~9200 BP (Richmond, 1986). Analysis of pollen collected from lake cores in Horseshoe Park, a montane glacial trough adjacent to Beaver Meadows, indicates treeline circa 12000 BP was 600 m lower than at present (Rainey, 1987).

There is evidence of a warm dry period in the Front Range from 10000 to 3500 BP (Benedict, 1979; Rainey, 1987; Short, 1985; Benedict et al., 2008; Muhs and Benedict, 2006; Fall, 1997; Elias et al., 1986), which is associated with the widely recognized Holocene altithermal. Treeline within this period is estimated to be at least 145 m higher than present based on dating of recently exhumed spruce trees from persistent snowbanks (Benedict et al., 2008). Within RMNP, paleoenvironments reconstructed from pollen, insect fossils and stratigraphic analysis of organic deposits suggest that the period of maximum warmth was between 6800-3500 BP (Elias et al., 1986).

The climate in the last ~4,000 years in the Front Range was similar to today; relatively cool and dry. Fluctuations in temperature during this period are recorded by alpine cirque glaciations (Richmond, 1986; Benedict, 1979) and prehistoric human land use at high altitudes (Benedict, 1999). Temperatures were similar but more severe during the Little Ice Age from ~700-100 BP (Fall, 1985) and may have been drier and warmer during the Medieval Optimum, a period from ~1050-750 BP (Mann et al., 2009), but this period of widespread drought has not been documented in local climate reconstructions.

1.2.4 Sedimentation

In order for sedimentation rates to locally increase in a basin, the rate of delivery of sediment must increase and/or the efficiency of the trapping and storing of sediment must increase. In the case of Beaver Meadows, sediment supply from native weathered bedrock is minimal. The Rocky Mountain bedrock surface is eroding on the order of 5 m/my ($5x10^{-4}$ cm/y), measured over the course of the Holocene (Anderson et al., 2006), which is 2-3 orders of magnitude smaller than the aggradation rates estimated from sites of sediment accumulation (Table 1.2). In the Lulu City wetland on the west slope of the divide, Rubin (2010) found aggradation rates of 0.04-0.15 cm/y between 4250 BP to 200 BP. He attributed aggradation to episodic debris flows and overbank deposits. In Hoseshoe Park, just

north of Beaver Meadows, Rainey (1987) found sedimentation rates of 0.025 cm/yr between 12,190 to 8200 BP, 0.089 cm/y during a warming trend between 8200-6075 BP, and 0.035 cm/y from 6075 BP to present. Based on cores from Green Lakes, Harbor (1984) found alpine sedimentation rates to be 0.15 cm/y over the last 5,000 years.

Many researchers have noted the abundance of eolian silt and clay sized particles in the Front Range (Rainey, 1987; Graf, 1997; Dethier et al., 2003; McMillan, 1984; Caine, 1986). Muhs and Benedict (2006) tested whether silts in alpine soils were locally derived. Trace element geochemistry of the soils showed that the sand fraction was locally derived, but the silt portion was mostly blown in from the semiarid North Park and Middle Park basins to the west. Thus, the silt and clay sized particles comprising the vast majority of the alluvium in Beaver Meadows are likely eolian in origin. Andrews et al. (1985) concluded that much of the eolian silt in the Colorado Front Range was deposited during the mid-Holocene, with maximum eolian silt accumulation between ~7880 and ~5500 BP. Similarly, Rainey (1987) noted an increase in sediment deposition in Horseshoe Park, ~3 km north of Beaver Meadows, during the Mid Holocene between 8200 and 6075 BP. These increased sedimentation rates correspond with the climatically dry altithermal and with a transition to sparser vegetation in nearby semi-arid basins (Fall, 1997).

Caine (1986) found that both coarse and fine sediments on hillslopes in the alpine zone are decoupled from stream channels. Lack of evidence of debris flow on the hillslopes surrounding Beaver Meadows and lack of suspended sediment in Beaver Brook support this decoupling even at lower elevations. A study of soil erosion on a Pinedale moraine found that the morainal deposits in the subalpine zone were stabilized soon after glaciation and only the surficial fine sediments and soil horizons are mobilized after sporadic erosional events (McMillan, 1984). During times of wetter climate (more rain and more frequent and intense summer convective storms), weathering rates may have been slightly higher (but probably not by much) and mass movements more frequent. However, studies of Holocene climate in the Front Range suggest that for most of the Holocene it was drier (and either cooler or warmer) than it is today (see section 1.2.3). I suggest that at this site it is unlikely there was a large increase in sedimentation due directly to a wetter climate; this merits further investigation but is not within the scope of this project.

Slope instability due to disturbances such as fire and beetle kill generally increases local erosion rates. Fire intensity and occurrence in the montane zone include both high and low intensity fires which burn areas of approximately 100 ha at intervals of 40-100 y (Veblen and Donnegan, 2005).

Sediment input due to fire would be episodic post disturbance. After the Ouzel fire in 1978, which burned 425 ha of the park, 0.22 cm of sediment was trapped by downed trees on the north-facing slope of a moraine (McMillan, 1984). This measurement recorded sediment transport and deposition over an eleven-year period following the fire, which averages to 0.02 cm/y. This measurement was obtained on the north-facing slopes, but post fire erosion is thought to have been less on the north slopes than the south slopes due to greater infiltration capacity. Post fire erosion removed at least 1 cm of soil from the south-facing slopes, but due to a relative lack of downed trees, most of the eroded sediment was not trapped on the hillslope and could not be recorded. Unfortunately, I could not find background soil erosion or creep rates for slopes within the montane zone. However, soil creep measurements made in alpine meadows and solifluction lobes and terraces range from 0.03-2.21 cm/y (Caine, 1986). I suggest that background creep measurements for soils on slopes surrounding Beaver Meadows are <0.05 cm/y, but this would be a worthwhile measurement to obtain through a rigorous field study.

In an environment where the major source of sediment is eolian and the streams are supply limited, Beaver Meadows must have been efficient at trapping and storing sediment in order to accumulate an appreciable amount of Holocene fill. Under current conditions, incision by Beaver Brook, clear water, and no evidence of frequent overbank flooding indicate that sediment is currently being removed from the basin, most likely at faster rates than surficial eolian deposition or soil creep.

The activities of the industrious beaver may have had a big impact on the trapping and storing of sediment in Beaver Meadows. Beaver dams locally raise base level, which in turn lowers local gradients and creates settling ponds for fine sediments. Beavers do not just facilitate sedimentation within their ponds but also on the active floodplain and even on relict terraces by enhancing the extent and duration of overbank flows (Westbrook et al., 2010). Reported modern and Holocene sedimentation rates in beaver ponds are summarized in Table 1.2.

The hydrologic, geomorphic and ecologic effects of beaver ponding are well documented (Mitchell and Cunjak, 2007; Westbrook, 2005; Cooper et al., 2006; Bigler et al., 2001; McKinstry et al., 2001; Rosell et al., 2005; Gurnell, 1998; Ruedemann and Schoonmaker, 1938; Mills, 1913). The presence of beaver ponds raises groundwater levels and creates complex valley bottom stream geometry advantageous for both aquatic species and riparian vegetation. In the mountain environment of Colorado, beavers often build a string of dams (some active and some not) up and down a valley bottom (Figure 1.9). Ives (1942) defined the term beaver-meadow complex to describe the interrelation between

beavers, sedimentation and plant growth due to a string of dams occupying a valley bottom. Ives claimed that the beaver-meadow complex is a post-glacial phenomenon responsible for the persistent large wet meadows in the mountainous regions of Colorado.

It has been subsequently assumed, without rigorous investigation, that beavers, through the creation of these contemporary meadow complexes, had a large impact on the long term scale and rates of sedimentation. This seems a reasonable conjecture given the abundance of beavers in Colorado historically (Wohl, 2001; Olson and Hubert, 1994; Rutherford, 1964; Naiman et al., 1988) and the effectiveness of contemporary beaver dams in trapping sediments (Table 1.2). Recently, Persico and Meyer (2009) studied sedimentation due to Holocene beaver damming in Yellowstone. They estimated that tens of meters of stacked sediment would be required to create the beaver-meadows complexes described by Ives (1942) and Ruedemann and Schoonmaker (1938) and thus concluded that the patchy distribution of beaver deposits in Yellowstone does not support the extensive aggradation of beaver-related sediment as described by those authors.

In a system like Beaver Meadows, where sediment influx is not great, beavers may have an important role trapping the sediment delivered to the valley. If beavers did have a significant impact on sedimentation in Beaver Meadows, the sedimentation rates would be episodic in space since beaver dams may not have covered the entire valley bottom and different dams were built in different locations over time. Beaver dam sediments could also be episodic in time as beaver populations increased or decreased depending on the climate, predation or overpopulation of grazers. For example, a notable absence of beaver occurred in Yellowstone during 700-1000 BP, which Persico and Meyer (2009) attribute to the Medieval Climatic Anomaly of widespread drought.

In addition to beaver damming, there is topographic evidence that the catchment was dammed by a Bull Lake terminal moraine ~130-140 ka. This dam was probably breached by glacial meltwater during glacial retreat and there is no evidence of a subsequent glacial dam during the Pinedale glaciation (10-30 ka). Some glaciofluvial sediments of poorly sorted cobbles, gravels, sands and silts may have been trapped and deposited behind the dam.

Table 1.2: Compilation of sedimentary deposition and erosion rates in the Rocky Mountains and vicinity.

Study	Location	Type	Elev (m)	Rate[1] (cm/y)	Time Frame
Anderson et al. (2006)	Colorado Rockies	Bedrock erosion on exposed surfaces	>2740	5×10^{-4}*	Holocene
Caine (1986)	Colorado Rockies, East Slope	Eolian Influx	3550	14 g/y	Modern
Caine (1986)	Colorado Rockies, East Slope	Soil Creep	3550	0.025-2.21	Modern
McMillan (1984)	Colorado Rockies, East Slope	Post Fire Slope Erosion	2930	0.02*	Modern
Caine (1986)	Colorado Rockies, East Slope	Lake Sedimentation	3550	0.15	Holocene
Rainey (1987)	Colorado Rockies, East Slope	Lake Sedimentation		0.025-0.089	Holocene
Rubin (2010)	Colorado Rockies, West Slope	Valley Bottom Sedimentation	2830	0.04-0.15*	Holocene
Rubin (2010)	Colorado Rockies, West Slope	Valley Bottom Sedimentation	2830	0.45*	Modern
Ives (1942)	Colorado Rockies	Beaver Pond	>2000	0.0076-0.025*	Holocene
Ives (1942)	Colorado Rockies	Beaver Pond	>2000	0.635*	Modern
Persico and Meyer (2009)	Yellowstone, Wyoming	Beaver Pond	1700-2700	0.035-0.625*	Holocene
Persico and Meyer (2009)	Yellowstone, Wyoming	Beaver Pond	1700-2700	5*	Modern
Butler and Malanson (1995)	Glacier Ntl Park, Wyoming	Beaver Pond	NR	4-39	Modern

1. Starred values were either converted to cm/y from original reported units or computed from reported thicknesses and time frames

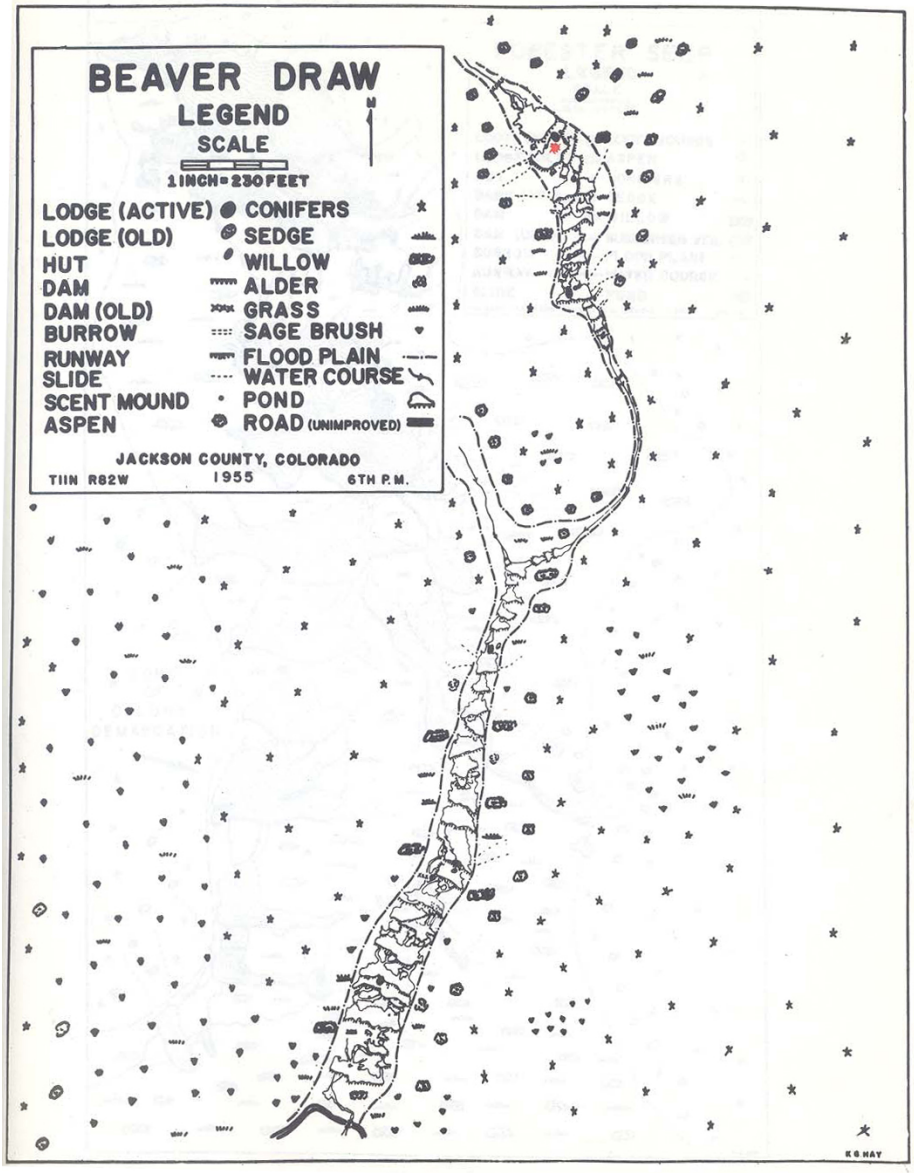

Figure 1.9: The beaver-meadow complex. Drawing by by Hay (1955). Beaver Draw is located Northwest of RMNP on the North Fork of the North Platte River, Colorado. Note how the string of ponds almost completely fill the floodplain. The red dot on the upper part of the reach marks the location of a food cache.

1.2.5 Historic land use and sedimentation

Most national parks are heavily managed and in many cases were greatly affected by human land use prior to and after establishment. RMNP, in particular, had a long history of human land use that altered the landscape and its ecology. Prior to studying the historic variability preserved in the sediments within Beaver Meadows, it is important to recognize the historic land use of the meadow and how it may have affected the sediment record.

Beaver Meadows was inhabited by humans prior to settlement of the area by Europeans in the mid 1800s. There is evidence that the Utes as well as the Shoshone visited the region surrounding Estes Park frequently during the summer and hunted game, but did not make permanent camps (Buchholtz, 1983). An early settler, Abner Sprague, noted a fortified mound at the west end of Beaver Meadows, which led him to believe that the meadows was a battle ground between tribes and the mound was where the weaker party made their last stand. However, Buchholtz (1983) speculates that this mound could actually have been part of a game drive system.

Game drives included using fire to drive game to ambush sites such as Beaver Meadows. A prehistoric human-induced increase in fire frequency may have affected slope stability in the upper catchment, leading to increased sedimentation in Beaver Meadows. In the 1920s the park started suppressing natural fires and only four fires have occurred since that time, the largest being the Ouzel fire mentioned earlier; none of these fires include the Beaver Meadows catchment. Natural fires are usually started by lightning strikes. A change in climate may affect frequency of ignition throughout the Holocene. Natural ignition has declined 75% since 1930, apparently due to lack of flammable materials because of overgrazing and decrease of human-set fires since Indian removal (Hess, 1993).

John Estes was the first European to permanently settle in Estes Park in 1860. Among other early settlers was John Hupp, who settled in Beaver Meadows in 1875 (Mills, 1905). The Hupp family raised cattle and farmed hay in the meadow. In 1902 Pieter Hondius Sr. bought the land (National Park Service, 1939) and, according to a personal communication between Graf (1997) and P. Hondius Jr. in 1995, cattle were grazed on the land until between 1910 and 1920. Although RMNP was established in 1915, Beaver Meadows was not incorporated into RMNP until 1932 and hay production in the meadow continued until that date.

Hay production and grazing in the meadow did not disturb appreciable depths of the subsurface

or affect the interpretations in this study. Cattle grazing had a similar (or most likely lesser) impact on the meadow than the current overgrazing of the meadow by elk. Grazing by elk and cattle probably compacted the uppermost portion of the soil to some degree. At the time, hay seed was often spread in the meadow without tillage and/or native grasses were harvested for hay. If the soil was tilled, a recent study of hand and horse drawn tillage methods currently being employed in Africa shows that this type of tillage only disturbs the upper 14 cm of the subsurface (Tsimba et al., 1999).

Hondius did make one major alteration to the hydraulics of the meadow when he built the Hondius-Beaver waterline between 1906 and 1908. This line diverted water from Beaver Brook to supply water to the Hondius homestead and to subdivided lots in Hondius's holdings east of the meadow. (Figure 1.10). The waterline consisted of a shallowly buried iron pipe (<0.5 m) and some clay drainage tiles. In 1932 Beaver Meadows was incorporated into RMNP, the Hondius homestead was removed and the waterline supplying the home was severed. An estimated 0.01 m^3/s flowed from the severed pipe into the western part of the meadow (Graf, 1997). A water right of 0.33 ft^3/s (0.09 m^3/s) was allocated in 1939 and the diversion remained in operation until the late 1990s, when the Park Service became concerned that the diversion was harmful to the riparian and wetland communities in Beaver Meadows. Graf (1997) studied the effects of the water diversion on the meadows and subsequently the diversion was discontinued and the water flowing from the severed Hondius homestead pipeline was stopped. The original iron pipe is still shallowly buried along with a 2" pvc replacement pipe. The subsurface disturbance due to the laying of the pipeline was minimal since it was shallowly buried (<0.5 m below ground surface) and the disturbance was localized around the pipe.

Along with the Hondius-Beaver diversion, heavy trapping of beaver during the early 1800s may have led to subsequent lowering of the water table in the meadows as well as a decreased ability of the system to trap fine sediments. Accounts of tribes from the South Platte region trading beaver pelts with Europeans date back to 1805 (Rensch, 1935). Heavy trapping by Europeans began in 1815 and by 1831 fur areas were depleted. After 1831 the fur trade mainly dealt in buffalo instead of beaver.

Once RMNP was established in 1915, beaver began to make a comeback. A report in 1947 states that beaver were doing well and populations were likely to increase (Packard, 1947). Some concern was expressed about overgrazing by a herd of 200 elk. Six beaver lodges on Beaver Creek

(Brook) were noted and a total of 890 were estimated for the park. Beaver populations in RMNP appeared to be doing well until 1976, when there was a sudden noticeable decline in beaver, which prompted another beaver survey (Stevens and Christianson, 1980). No beaver were reported for Beaver Meadows in this second survey and only 108 were reported for the whole park (88% decrease from 1932). The decline in beaver was reported to be related to a rising elk population (1,100 by 1979; an 82% increase since 1932), lowering of water tables due to a dry year and also possibly to an outbreak of bubonic plague among rodents. Change in woody vegetation noticed in aerial photographs between the fall of 1947 and the fall of 1987 in Beaver Meadows due to overgrazing is drastic (Graf, 1997). A survey in 1998-1999 found only seven beaver lodges within RMNP (Mitchell et al., 1999). Using the technique employed in the previous two studies of assuming six beavers per lodge, this would represent only 42 beavers, a 95% decrease since 1932. The survey did note that two sites without lodges had signs of recent beaver activity such as cuttings and dens, thus the estimate of 42 is a lower bound for the beaver population at that time. The elk population during the time of this study was estimated to be between 2,800 and 3,500, a 93% increase from 1932. That the elk have a direct effect on the beaver is likely, not only from vegetation change, but because for every percent increase in elk there is approximately the same percent decrease in beaver (Figure 1.11).

Currently, an estimated 600-800 elk winter in RMNP and 1000-1300 winter in Estes valley outside the park (Terese Johnson, RMNP biologist, personal communication, Sept, 2010). Although elk numbers are now down due to culling and birth control efforts, Beaver Meadows cannot support a beaver population due to lack of suitable vegetation and a low water table (Mitchell et al., 1999). Close to two centuries of beaver absence directly and indirectly related to human land use (human hunting removed the wolves that would have limited the elk population) has most likely slowed sedimentation rates in the meadow. If beavers are to be transplanted in Beaver Meadows as a restoration tool, extensive vegetation planting, continued elk management and artificial efforts at bringing the water table up will likely have to be employed.

RMNP has become increasingly popular to tourists over the last century and in 1999 RMNP had close to three million visitors. RMNP is working hard not to just manage the elk, but to manage the people as well. In 1980, Ranger Larry Van Slyke put it this way, “today we are people managers, managing people making an impact on the environment” (Buchholtz, 1983).

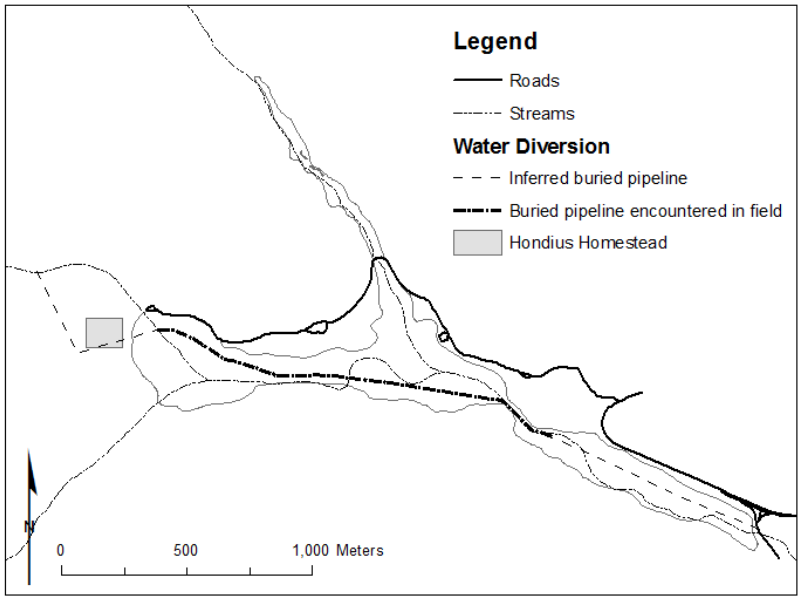

Figure 1.10: Location of the Hondius waterline and homestead.

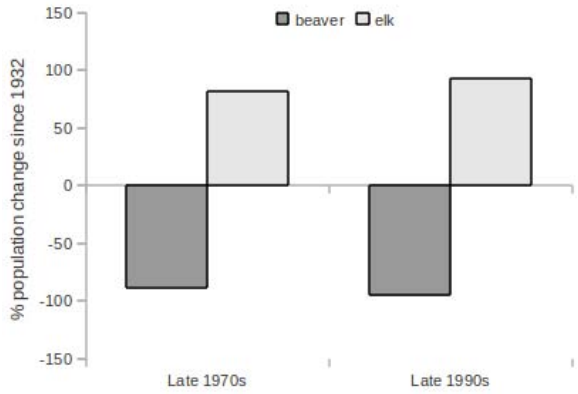

Figure 1.11: Comparing percent changes in elk and beaver in RMNP since 1932. Note that for every fractional increase in elk population, there was a corresponding fractional decrease in beaver.

1.2.6 Previous research in Beaver Meadows: An annotated bibliography

Several previous studies have been conducted in Beaver Meadows. I have mentioned some of these studies already, but as they will be referenced multiple times within this thesis, a short summary of each was deemed pertinent and necessary. In the absence of recorded coordinates, I re-plotted data locations in Beaver Meadows from the original printed maps using landmarks (Figure 1.12)

Graf, D.D., 1997. Effects of water diversion in Upper Beaver Meadows Rocky Mountain National Park. MS thesis, Colorado State University, Fort Collins, CO.

Graf installed 42 shallow wells and 13 piezometers for the study of surface-groundwater interactions in WBM upstream of the confluence with NBM (Figure 1.12). Graf conducted his study because the park service was concerned that the century-old Hondius diversion was drying the meadow. I used the auger core descriptions to augment interpretation of the alluvium. For most auger holes a complete sediment description was not supplied, but the total depth was. From my experience coring in that part of the meadow, augers generally are able to penetrate through alluvium but are stopped when they encounter the underlying till. In general, I used the max depth of each auger from this study as a minimum depth of alluvium.

Locke, W.W., 1987, Low-Energy Seismic Survey of Quaternary Materials, Rocky Mountain National Park, Colorado, The Mountain Geologist, Vol. 24, No.2, p 45-49.

In this study Locke experimented with using seismic refraction techniques to map subsurface Quaternary deposits in RMNP. Particularly pertinent to this study are two seismic lines he ran in Beaver Meadows, WBM and EBM. On Figure 1.12, I re-named these seismic lines so that Locke's EBM=Locke1 and Locke's WBM=Locke2. The re-naming was necessary to avoid confusion since I have abbreviated my study areas the same, WBM and EBM. Locke estimated depth to bedrock to be ~11 m bgs (below ground surface) under Locke1. Locke2 started on bedrock, then the contact deepened to ~5 m bgs under Beaver Brook and to ~20 m bgs near where the line crosses the trail. In addition to the depth estimates for the valley fill/bedrock contact, I used Locke's estimates of seismic velocities to help interpret my own seismic refraction lines.

Packard, F.M., 1947. A survey of the beaver population of Rocky Mountain National Park, Colorado. Journal of Mammalogy 28 (3), 219-227.

Packard conducted beaver population surveys in RMNP in 1939 and 1940. He paced each stream in the survey to identify beaver lodges and assumed six beavers per lodge. The forms and maps associated with the survey were reported to be stored at the offices of RMNP in Estes Park. Unfortunately, upon inquiry, these maps were not found. Nonetheless, Packard identified six lodges along Beaver Creek (Brook). He states that three of the colonies within Beaver Meadows appear to be doing well. It is unclear from his report if all beaver colonies were found within the meadow or some were found along Beaver Brook above the meadow. Packard also mentions that although Beaver Meadows has considerable habitat suitable for beaver, most of the upper meadow lacks aspen and so the beaver colonies would have to subsist on grasses and willows heavily browsed by a band of over 200 elk. A subsequent RMNP beaver census in 1980 did not include Beaver Meadows, so presumably no beavers were there at that time (Stevens and Christianson, 1980).

Welder, F.A, 1971. Ground-water reconnaissance study of selected sites in Rocky Mountain National Park and Shadow Mountain National Recreation Area. USGS Open File Report 71001.

The purpose of this study was to determine the feasibility of obtaining ground-water supplies for various campgrounds, picnic areas, ranger stations and living quarters within RMNP and Shadow Mountain National Recreation Area. One of the sites within this study was Beaver Meadows, where both a test hole and an observation well were drilled (Figure 1.12). The drill logs are summarized in Table 1.3. Both holes terminated at bedrock ~12 m below ground surface. This study was especially useful for verification of the interpretation of the bedrock/valley fill contact as well as the valley fill/alluvium contact within this thesis.

Table 1.3: Two drill logs down to bedrock from Welder (1971).

Observation Well (Test Hole 14)			Observation Well (Test Hole 15)		
Description	I (m) [1]	C[2]	Description	I[1] (m)	C[2]
Clay, sandy, organic, black, (boulders at 3.7 m)	0-3.7	A	Clay, sandy, (boulder at 0.9 m)	0-1.5	A
Clay, sandy, black, contains streaks of gravel	3.7-4.9	A	Sand, fine to coarse, contains clay and fine to coarse gravel (water level estimated at 3.7 m)	1.5-6.4	A?G?
Gravel, fine to medium; contains brown clay (water level at 1.7 m)	4.9-5.5	G	Clay	6.4-6.7	A?IG?
Gravel, fine to medium; contains brown clay and cobbles	5.5-6.1	G	Sand, fine to coarse, fine to coarse gravel; contains brown clay (boulder at 11 m)	6.7-12	G
Clay, brown, and fine to coarse sand	6.1-7.6	G	Granite Bedrock	12	B
Clay, brown; contains fine to coarse sand and fine to coarse gravel	7.6-11	G			
Sand, coarse, and medium gravel; contains clay	11-12	G			
Granite Bedrock	12	B			

1. Interval in meters below ground surface, value converted from reported intervals in inches.

2. Codes for my interpretation of the subsurface. A=Alluvium, G=Glacial, IG= Interglacial or B=Bedrock. Glacial Deposits would include outwash or other meltwater deposits. From augering, we know that post glacial clays are black, not brown.

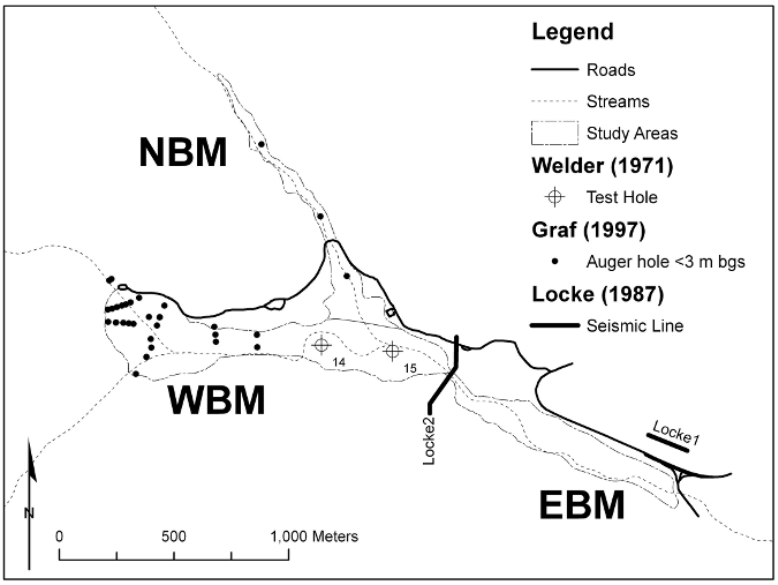

Figure 1.12: Location of data from previous studies in Beaver Meadows.

2 METHODS

2.1 Brief Overview of Geophysical Techniques

GPR profiles provide information regarding primary depositional structure and SSR is very useful in identifying boundaries between layers of markedly different lithologies (Reynolds, 1997; Neal, 2004). This study uses GPR to identify depth to bedrock, till, alluvium and buried beaver pond deposits and SSR to identify depth to bedrock when bedrock was too deep to image with the GPR.

GPR detects electrical discontinuities in the shallow subsurface by transmitting high frequency electromagnetic waves in the megahertz range. GPR profiles are generated by recording the time between transmission and reception of a wave reflected by contrasts in dielectric properties caused by different lithologies or grain size. With appropriate resolution, data processing, and interpretation, GPR profiles accurately provide information regarding primary depositional structure.

Seismic refraction uses two-way travel times of compressional p-waves refracted between layers of differing velocities to estimate the subsurface velocity profile. Seismic refraction is very useful in identifying boundaries between layers of markedly different lithologies at many scales, including: global, crustal and near-surface. Near-surface seismic refraction (SSR) techniques are often employed by researchers interested in the depth to bedrock underneath shallow unconsolidated Quaternary deposits (Leopold, 2008; Peirson, 1991; Lennox, 1967).

For a more thorough description of GPR and seismic refraction theory and techniques, refer to: Neal (2004); Reynolds (1997); Baker et al. (2007); Schrott and Sass (2008); and Jol (2009).

2.2 Data Collection

Geophysical data were collected in the summer of 2009 and supplemental field data were collected during the summers of 2009 and 2010. Since geophysical data are non-unique (multiple interpretations for the same signal), it was necessary to also collect field data to substantiate geophysical interpretation. Supplemental field data included surficial field observations (such as location of berms and boulders), description of cutbank exposures, and descriptions of hand auger holes (maximum

2 m depth). Figures 2.1 and 2.2 show the location of the supplemental data and the geophysical transects. Many of the core descriptions were supplied by Lina Polvi, which are presented in her dissertation (Polvi, in prep). Tables containing descriptions and coordinates of all supplemental data are included in Appendix A.

A dense coverage of over 4 km of common offset GPR data and six common midpoint (CMP) surveys were completed using Sensors and Software Pulse Ekko PE100 100 mHz antennae (Figure 2.2 and Table 2.1). Common offset surveys are performed along a transect and generate profiles of reflectors that represent subsurface lithology. CMP surveys are performed to estimate subsurface radar velocities so that the two-way travel times (TWT) collected by the common offset surveys can be converted to depths. Figure 2.3 depicts the difference in data collection for common offset and common midpoint surveys. Common offset data were acquired at a 0.25 m step size using 1 m spacing between antennae, which were placed parallel to the survey line. CMP data were collected by placing the transmitter and receiver antennas side by side (starting offset=0m) and then progressively moving them apart by a 0.20 m step size with the exception of x3, which was collected with an 0.25 m step size.

Four of the GPR transects, BT2, BT4, BT6 and BT11, were resurveyed using SSR (Figure 2.2, Table 2.1). For each seismic transect, a string of 24 geophones was laid out with 2 m spacing between geophones. P-waves were generated by striking an aluminum metal plate with a hammer (shots) at distances of 2, 4 and 6 m past the ends of the line on each side. This reversal of the survey was necessary in order to pick up dipping bedrock contact. The line was then advanced, overlapping the last 6 geophones, and new shots were taken.

Table 2.1: Summary of GPR and SSR Profiles.

ID	Length (m)	UTM E (m)	Start N (m)	UTM E (m)	End N (m)	Technique(s)
BL1	2000	447835	4469072	449734	4468679	GPR
BL2	600	448612	4469129	449199	4469013	GPR,SSR
BT1	392	447868	4469321	447957	4468941	GPR
BT2	384	448048	4469304	448048	4468923	GPR
BT3	200	448178	4469182	448173	4468985	GPR
BT4	173	448336	4469190	448362	4469021	GPR,SSR
BT5	145	448620	4469169	448620	4469026	GPR
BT6	270	448860	4469228	448833	4468966	GPR,SSR
BT7	268	449069	4469173	449020	4468917	GPR
BT8	140	449209	4469085	449194	4468951	GPR
BT9	44	449340	4468956	449308	4468926	GPR
BT10	123	449494	4468856	449463	4468740	GPR
BT11	190	449665	4468843	449579	4468676	GPR,SSR
BT12	117	449739	4468717	449694	4468610	GPR
AL1	700	448860	4469228	448593	4469851	GPR
AL2	284	448577	4469848	448434	4470069	GPR
AT1	47	448489	4470014	448445	4469991	GPR
AT2	53	448466	4469934	448509	4469969	GPR
AT3	29	448549	4469859	448576	4469879	GPR
AT4	55	448701	4469754	448660	4469714	GPR
AT5	43	448726	4469636	448763	4469650	GPR
AT6	100	448804	4469346	448919	4469329	GPR
m1	—	447899	4469079	———	———	CMP
m2	—	449623	4468762	———	———	CMP
m3	—	448850	4469123	———	———	CMP
x1	—	447835	4469025	———	———	CMP
x2	—	448267	4469054	———	———	CMP
x3	—	448351	4469092	———	———	CMP

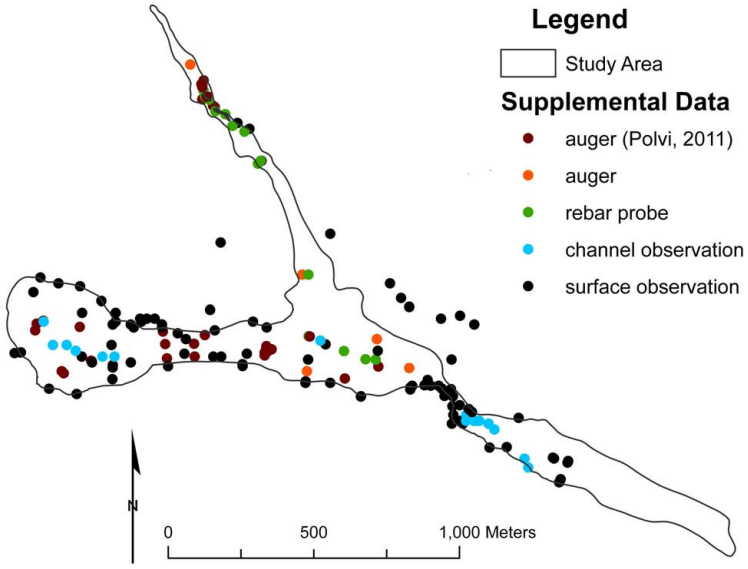

Figure 2.1: Location map of supplemental data. The Easting (E) and and Northing (N) entries are in UTM NAD83 Zone13N and mark the start and finish location of each survey line. CMP surveys are located by just one set of coordinates.

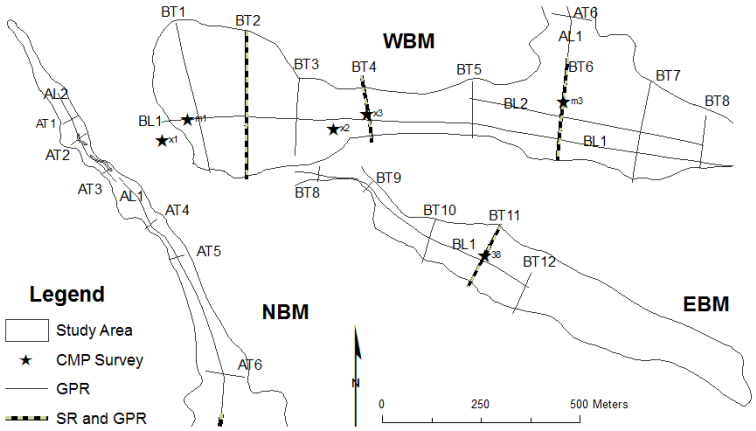

Figure 2.2: Location map of geophysical data

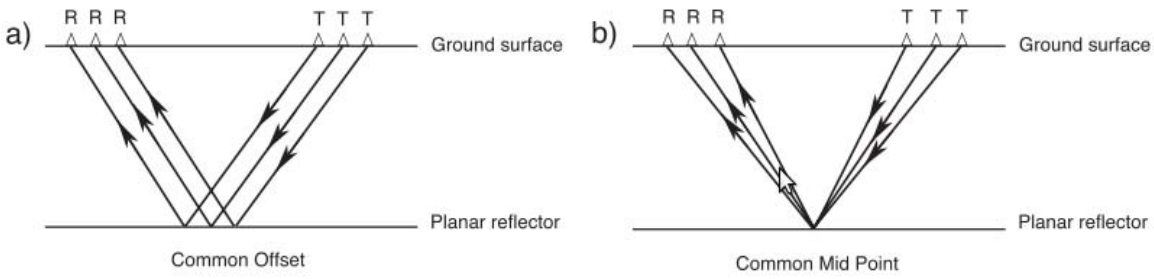

Figure 2.3: Schematic illustrations of common offset and midpoint data collection. Figure from Neal (2004). R=Receiver and T=Transmitter.

2.3 GPR Data Processing

2.3.1 Estimating subsurface radar velocities

The CMP surveys from Beaver Meadows were analyzed using semblance plots generated by Sensors and Software's Ekko View Delux program (Sensors and Software, 2003). In order to determine if there were horizontal velocity differences related to above-ground vegetation, near-surface substrate characteristics, and apparent saturation, the six surveys on Figure 2.2 were grouped into two classes, mesic and xeric. Table 2.2 summarizes the CMP analysis results for each survey within these two classes.

In Beaver Meadows, mesic areas are dominated by hummocky graminoids rooted in saturated, fine sediments including clay, silt and some sand. The semblance plots for mesic surveys (Figure 2.4) show velocities ranging from 0.05-0.06 m/ns. In contrast, xeric areas are dominated by sage with some herbs rooted in damp to dry coarser sediment including cobbles, sand, gravel and silt. The semblance plots for xeric surveys (Figure 2.5) show velocities ranging from 0.10-0.12 m/ns. The mean velocity using all six surveys is approximately 0.08 m/ns with a standard deviation of 0.03 m/ns.

The boxplots in Figure 2.6 demonstrate that there is a notable difference in velocity estimates between wet areas supporting mesic vegetation (mean=0.06 m/ns) and dry areas supporting xeric vegetation (mean=0.11 m/s). Due to the low number of data points (count=6), a more rigorous statistical analysis was not done. The velocity estimates obtained from the CMP surveys are within the known velocity ranges for saturated and unsaturated clay, silt and sand (Table 2.3). I did not

use the average velocity of 0.08 m/ns to universally convert the TWT axis to a depth axis since the data suggest that radar velocities are heterogeneous laterally depending on the level of saturation. Instead, I retained the TWT axis and created a velocity contour map (Figure 2.7) which was used to convert any TWT to a depth at specific locations.

I created the velocity contour map by using knowledge about: the distribution of vegetation types, field saturation conditions and bedrock geology to interpretively contour the subsurface velocities in Beaver Meadows (Groshong, 2006; Tearpock and Bischke, 1991). In addition to the six CMP data points, I supplemented the velocity coverage with velocity estimates obtained from diffraction hyperbolas along each profile. To obtain the diffraction velocity points, I measured the velocity of one to six diffraction hyperbolas within a 10 m interval and averaged them to obtain a velocity point every ~10 m along each GPR profile.

Table 2.2: Summary of CMP radar velocity results. V_r is the radar velocity and TWT is the TWT of the reflector from which the velocity was measured.

ID	Class	V_r	TWT	Surface particles
m1	mesic	0.05 m/ns	40 ns	sand, silt clays
m2	mesic	0.06 m/ns	50 ns	sand, silt, clays
m3	mesic	0.06 m/ns	20 ns	sand, silt, clay
x1	xeric	0.12 m/ns	40 ns	boulder, cobble, gravel, silt
x2	xeric	0.11 m/ns	30 ns	gravel, sand, silt
x3	xeric	0.10 m/ns	30 ns	gravel, sand, silt

Table 2.3: Radar velocities within selected geologic materials. Table compiled from Neal (2004) and Baker et al. (2007). Where there were conflicting intervals for the same substrate, the intervals were compiled so that they encompassed the widest velocity range.

Material	Velocity (m/ns)
fresh water	0.03
saturated clay	0.05-0.08
saturated sand	0.05-0.09
saturated silt	0.05-0.07
saturated sand and gravel	0.06
unsaturated silts	0.05-0.13
unsaturated sand and gravel	0.09-0.13
till	0.10-0.12
granite	0.12-0.15
unsaturated sand	0.12-0.17
unsaturated clay	0.12-0.21
air	0.30

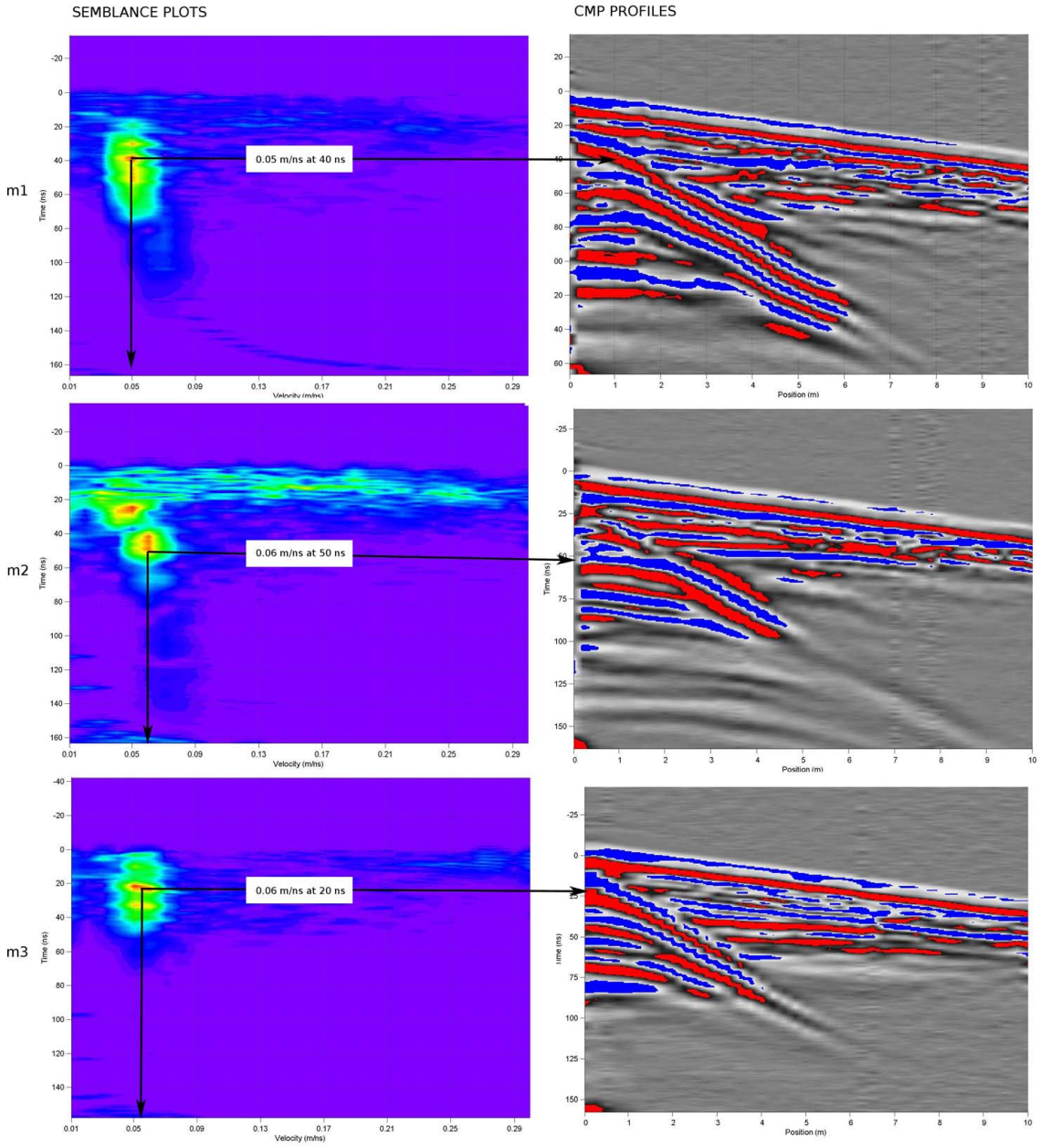

Figure 2.4: Semblance and profile plots from the mesic CMP analysis.

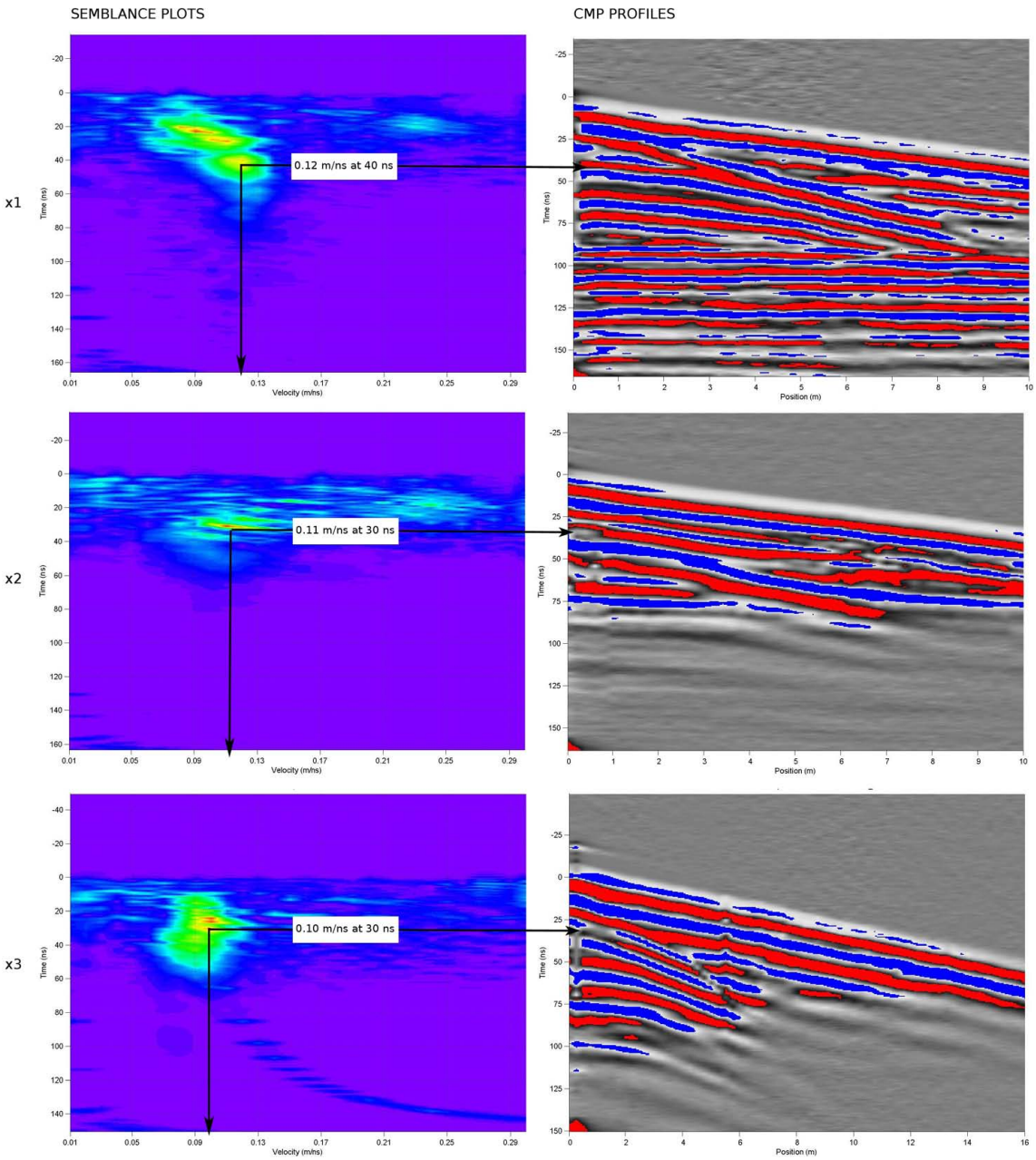

Figure 2.5: Semblance and profile plots from the mesic CMP analysis.

.

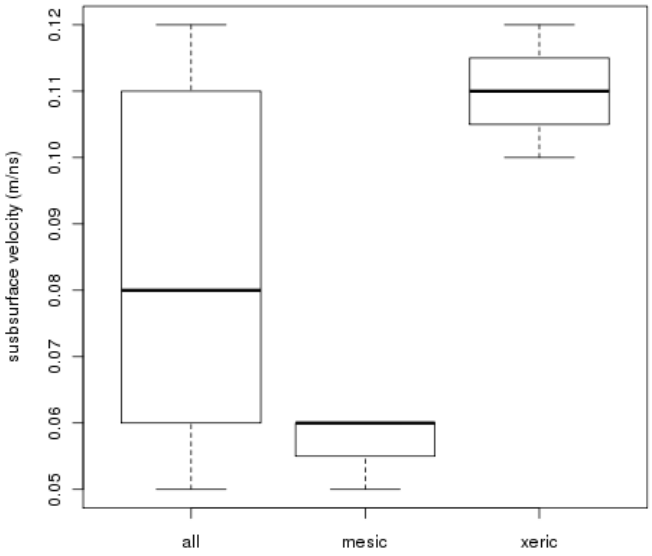

Figure 2.6: Boxplots of radar velocities. The first boxplot shows all the CMP results grouped together, the second and third boxplots break up the data into mesic (wet) and xeric (dry) CMP locations. These plots suggest lateral heterogeneity of velocities within the study area based on saturation.

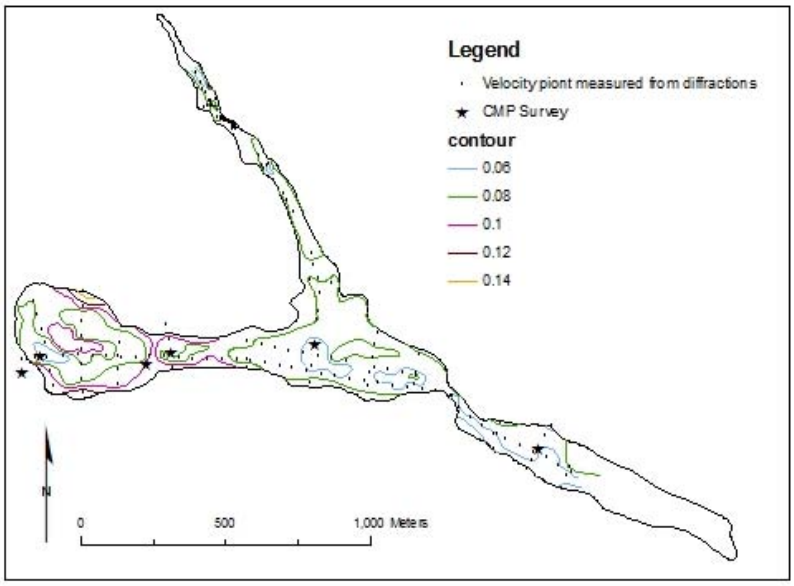

Figure 2.7: Radar velocity contour map

2.3.2 Computing the vertical resolution

The vertical resolution measures the ability to differentiate between two adjacent signals and can be thought of interpretively as the thickness of the thinnest beds that can be resolved. From my analysis, the average vertical resolution from all profiles in EBM and WBM transverse to the longitudinal valley axis is 0.32 m with a range from 0.28-0.36 m. The theoretical vertical resolution is calculated from the center frequency of the antennae and a subsurface velocity:

$$R_v = \frac{v}{4 \times f_c} \tag{2.1}$$

where R_v =vertical resolution , v=subsurface velocity and f_c =center frequency. This equation is a combination of two facts: the wavelength (λ) is equal to the velocity divided by the frequency, $\lambda = v/f$, and the vertical resolution is approximately one quarter of the wavelength, $R_v = \lambda/4$ (Reynolds, 1997; Jol, 1995). Thus, for a center frequency of 100 mHz and an estimated velocity of 80 m/ns (0.08 m/ns), which is the average velocity from the CMP analysis,

$$R_v = \frac{80\ m/ms}{4 \times 100\ mHz} = 0.20\ m \tag{2.2}$$

However, the 100 mHz center frequency for the Sensors and Software 100 mHz antenna is measured in air (Sensors and Software, 2003). This means that the actual return center frequency when data were collected in the field is somewhat less than 100 mHz and the resolution will not be as thin as the theoretical 0.20 m calculated above. The actual center return frequency can be identified from the average amplitude spectrum (AAS) plot, which plots amplitude versus frequency (Figure 2.8). For BT4, the vertical resolution, assuming a velocity of 80 m/ms (0.08 m/ns), is:

$$R_v = \frac{80\ m/ms}{4 \times 62\ mHz} = 0.32\ m \tag{2.3}$$

Using the same method as described for BT4, I computed the vertical resolution for each transect survey line in WBM and EBM. These values are reported in Table 2.4.

Table 2.4: Summary of GPR center return frequencies (f_c) and corresponding vertical resolutions (R_v).

Transect	f_c (mHz)	R_v (m)
BT1	60	0.33
BT2	71	0.28
BT3	61	0.33
BT4	62	0.32
BT5	63	0.32
BT6	71	0.28
BT7	67	0.30
BT8	61	0.33
BT9	65	0.31
BT10	55	0.36
BT11	59	0.34
BT12	69	0.29

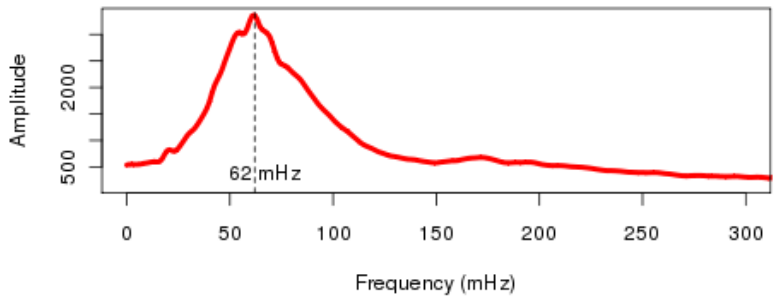

Figure 2.8: Average amplitude spectrum. Plot was generated from the gained BT4 profile. The center return frequency is 62 mHz.

2.3.3 Processing the common offset surveys

Basic

By overcoming some of the inherent limitations in the raw data, processed data provide clearer images of the subsurface and thus allow for more confident sedimentological interpretation (Neal, 2004). Table 2.5 describes and Figure 2.9 diagrams the basic processing steps performed on the common offset profiles. The profiles were processed using Ekko View Deluxe software by Sensors and Software, Inc. and Figure 2.10 is a comparison of a raw to porcessed common offset profile for BT4, following the processing flow diagrammed in Figure 2.9.

A gain corrects radar attenuation due to geometric spreading by increasing the signal strength of weaker signals at later times. Two typical types of gains are AGC (Automatic Gain Control) and SEC (Spreading and Exponential Compensation). The AGC gain equalizes signals by applying a gain which is inversely proportional to the signal strength. The AGC gain is popular in sedimentological studies since it helps resolve continuity of reflectors regardless of amplitude (Neal, 2004). However, once an AGC gain has been applied, information regarding relative amplitudes is lost and one cannot make inferences about the relative strength of one reflector compared to another. The SEC gain corrects for exponential energy loss due to geometric spreading through a combination of a linear time gain and an exponential function. By using an SEC gain, information regarding relative signal strengths is retained. The downside of the SEC gain is that continuity of reflectors could be lost in a zone of low amplitudes.

An SEC gain (max=150, attenuation 5 decibels/meter) and topographic correction using a velocity of 0.08 m/ns was applied (Figure 2.10). Note that timezero begins below the first two horizontal reflectors. These upper reflectors are the direct arrival and the ground wave and do not represent subsurface stratigraphy. These two reflectors were ignored during the analysis of the subsurface stratigraphy. Since SEC gains retain information about relative amplitudes, the black and white colors on the GPR profiles correspond to high amplitudes while grey colors correspond to low amplitudes.

For this study, both AGC and SEC gains were tried and were found to be very similar. Through iterative processing, an AGC gain of max=150 and an SEC gain of max=150, attenuation=5 decibels/meter were chosen for comparison (Figure 2.11). The AGC and SEC gains are similar. In both cases, the time amplitude spectrum plots show good correction of geometrical spreading since the

amplitude remained relatively constant for the bulk of the profile. Even though the SEC gain is less commonly used in sedimentological studies, I chose to use the SEC gain on all profiles. The SEC gain showed adequate continuity of reflectors and had the added benefit of retaining information regarding the relative strengths of reflectors, which could be used to make preliminary inferences about subsurface materials. There is an interesting dip in amplitude on the SEC profile corresponding to the contact between diffraction-rich reflectors and the overlying continuous reflectors, which may be useful in interpretation.

Table 2.5: Summary of process steps. More detailed description of processing steps are reported in Neal (2004); Annan (1999); Sensors and Software (2003); Jol (2009).

Step	Description
1)	**Data Cleaning.** This included correction of any field data entry errors and polarity reversals, as well as deletion of duplicate traces.
2)	**Alignment of First breaks.** A routine step that corrects the misalign- ment of the first break and realigns all reflections beneath it appropriately.
3)	**Merge Files.** Relevant data files were merged so that each transect con- sisted of only one file instead of many.
4)	**Repick Timezero.** Timezero was re-picked for the merged file to correct traces which may have drifted up or down
5)	**Dewow.** A routine data step that filters out low-frequency noise induced by signal saturation of the receiving antenna.
6)	**Gain.** Corrects radar attenuation due to geometric spreading and ex- potential dissipation of energy by increasing the signal strength of weaker signals at later times.
7)	**Migration.** Re-positions subsurface reflection events by removing diffrac- tions and dip displacements.
8)	**Topographic Correction.** Corrects for misalignment of signals due to topography.

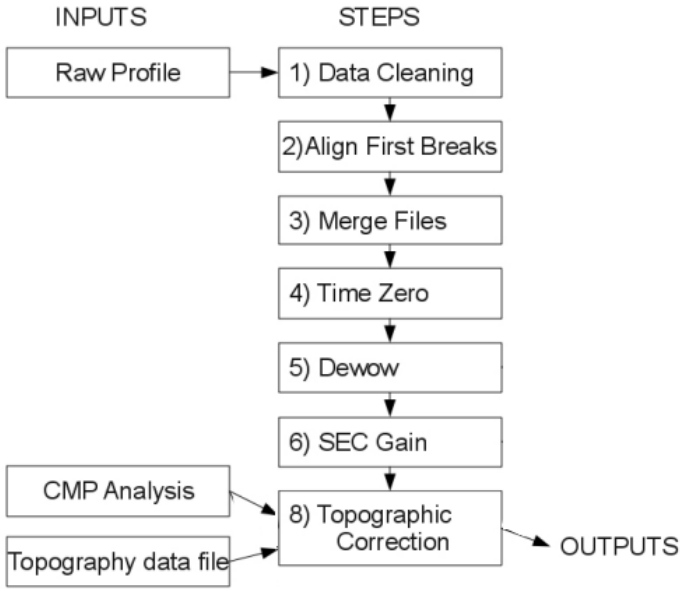

Figure 2.9: Flow chart of basic GPR processing steps. Inputs included the raw data files, results from the CMP analysis,topography data files generated from a total station survey of all transects. Processing steps are summarized in the text.

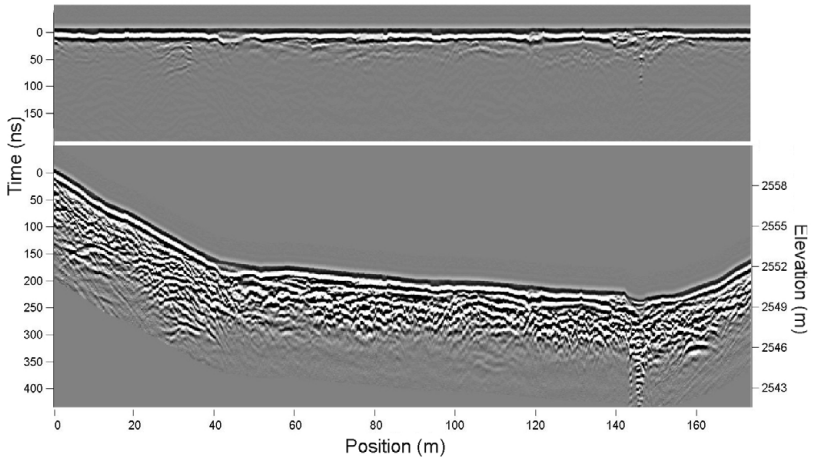

Figure 2.10: Comparison of raw and processed GPR profiles. Comparison of the unprocessed profile (top) to the processed output profile (bottom) for transect BT4 following procedures outlined in Figure 2.9 and Table 2.5. An SEC gain (max=150, attenuation=5 decibels/meter) and topographic correction using a velocity of 0.08 m/s was applied to the processed profile.

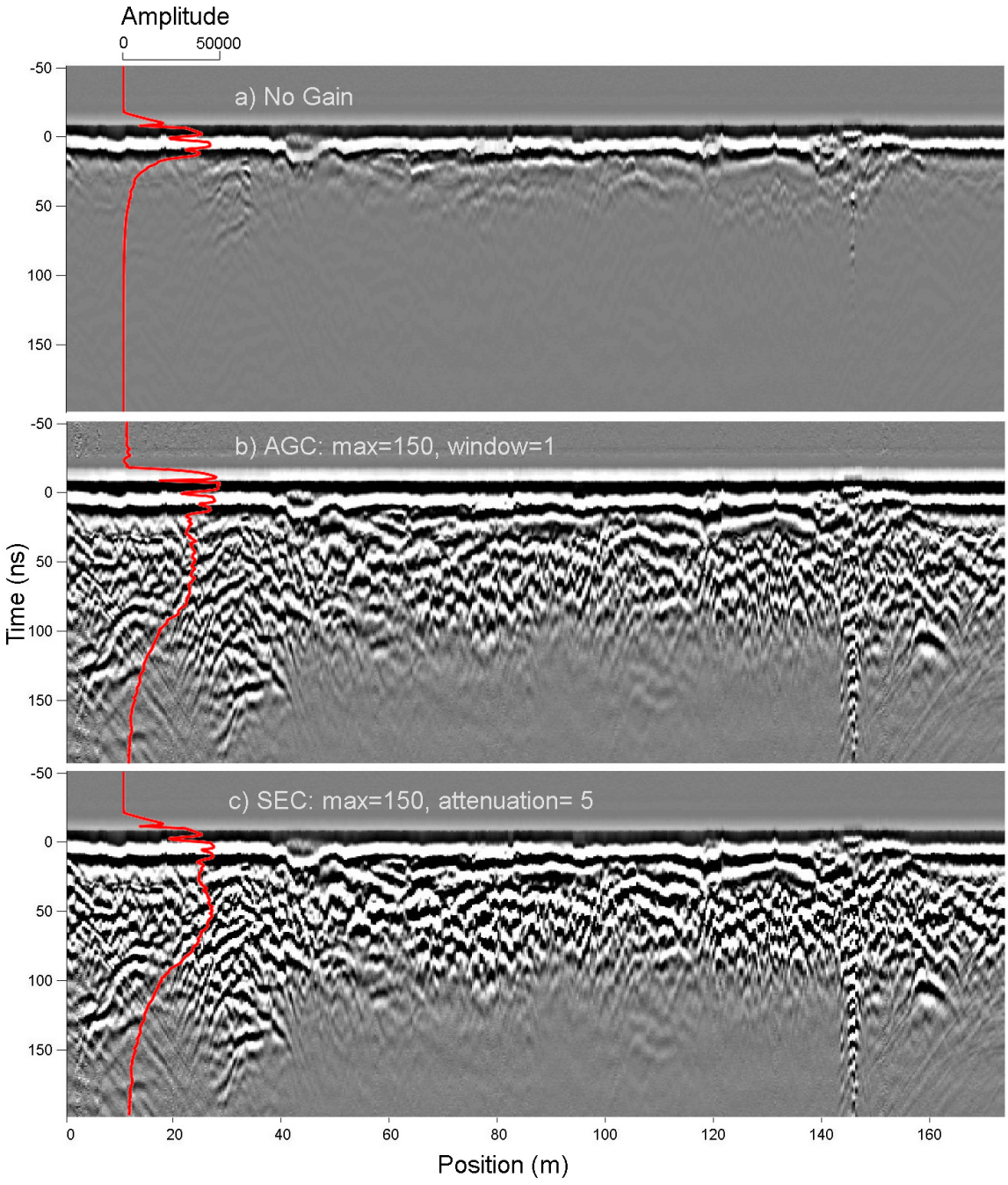

Figure 2.11: Comparison of no gain to AGC and SEC gains for transect BT4. The thick red line represents the time amplitude plot for each profile. (a) No gain has been applied. (b) An AGC gain with max=150 has been applied. (c) An SEC gain with max=150 has been applied.

Advanced

Advanced processing techniques such as migration, filtering and deconvolution are generally performed to resolve unwanted systematic noise. What follows is a summary of systematic noise encountered in Beaver Meadows and why these advanced techniques were not used. Figure 2.12 is a collection of images showing the three main types of systematic noise found in the profiles: surface reflections, multiple ringing and diffractions.

Reflections of surface features in subsurface profiles are created when electromagnetic energy transmitted by the GPR antennae is lost into the air and the receiver detects reflected radar waves from objects of high electrical contrast on the surface. Surface reflections can be caused by poles, trees, metallic fences, valley walls, boulders and irregular surface topography. Surface reflections are identified on profiles as hyperbolas with the velocity of air (0.3 m/ns). Surface reflections are especially prevalent in profiles when unshielded antennae are used. Sensors and Softwares PE100 system used in this study is unshielded and so recognition of these surface reflections prior to interpretation is important.

During surveying, careful notes were taken about potential sources for surface reflections. Surface reflections were most commonly found on the edges of the transverse profiles (feature a on Figure 2.12), but occasionally were found in the middle of profiles (feature b on Figure 2.12). Surface reflections located on the edges of the transverse profiles were due to the valley walls and presence of trees. Surface reflections located in the middle of the sections were due to location-specific surface objects such as fences and large surface boulders. Surface reflections could be resolved by migrating the data at the velocity of 0.3 m/ns, but this would over-migrate the data that I am trying to interpret. The best solution was to simply recognize the surface reflections and then ignore them.

Multiple ringing is caused by radar waves bouncing back and forth between a high conductivity reflector and an antennae, resulting in multiple reflection events. The multiple reflection events are dominated by a single low frequency that often obscures 'true' reflectors. Features c and d in Figure 2.12 were both due to a field protocol which allowed the transect to be surveyed at the same time that the GPR data were being collected. Feature c was created when the person holding the receiving antennae also held the metal survey rod parallel to the antennae. Feature d was created when a person with the metal survey rod positioned it vertically too close to the receiving antennae while getting a data point. These problems were identified in the field but not before transects BT1,

BT2, BT3, and the first 100 meters of BT6 were collected. In some of the other transects, similar artifacts may be due to other objects with high conductivity, such as metal fences or buried metal pipes. Curiously, every time the antennae crossed small streams or standing water bodies, multiple ringing was created (feature e on Figure 2.12).

Multiple ringing is the most disruptive source of noise in the profiles so I attempted to remove it through deconvolution and frequency filtering. Bandpass frequency filtering is used to filter unwanted noise outside of a certain specified bandwidth (Sensors and Software, 2003). By inspecting the average amplitude spectrum (AAS) plot of the unfiltered data (Figure 2.13a), I chose the corner frequencies 20, 30, 100, and 110 mHz. I centered the corner frequencies about 70 mHz, which is approximately the return center frequency for the transect shown. I set the bandwidth to be the narrowest that I could make it without filtering out frequencies within the natural bandwidth of the data. By comparing the non filtered data with the filtered data (Figure 2.13), it is apparent that some minor high frequency background noise has been eliminated but that the lower frequency multiple ringing has not been altered.

Deconvolution is often used in seismic processing to remove multiple ringing but has had only limited success with radar data (Neal, 2004). Deconvolution attempts to convert a radar wavelet into as close to a spike as bandwidth will allow. The deconvolution algorithm in EKKO View Deluxe uses the GPR center frequency to constrain the wavelet estimation process (Sensors and Software, 2003). To apply deconvolution, four main parameters are needed; (1) return center frequency, (2) filter width, (3) delay (0.5 times the filter width) and (4) spike width. In Figure 2.13b, return center frequency = 71 mHz estimated from the AAS data, filter width=20 ns, delay=10 ns and spike width=2 ns. The deconvolution did resolve the multiple ringing to some degree, but it also made the rest of the data fuzzier and harder to interpret.

Due to the ineffectiveness of bandpass filtering in resolving the multiple ringing and the loss of data quality with deconvolution, I chose to use neither when processing the data. Thus, the profiles were interpreted with the multiple ringing intact. However, since multiple ringing is easily identifiable, it was easily ignored during interpretation.

Diffractions are hyperbolas, which are generated by reflection off isolated reflectors, such as buried pipes, joints, isolated boulders or abrupt truncation of lithology (Neal, 2004; Beres et al., 1999; Vandenberghe and van Overmeeren, 1999). The presence of diffractions has implications for interpretation. Diffractions disrupt the radar stratigraphy and may need to be collapsed through

migration in order to accurately portray the subsurface reflections for interpretation. However, diffractions are also very useful in interpretation. The presence of many scattered diffractions within a facies (such as the diffractions shown in Figure 2.12) may lend weight to the argument for a sedimentary layer composed of many large boulders such as a glacial lag or till. The location of a diffraction may also point towards an abrupt change in lithology associated with intersecting channels, the boundary between a channel and its floodplain, or channel bottoms (Vandenberghe and van Overmeeren, 1999). However, diffractions must be interpreted with care since they can be created by many different types of isolated objects. The presence of a buried metal water conveyance pipe in Beaver Meadows is a concern for identifying whether the diffractions were caused by lithology. However, the location of this pipe is known and was presented in the introduction (Figure 1.10).

Profile migration collapses diffraction hyperbolas to obtain more accurate representation of the subsurface layering (Neal, 2004; Sensors and Software, 2003). Almost all the profiles had ubiquitous scattered diffractions on the bottom half of the profiles and a few isolated diffractions within overlying, continuous to moderately continuous reflectors. These scattered diffractions corresponded well with where glacial till outcropped on the surface and thus were probably generated by buried boulders (section 3.1.2). To resolve these diffractions, I migrated the SEC gained BT4 profile with a 0.11 m/ns velocity, which was the velocity determined through the CMP analysis associated with till deposits.

Figure 2.14 compares the unmigrated to the migrated profile. The velocity of 0.11 m/ns resolved the diffractions at depth, but over migrated the upper portion of the profile, creating concave-up features disrupting the sedimentary structure. This suggests vertical heterogeneity of radar velocities associated with different sedimentological units. Given the study goal of differentiating glacial deposits from overlying alluvium, I decided not to use migration to collapse the diffractions. Collapsing diffractions made sedimentary structure within the diffraction-rich layer easier to interpret, but I am less interested in the sedimentary structure within the diffraction-rich layer and more interested in identifying the contact between the diffraction layer and the overlying reflector. Migration also disrupted the sedimentary structure of the overlying layer, which I am interested in characterizing.

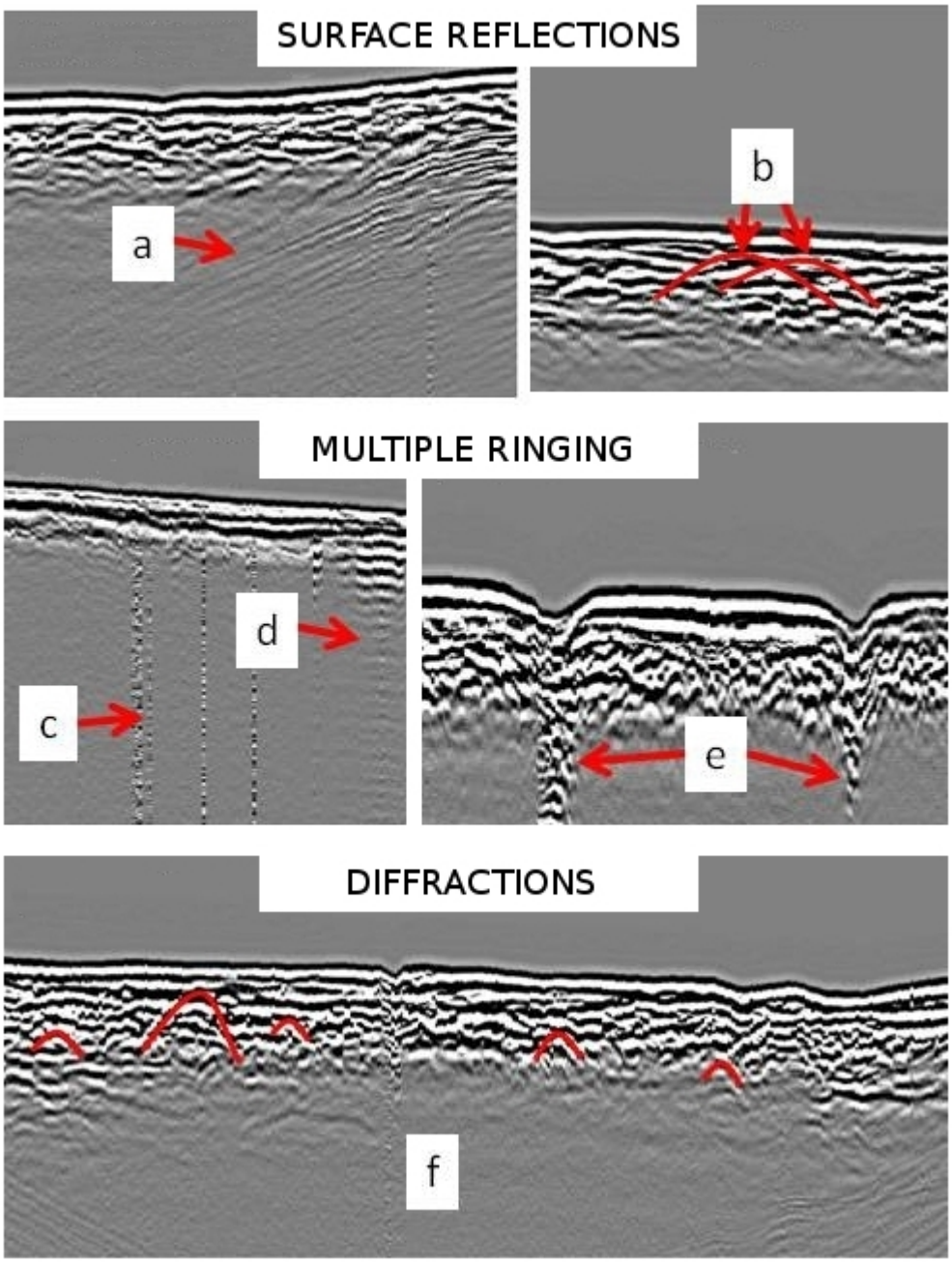

Figure 2.12: Systematic noise in GPR profiles. Three general categories of noise are shown: surface reflections, multiple ringing, and diffractions. Feature a is a surface reflection that is due to the proximity of valley walls and trees. Feature b is a surface reflection due to the presence of a nearby surface object with high electrical contrast. Features c and d show multiple ringing due to a metal survey rod being held too close to the antennae during data collection. Feature e is multiple ringing due to the crossing of a stream. Feature f shows examples of diffractions caused by isolated objects in the subsurface, such as boulders.

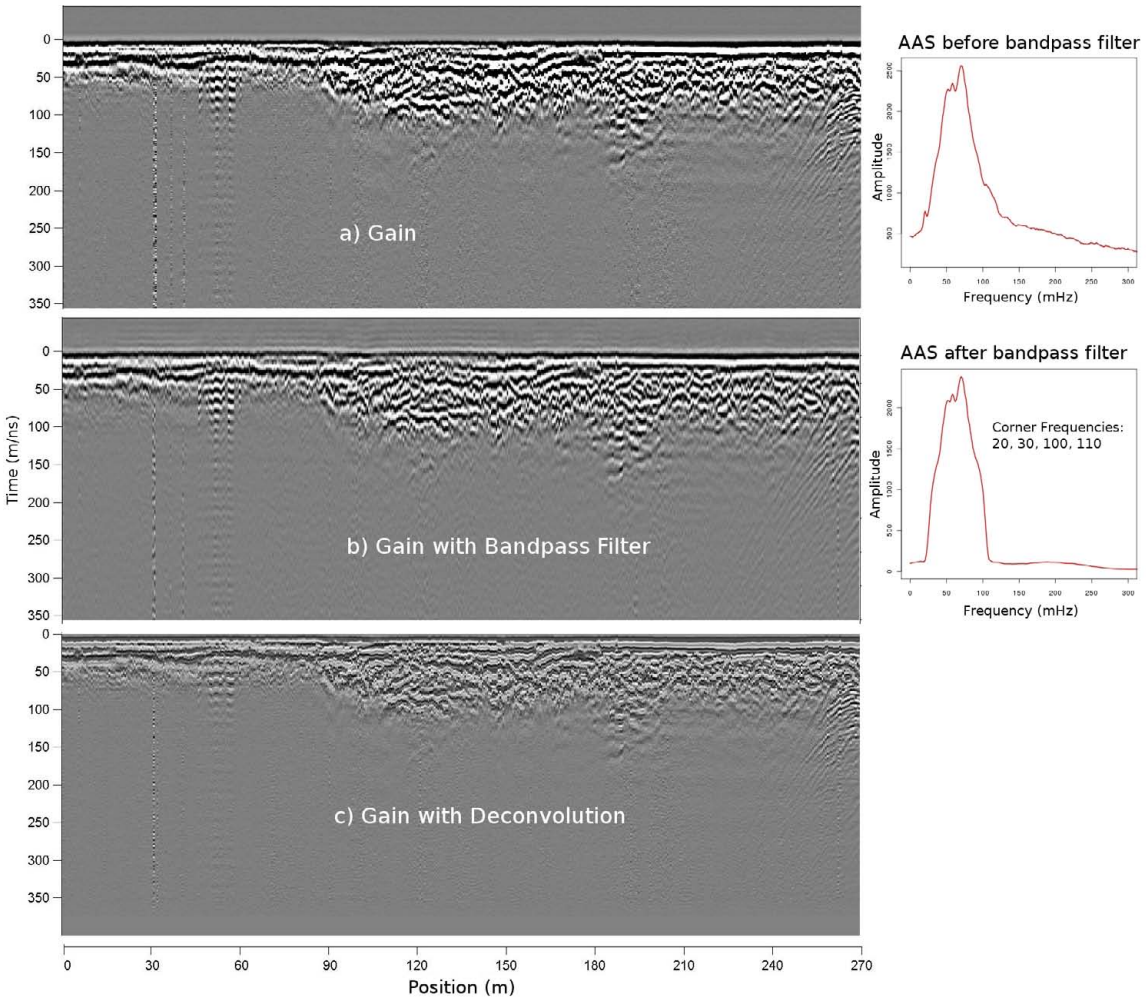

Figure 2.13: Bandpass filter and deconvolution of BT6. a) Transect BT6 with an SEC gain (max=150, attenuation=5 decibels/meter). Average Amplitude Spectrum (AAS) plot to the right shows a return center frequency of 71 mHz. b) Bandwidth frequency filter applied with corner frequencies at 20, 30, 100 and 110 mHz. AAS plot to the right shows frequency distribution after filtering. c) Deconvolution applied with return center frequency = 71 mHz, filter width=20 ns, delay=10 ns and spike width=2 ns.

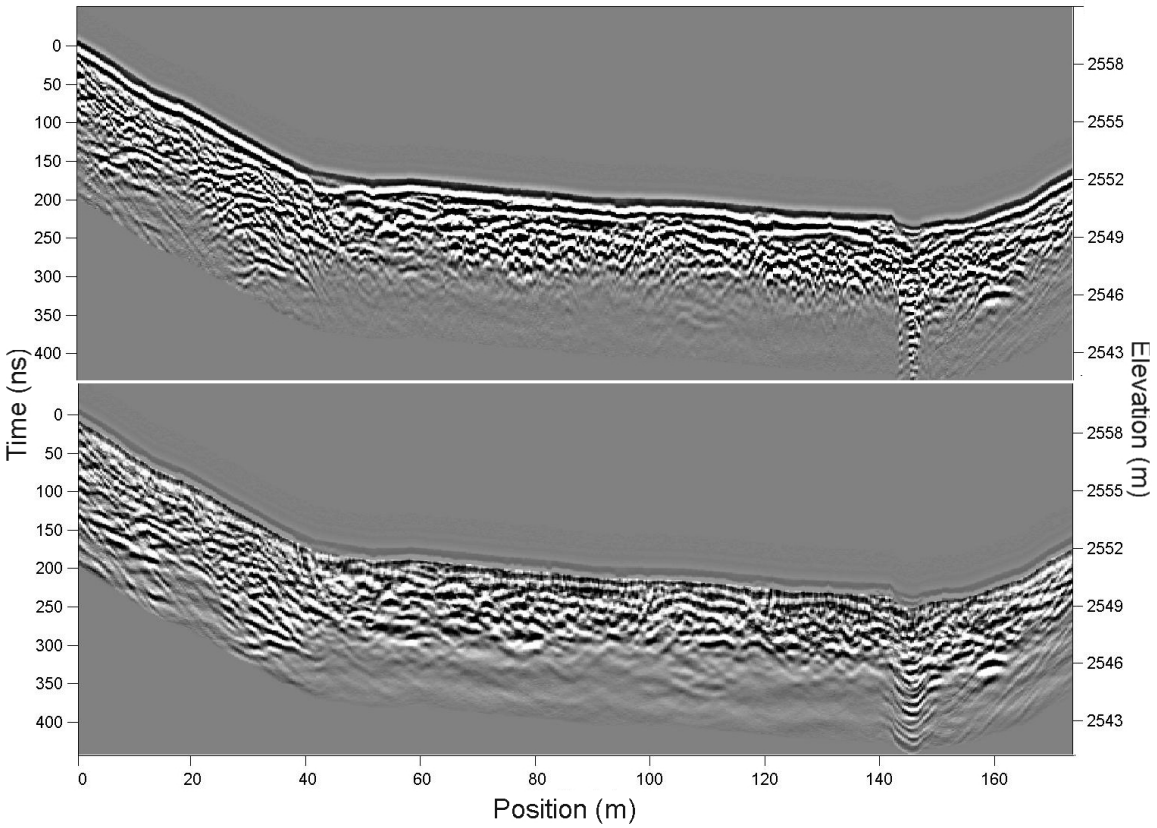

Figure 2.14: Migration of BT4. Comparison of unmigrated data (top) to migrated data at 0.11 m/ns (bottom). An SEC gain (max=150, attenuation=5 decibels/meter) was applied to both profiles.

2.4 SSR Data Processing

The SSR subsurface velocity profiles for BT2, BT4, BT6 and BT11 were generated by tomography of travel time curves using SeisImager software packages. Travel time curves were created from first break picks using Pickwin and tomography was applied in Plotrefa. The signal to noise ratio ranged from high to low throughout the study area (Figure 2.15). There were both low and high frequency systematic noise in the datasets (Figure 2.16). Low frequency noise appeared in the data occasionally when a car or plane went by. Unfortunately, there are many visitors to RMNP and thus it was impractical to pause data collection for every car. High frequency noise significantly increased in areas of saturated ground containing numerous hummocks, occasionally rendering the data so noisy as to be uninterpretable (Figure 2.15). When signal to noise was especially low, data were not used.

Tomography models for all four surveys are presented in Appendix C, along with raypath coverage and modeled versus observed travel time curves. The initial model parameters included topography, constraints on the maximum and minimum velocities of 300 m/s and 6,000 m/s, and maximum depth of investigation of 30 m . The tomographic velocity inversion was iterated 10 times, after which no significant changes were noted in any of the transects. The raypaths had decent coverage and the RMSE for each line was <3 ns.

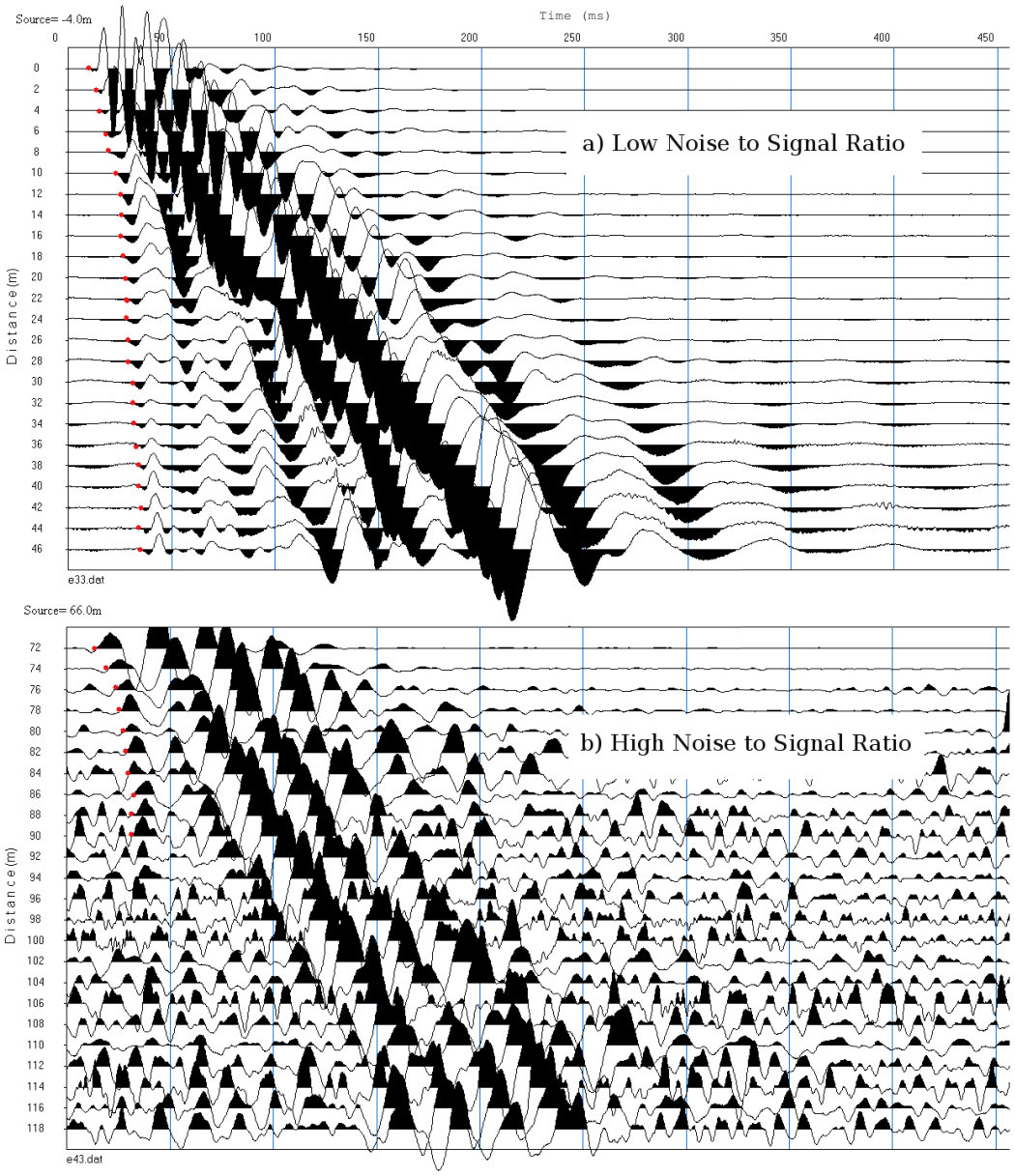

Figure 2.15: Comparison of first break picks. Red dots mark location of first break picks. a) First arrival data from BT6 with a high signal to noise ratio. Survey collected on dry ground. b) First arrival data from BT11 with a low signal to noise ratio. Survey collected on mushy wet ground with grassy hummocks. Notice that first breaks were not picked when the noise drained out the first arrival data.

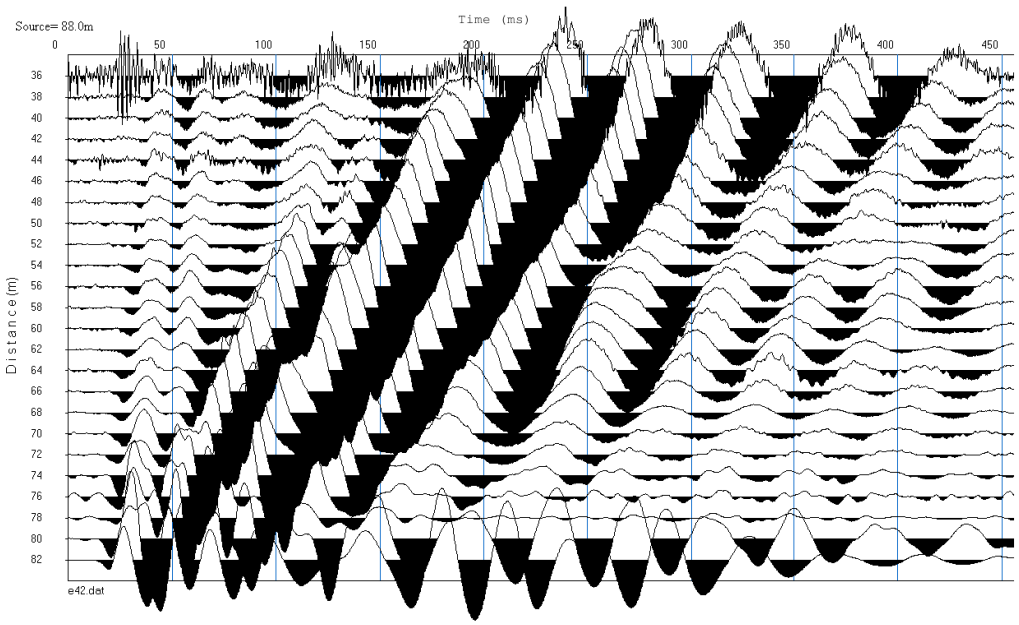

Figure 2.16: Low and high frequency noise The high frequency noise on geophone 36 was caused by the placement of the geophone in a grassy hummock. The long period low frequency noise apparent throughout the dataset was caused by the passing of a car.

3 RESULTS

3.1 Geophysical Data Analysis and Interpretation

In this section, I analyze, interpret and discuss both the GPR and SSR data profiles. I develop radar stratigraphy with interpretations for Beaver Meadows, which could later be used as type radar stratigraphy for similar valleys in studies throughout the Rockies. I also identify the valley fill/alluvium contact on the GPR profiles and the bedrock/valley fill contact on both GPR and SSR profiles. Results and discussion relating to average thickness, volumes and percentages of deposits throughout the entire meadow are presented in section 3.2.

3.1.1 Radar stratigraphy

Radar stratigraphy includes the description of radar facies, radar packages, and radar surfaces (Neal, 2004). Radar facies are sets of reflectors characterized by distinctive congurations of shape, dip, relationship and continuity. Radar packages are depositional units of genetically related strata. Radar surfaces are surfaces of discontinuity representing depositional breaks in stratigraphy which bound radar facies and radar packages, thus identification of radar surfaces facilitates identification of facies and packages. In Beaver Meadows, I identified three main radar surfaces; concordant, truncated, and onlapping.

Figure 3.1 summarizes the radar facies and packages in Beaver Meadows. Five facies were identified; F0, F1, F2, F3, and F4. F0 is reflection free. F1 is easily identifiable as it is diffraction-rich, chaotic, and discontinuous. F2 has noticeably less diffractions than F1 and the reflectors are horizontal, wavey, subparallel, and discontinuous to moderately continuous. F3 has thick, parallel, continuous reflectors. F4 has inclined, parallel to subparallel reflectors.

Two main radar packages were identified, P1 and P2. P1 is mainly comprised of facies F1 with a noticeable increase of F2 in EBM. P2 is complex and contains all of the facies, but is noticeably dominated by F3. P1 stratigraphically underlies P2 in WBM and EBM, but is absent in NBM. In WBM and EBM, P2 is a wedge, thickest to the south and thinnest to the north. The wedge abruptly terminates with the bottom boundary onlapping onto a radar facie characterized by a lack

of reflectors. For most of the study area there is no clear lower bounding radar surface to this package; rather, it attenuates into a facie of no reflectors. P1 is bounded on the top by P2, which either onlaps or is concordant to P1. The upper boundary of P2 is concordant with the ground surface unless stream incision is present, in which case it is truncated.

Table 3.1: Radar stratigraphy for Beaver Meadows. Example facies from profiles in Beaver Meadows. Wedge and drape images are from Neal (2004)

Facies		
F0		Reflection free
F1		Discontinuous, chaotic, many diffractions
F2		Discontinuous to moderately continuous, wavey, subparallel, subhorizontal, minor diffractions
F3		Continuous, horizontal, parallel, thick
F4		Moderately continuous, inclined, subparallel to parallel
Packages		
P1	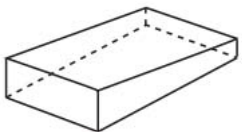	Wedge, which includes F0, F1 and F2. This package thins to the north and is absent in NBM.
P2	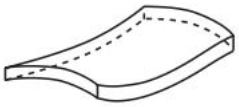	Filled drape, which includes F1, F2, F3 and F4. This package drapes over the underlying topography. Where the underlying topography was low, the drape was filled in so that it had a drape-like lower contact but a flat surface at the top, thus I am calling it a filled drape.

3.1.2 Interpretation of radar stratigraphy and seismic profiles

Bedrock/valley fill and glacial/alluvium Contacts

Surface exposures of till and bedrock as well as subsurface data from cores and auger holes led to a confident interpretation of P1 as glacial and P2 as alluvium. The contact between these two packages is the glacial/alluvium contact. Figure 3.1 shows the correlation between the interpreted glacial/alluvium contact on GPR profiles with cores and a cutbank exposure. In the NBM and the northern edge of WBM, where bedrock was near the surface and P1 is absent, the bedrock/valley fill contact was identified on the GPR as a sharp transition between F0 and P2 (Figure 3.2). Since glacial deposits (P1) are absent at these locations, the bedrock/valleyfill contact is a bedrock/alluvium contact. This contact was field verified with auger holes in NBM and along the northern boundary of WBM, from which ± 0.5 m uncertainty was estimated for the depth to the contact. C^{14} dating by Polvi (in prep) confirmed that the alluvium deposited directly on top of pre Cambrian bedrock is Holocene in age. This implies that Pleistocene alluvium deposition beyond the maximum glacial extent was not preserved. Where the contact between F0 and F2 was not sharp but gradational (Figure 3.2), F0 was interpreted to be part of P1 and the gradational contact was attributed to attenuation of the radar waves through glacial till.

Throughout most of WBM and all of EBM, the bedrock contact was too deep to detect with the shallow penetration of the GPR, thus seismic refraction was used to image the bedrock contact in those study areas (see Appendix B for all seismic profiles). The bedrock/valley fill interface was interpreted from the velocity profiles by noting a steep gradient in velocity corresponding to a velocity change from the range of valley fill, <2700 m/s, to that of crystalline bedrock, >3500 (Table 3.2). In Beaver Meadows this sharp velocity gradient occurred at ~3000 m/s, which is consistent with data gathered by Locke (1987). This velocity is slightly slower than typical velocities found for granite elsewhere (Table 3.2). I estimated the error of this contact to be ± 1 m based on how much higher or lower I could draw the contact based on my criteria. Setting the boundary at this velocity matched well with drill hole data (Figure 3.3). The seismic profiles did show some undulation at the valley fill/bedrock contact. This could reflect undulations in the bedrock or may result from the quality and spatial resolution of the data. The anomalous high mound shown in the middle of transect BT11 (Appendix C) is worthy of note. This mound shown was ignored as a true subsurface structure because it was modeled from missing and noisy data.

Surprisingly, the shallow bedrock boundaries interpreted from the GPR lines did not line up with the >3000 m/s velocity contour, but with a much slower one at >900 m/s (Figure 3.2). I am fairly confident that the bedrock boundaries interpreted from the GPR profiles are accurate as they were field verified with multiple auger holes; I am similarly confident that the deeper bedrock contacts on the SSR profiles are accurate as they match up with drill hole data and previous seismic work. This implies that the bedrock closer to the surface has a slower velocity and interpretation of the bedrock contact cannot be solely based on one iso-velocity contour. Similarly to my findings, in Beaver Meadows Locke (1987) found that granite bedrock at the surface had velocity of >1000 m/s, which was interpreted to be a highly weathered zone. The interpretation that these low velocities represent a weathered zone is not unreasonable. Press (1966) summarizes a velocity range of 300-900 m/s for a "weathered layer" and Barton (2007) reports modeled p-wave velocities for hard rocks at shallow depths as low as 1.1 m/s in a 'weakness zone' with high joint density and weathering. I combined the interpretations from the GPR and SSR profiles to obtain bedrock contacts along each SSR profile. Figure 3.2 shows the SSR profile for BT2 with and without the bedrock interpretation.

Table 3.2: Summary of p-wave velocities in m/s.

	Global[1]	This Study[2]	Locke[2] (1987)	Tinsley[3] (1978)	Schjins[4] (2009)
Air	330				
Water	1450-1530				
Soil	100-500		420-620	325-475	
Alluvium	500-2200		350-750		320-520
Saturated Alluvium				1505-1655	
Till	430-2700		640-1130	910-1230	1640-1960
Weathered layer	300-900	>900	>1100	2340-2940	
Unweathered Granite	4600-6200	>3000	>3260		4900-6580
Schist/Gneiss	3500-7500	>3000			

1. Range of values compiled from Reynolds (1997); Barton (2007); Press (1966)
2. Beaver Meadows, RMNP, Colorado Front Range
3. Sierra Nevada Mountains, California
4. Finland

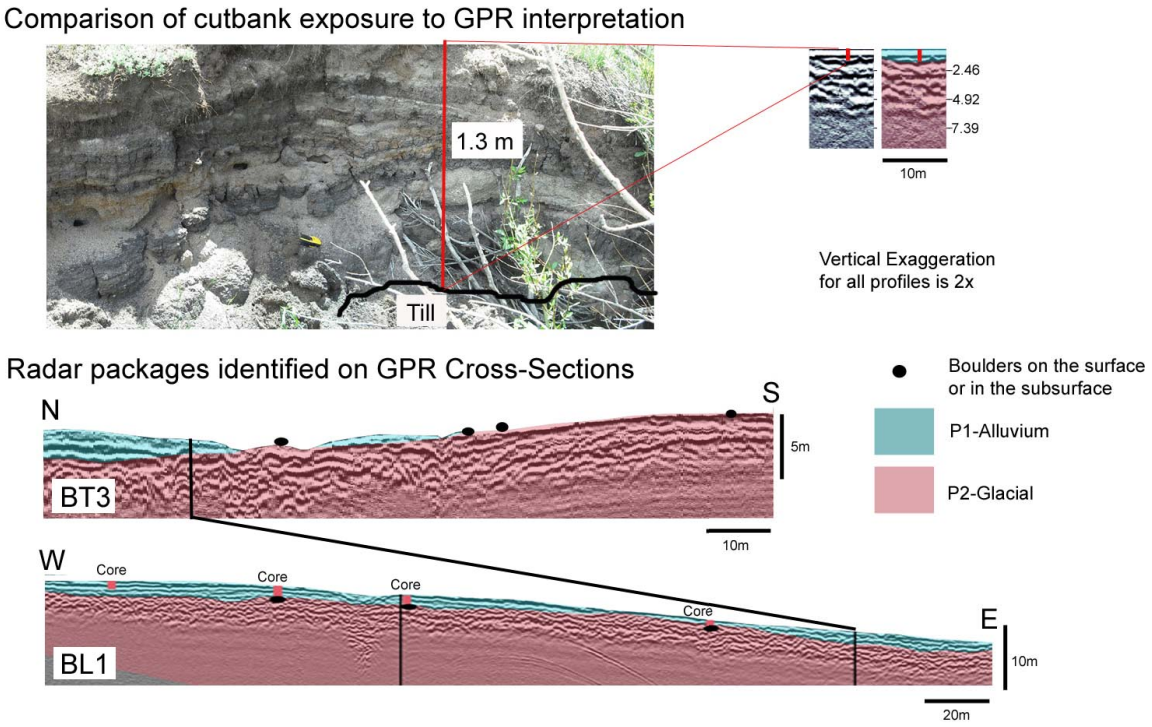

Figure 3.1: Field verification of the glacial/alluvium contact. Comparison of the glacial/alluvium contact with cores and a cutbank exposure. The air wave and direct ground wave are not shown. Note that BT3 and BL1 cross each other at the location marked and that BL1 was drawn at a different scale in order to fit it on the page. The red vertical lines on BL1 represent auger holes. Boulders encountered at the base of an auger hole are marked. A representative stratigraphic column of the cutbank exposure is presented in Figure 3.4.

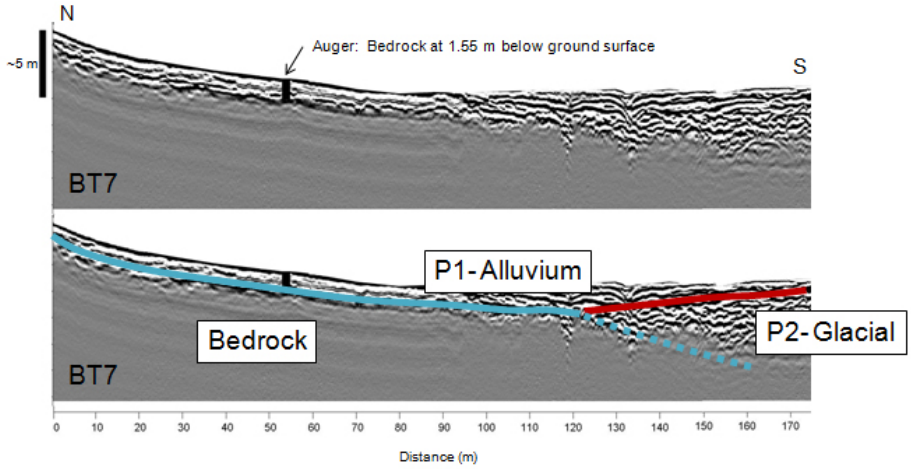

Figure 3.2: Identification of bedrock contact on GPR profiles. Using BT7 as an example, this figure shows that the interpreted bedrock contact is consistent with depth to bedrock noted in a hand auger core. The right side of the figure demonstrates the attenuation of the radar signal through glacial material. The air wave and the direct ground wave are not shown.

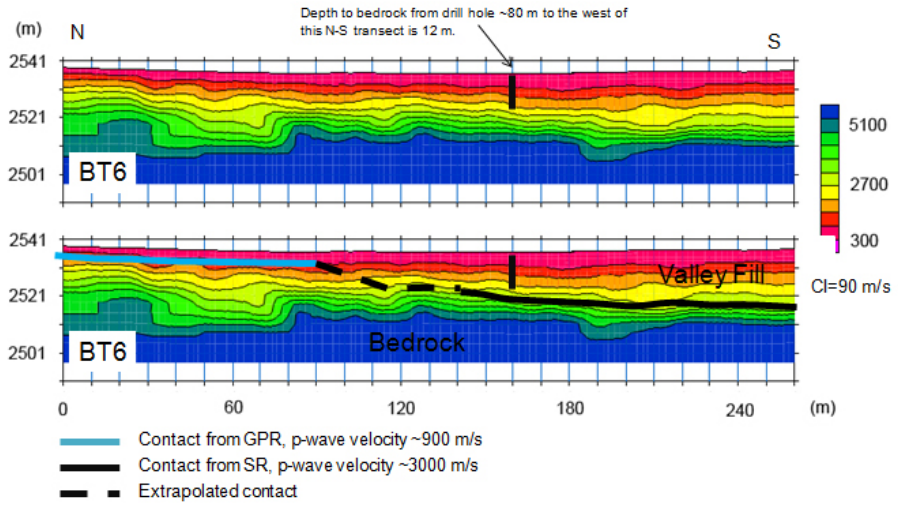

Figure 3.3: Identification of bedrock contact on SSR profiles. Using BT6 as an example, this figure shows the interpreted bedrock contact based on seismic velocity >3000 m/s (black line) and based on GPR profiles (blue line).

GPR facies

Table 3.3 presents the interpretation of the radar facies summarized in Table 3.1. All of the GPR profiles shown in Figure 2.2 and listed in Table 2.1 are presented along with interpretations in Appendix B. It is important to recognize that radar facies are non-unique; different deposits can generate the same radar signal, thus the facies within P1 (glacial) and P2 (alluvium) were interpreted based on the depositional setting (whether they are located within P1 or P2), the character of their bounding surfaces, surface field observations and auger descriptions. Figure 3.4 is a representative stratigraphic column of the cutbank exposure on Figure 3.1. This exposure displayed packages of sediment typical in auger holes throughout the valley (Appendix A) and is consistent with auger descriptions by Graf (1997).

Almost all auger holes had a surficial layer of ~0.3 m of silty loam soil (unit A on Figure 3.4), thus a ~0.3-0.5 m F3 reflector, which drapes the entire meadow, is interpreted to be soil. A layer of poorly sorted sands and gravels lying directly on top of boulders or bedrock is present in the majority of auger holes in WBM (unit D on Figure 3.4). This layer is interpreted to be glacial outwash due to its ubiquitous presence in WBM and its proximity to glacially deposited boulders. The thickness of this basal layer of sand and gravels is commonly less than the ~0.32 m vertical resolution of the GPR (section 2.3.2), therefore it was not directly tied to a particular radar reflector. I was able to identify F1 as the bouldery till underlying unit D due to the density of diffractions, which were caused by reflection off large boulders. Not only is it common to see diffractions from boulders but also from pockets of gravels and cobbles (Neal, 2004). Thus, when F1 was encountered within the alluvium, it was interpreted to be pockets of fluvial cobbles and gravel. F1 was most commonly found within the alluvium in the northwestern section of WBM where Beaver Brook enters the meadow. This is a natural location for the deposition of coarser material within the channel since the stream gradient abruptly decreases as it enters the meadow (Figure 1.3).

Stratigraphic units B (interlayered lenses of silts, clays and sand) and C (massive black clays) depicted in Figure 3.4 were found in most auger cores, although thicknesses, order and number varied. I am using the word clay within this thesis to refer to clay-sized particles, not clay minerals. Some examples of other configurations of B and C found in the valley are BC, BCB, CBC, CB, BCBC. The spatial heterogeneity of sections B and C vertically and horizontally suggests that the deposition of fines within these units occurred from spatially heterogeneous ponding. From 39 cores and cutbanks

in Beaver Meadows, Polvi found that 33-50% of sediment within the top 2 m was composed of sediment similar to units B and C and interprets them to be pond, pond/channel and pond/floodplain deposits associated with beaver damming. Furthermore, clay deposits similar to unit B were found directly behind existing topographical berms (Polvi, in prep), contained disintegrated wood and are consistent with descriptions of buried beaver pond deposits in strikingly similar valleys in Yellowstone (Lyman Persico, Personal Communication Nov 2010). Polvi (in prep) presents grain size analysis and C^{14} results obtained from auger holes in Beaver Meadows and discusses sediment dynamics and rates within the Meadow. The thickness, horizontal deposition, and fine sediment size of units B and C led me to interpret the majority of F3 within P1 as sedimentation associated with beaver damming.

In order to confirm the interpretation of F3 deposits as beaver-induced sedimentation, I identified a sub package of P2, P2a, interpreted to be genetically related strata associated with a beaver dam. This sub package was identified by imaging longitudinally and transversely over a topographic berm that was positively identified in the field as a buried beaver dam (Polvi, in prep). Figure 3.5 shows the un-interpreted and interpreted GPR profiles of the buried beaver dam. The dam was recognized as a facie of chaotic discontinuous reflectors (F1) that truncated parallel, continuous reflectors upslope (F3). The P2a package was therefore recognized as a wedge, thinning away from the dam, which contained abrupt truncation of F3 by F1 downslope. As shown in Figure 3.5, P2a packages can appear in a chain and stacked in offset to one another. This is consistent with the habit of beavers to build a chain of dams of different sizes to service one family, and with the temporal and spatial variability of damming (Gurnell, 1998).

Because the spatial distribution of the GPR lines, which are spaced approximately 200 m apart, may not cross all buried beaver dams within the valley, I generally interpreted F3 (laterally continuous thick reflectors) to be beaver pond deposits whether or not they were part of a P2a package. This interpretation of F3 is consistent with the stratigraphy of alluvium as described from augers and cutbank exposure described previously. Also, laterally thick, continuous, horizontal reflectors in this setting are indicative of relatively stable low energy deposition associated with ponding. At this site, the two plausible explanations for ponding of water are by beaver damming or glacial damming. Deposition of these sediments by glacial damming can be disregarded because Polvi (in prep) has shown that the alluvium is Holocene in age.

The two facies, F2 and F4, were not examined in detail because their relevance to investigating

the hypotheses of this thesis is minimal. F2 is interpreted to be associated with re-worked, or stratigraphically layered glacial deposits or re-worked alluvium. F2 notably increased within the glacial deposits below the location of the Bull Lake glacial dam (section 1.2.2) and thus may be associated with a pre Pinedale outburst flood. F2 may also be associated with structured outwash deposits. Further investigation into the deposition of F2 within the glacial deposits is outside the scope of this thesis, but I recognize that it could produce interesting results and be useful for mapping glacial deposits in the subsurface. F2 within the alluvium notably increased at the head of WBM where Beaver Brook enters Beaver Meadows. Aerial photographs of the meadow suggest that channel migration was greater in this part of the meadow (Polvi, in prep), and as stated before, it is a natural deposition zone. Both these facts support the interpretation of F2 as re-worked alluvium. The presence of F4 was very limited and confined to valley edges. F4 was interpreted to be colluvium because it was seen in the subsurface where alluvial fans encroached on the valley bottom or at the base of steep valley sides. Where F4 was interfingered with other facies, I interpret this to represent concurrent episodic hillslope deposition with valley floor aggradation.

Table 3.3: Interpretation of radar stratigraphy. Interpretation of radar facies and packages based on augering, and field observations of boulders and cutbanks in incised channels.

Facie	
F0	Glacial deposits when above bedrock contact and bedrock when below bedrock contact.
F1	Poorly sorted glacial deposits, channel gravels and cobbles, buried beaver dam, fractured bedrock.
F2	Re-worked glacial or stratified drift, re-worked alluvium including floodplain deposits.
F3	Soil overburden, stacked sequences of flat lying ponded silts clays and fluvial sands associated with beaver damming.
F4	Channel fill, colluvium.
Package	
P1	Glacial Deposits (Till and Outwash). Contains F0, F1, and F2.
P2	Alluvium (Post-glacial sedimentation). Contains F1, F2, F3, F4.

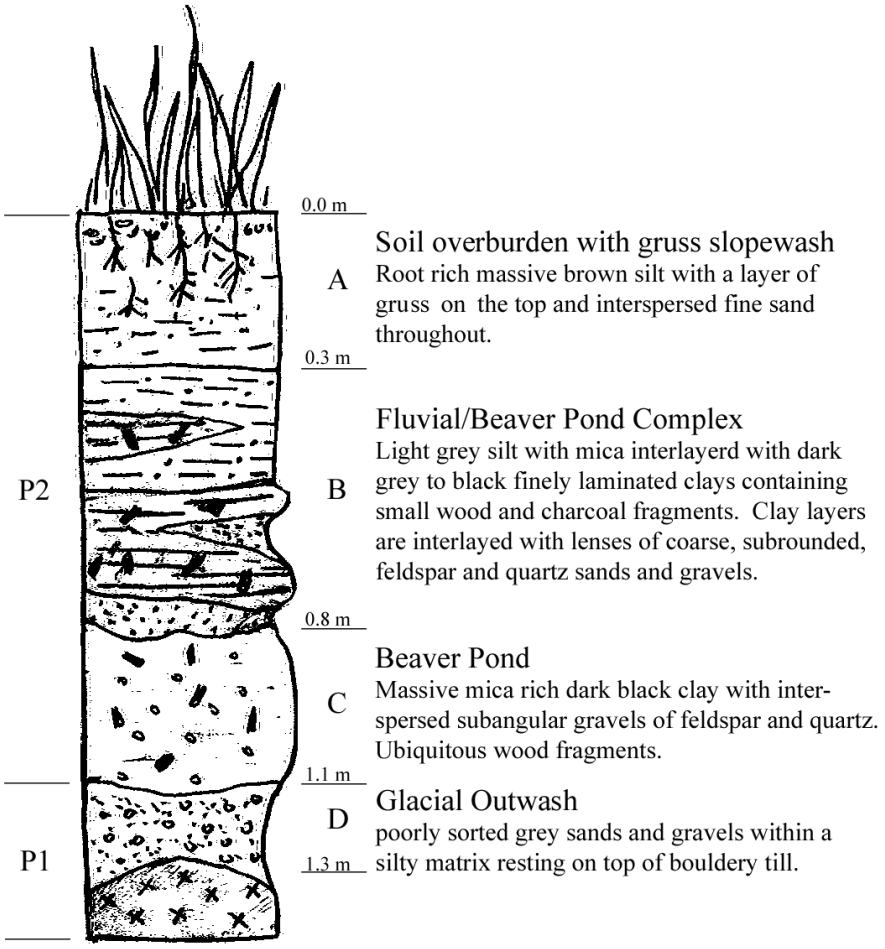

Figure 3.4: Alluvium stratigraphy. Stratigraphic column of the cutbank exposure shown in Figure 3.1. The stratigraphic units shown are representative of stratigraphi units in many auger holes throughout the meadow. P1 and P2 denote radar packages associated with glacial and alluvium deposits, respectively.

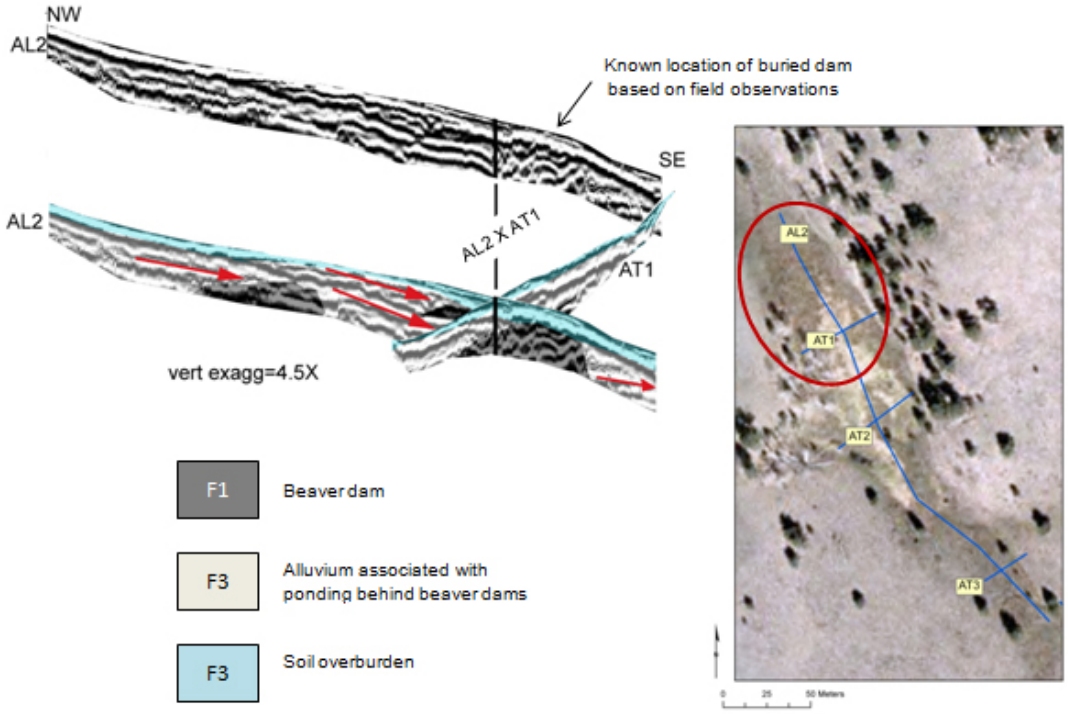

Figure 3.5: Identification of beaver dams in the GPR profiles. The type radar sub package, P2a, of genetically related strata associated with a beaver dam (radar sub package P2a), is recognized in NBM. Only the alluvium radar reflectors are shown. Below the alluvium is bedrock. The top image is the uninterpreted AL2 profile without the AT1 cross-section. The bottom is the interpreted image with the AT cross-section. The air wave and direct ground wave are not shown.

3.2 Testing the Hypotheses

Recall the first research hypothesis:

- $H1_o$: Alluvium does not constitute a substantial portion of valley fill (<25%).
- $H1_a$: Alluvium constitutes a substantial portion of valley fill (>25%).

To test $H1_o$, I calculated the fraction of alluvium in the valley fill. Once the bedrock/valley fill contact (C1) and glacial/alluvium contact (C2) were identified, depths from ground surface to C1 and C2 were noted approximately every 10 m along each transect. These points, as well as additional points from field observations, auger data and previous studies, were interpretatively contoured (Groshong, 2006; Tearpock and Bischke, 1991) to create isopach maps of valley fill and alluvium for the entire meadow. Two-way travel times to C1 and C2 taken from the GPR profiles were converted to depths using radar velocities estimated from the radar velocity contour map (section 2.7). An average velocity was not used to universally convert to depth estimates since radar velocity was significantly different across the valley (section 2.3.1). Volumes of valley fill (V_f) and alluvium (V_a) were estimated (Table 3.4) by the summation of the volumes between each iso-line. Volumes between iso-lines were estimated by multiplying the area by its mean thickness. Error associated with volume estimates for valley fill and alluvium were estimated by adjusting the mean thicknesses using the $\pm$ 0.5 m vertical error associated with the GPR contacts and the $\pm$ 1 m vertical error associated with the SSR contacts (section 3.1.2). For each study area, fraction of alluvium was calculated from the ratio of alluvium to valley fill, and mean thicknesses for the valley fill and alluvium were calculated by dividing the volumes for each by their surface areas (Table 3.4).

Most of the valley fill in Beaver Meadows is glacial in orgin with a thin (<2 m) alluvium drape. $H1_o$ was not rejected in the main meadows (EBM and WBM) because the alluvium is only ~15% of the valley fill. In NBM, $H1_0$ was rejected. This is unsurprising because NBM was never glaciated, directly implying that alluvium is 100% of the valley fill. Surprisingly, the thickness of alluvium in NBM (1.3 m), which has a much smaller drainage area and thus lower stream power, was comparable to the main meadow (1.5 m).

Figure 3.6 shows schematic cross-sections for WBM, EBM and NBM and Figure 3.7 compares the isopach of valley fill to the isopach of alluvium. In the main meadow the depth to bedrock is asymmetrical, deepening toward the south end of the valley. As summarized in Table 3.4, maximum

depth is 18-21 m at the southernmost end directly under the till. Minimum depth is 0 m adjacent to the northern slopes, which are composed of bedrock. Mean depth to bedrock in the main meadows is ~12 m. In EBM, boulders from a glacial lag protruded onto the surface and net alluvium aggradation was only ~0.7 m. In WBM, the thickest alluvium (~4-6 m) was located near natural deposition zones where Beaver Brook and the northern tributary enter the main meadows and along the margin of maximum glacial extent.

Now recall the second hypothesis:

- $H2_o$: Beaver-induced sedimentation does not constitute a substantial portion of alluvium (<25%).
- $H2_a$: Beaver-induced sedimentation constitutes a substantial portion of alluvium (>25%).

To test $H2_o$, I estimated the fraction of sedimentation due to beaver ponding in the alluvium from a ratio of areas along each GPR profile (Table 3.4). Ratios were calculated only within the study area bounds. It is important to recognize that the ratio of areas calculated along each GPR does not necessarily represent the average ratio across the entire meadow, but only along the transects surveyed; therefore, they are subject to uncertainties associated with the spatial distribution of the GPR profiles and the identification of subsurface beaver-related deposition. To obtain a rough estimate of volume of beaver-induced sedimentation within the alluvium, I raised the ratios of areas to the exponent 1.5. The main assumption behind this calculation is that the beaver-induced sedimentation is uniformly distributed. Although I recognize that this is probably not the case, this type of calculation is still valid for a first approximation, especially given the uncertainty associated with calculation of the ratio of areas, as mentioned previously.

Listed first as percent area along GPR lines and second as percent volume over the entire area, my first-order approximations for the percent of beaver-induced sedimentation in the alluvium are: ~43/28% for WBM, ~53/38% for NBM and ~74/64% for EBM. I have not provided error estimates since there are degrees of uncertainty that are not directly measurable, associated with the subjective interpretation of beaver-related deposits within the GPR and the placement of GPR profiles. Even with this uncertainty, these estimates are good first-order approximations, which are consistent with the 30-50% estimates of beaver-related sedimentation found in cores throughout Beaver Meadows (Polvi, in prep). These percentages lead to a rejection of $H2_o$, implying that beaver-induced sedimentation constitutes a substantial portion of the alluvium throughout the enitire meadow.

Beaver dams and areas of beaver-induced sedimentation are identified along each GPR profile in Appendix B. What is interesting is that the number of dams per cross-sectional area of alluvium is very similar for all the study area, on the order of 5×10^{-3} m^{-2} $\pm 3 \times 10^{-4}$ m^{-2}. Although the maximum thickness of alluvium was ~6 m, the maximum thickness associated with beaver-induced sedimentation was generally less than 3 m. There was evidence for valley bottom expansion in the GPR from ponded sediment. As indicated by an onlapping progradational sequence, Figure 3.8 shows stacked deposition of pond sediments widening the valley margin at the start of longitudinal profile BL1.

Figure 3.9 displays the spatial distribution of beaver dams identified in the GPR with beaver dams identified from an analysis of historical aerial photographs (1938-2001) by Polvi (in prep). The analyses of historical aerial photographs were done independently of the GPR analysis, and as Figure 3.9 shows, there was very good aggreement between the two with a possible bias towards under-identification of buried dams. This suggests that I may be underestimating the percent beaver-induced sedimentation (Table 3.4). The areas in which dams were missed were areas of a high density of dams because it was hard distinguish the GPR stratigraphy of single dams. In the GPR signal, areas of high dam density create a larger area of chaotic reflectors, thus resulting in loss of the abrupt truncation of upvalley flatlying reflectors, which were used as a main identification tool.

In addition to testing the hypotheses, I mapped the furthest glacial extent in the subsurface (Figure 3.10). The furthest subsurface glacial extent matched well with the small anomalous pre-Bull Lake deposit near the boundary between WBM and EBM. Based on my subsurface glacial extent, I also mapped a second anomalous bouldery deposit near the west end of WBM as pre-Bull Lake. Previously this deposit was not mapped as till as it is outside the natural topographic expression of the Bull Lake deposits.

.

Table 3.4: Summary of results. The main meadows is EBM and WBM while the entire valley is EBM, WBM and NBM.

	EBM	WBM	NBM	Main Meadows	Entire Valley
Volume Fill ($x10^5 m^3$)	21 ± 4	31 ± 7	1.1 ± 0.5	52 ± 5	53 ± 5
Volume Alluvium ($x10^5 m^3$)	1 ± 0.7	6 ± 2	1.1 ± 0.5	7 ± 2	8 ± 2
Mean Thickness Valley Fill (m)	16	10	1.3	12	10
Mean Thickness Alluvium (m)	0.7	1.8	1.3	1.5	1.3
Max Thickness Alluvium (m)	2.5	6.0	3.5	6.0	6.0
% Alluvium in Valley Fill	5	19	100	13	15
% Beaver Deposits in Alluvium-A[1]	74	43	53	46	49
% Beaver Deposits in Alluvium-V[2]	64	28	38	32	35
Number of Dams	6	28	16	34	50
Dams/Area Alluvium ($no./m^2$)	$4.8E^{-3}$	$4.9E^{-3}$	$5.3E^{-3}$	$4.9E^{-3}$	$4.5E^{-3}$

1. percent calculated from fractional area along each GPR profile. $100 \times (A/A)$
2. percent calculated by $100 \times (A/A)^{3/2}$, which estimates percent as a fractional volume, assuming uniformly distributed beaver-related deposition.

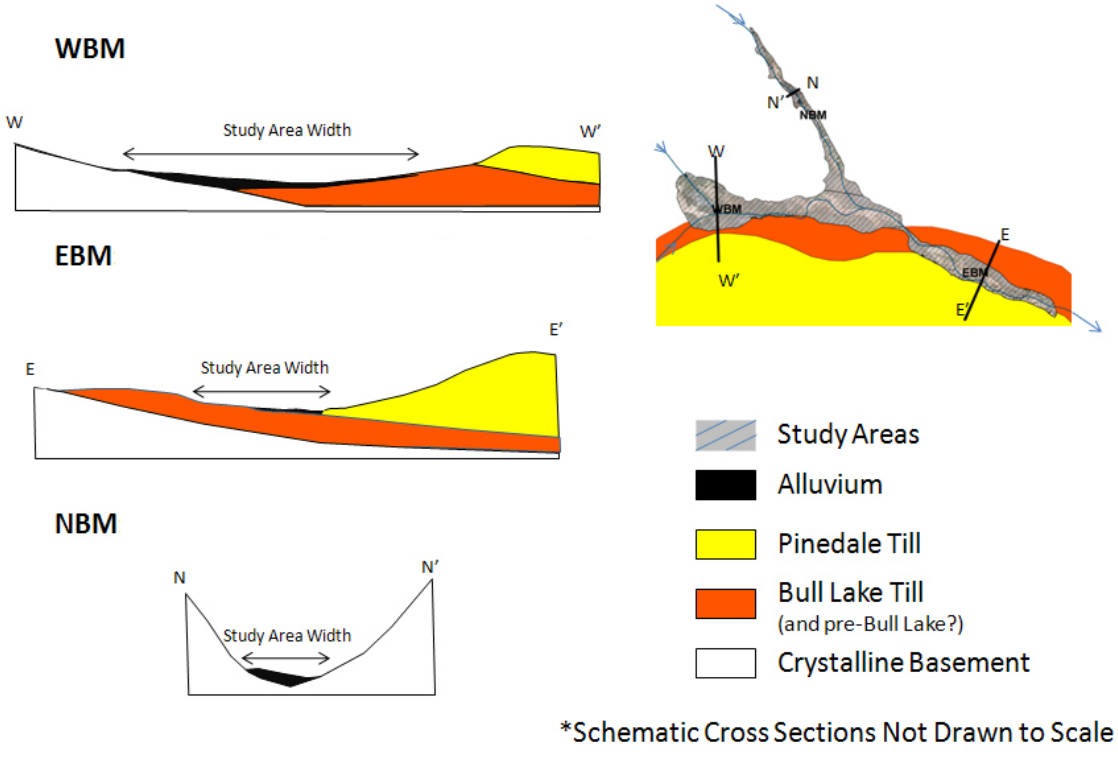

Figure 3.6: Schematic cross sections for EBM, WBM and NBM.

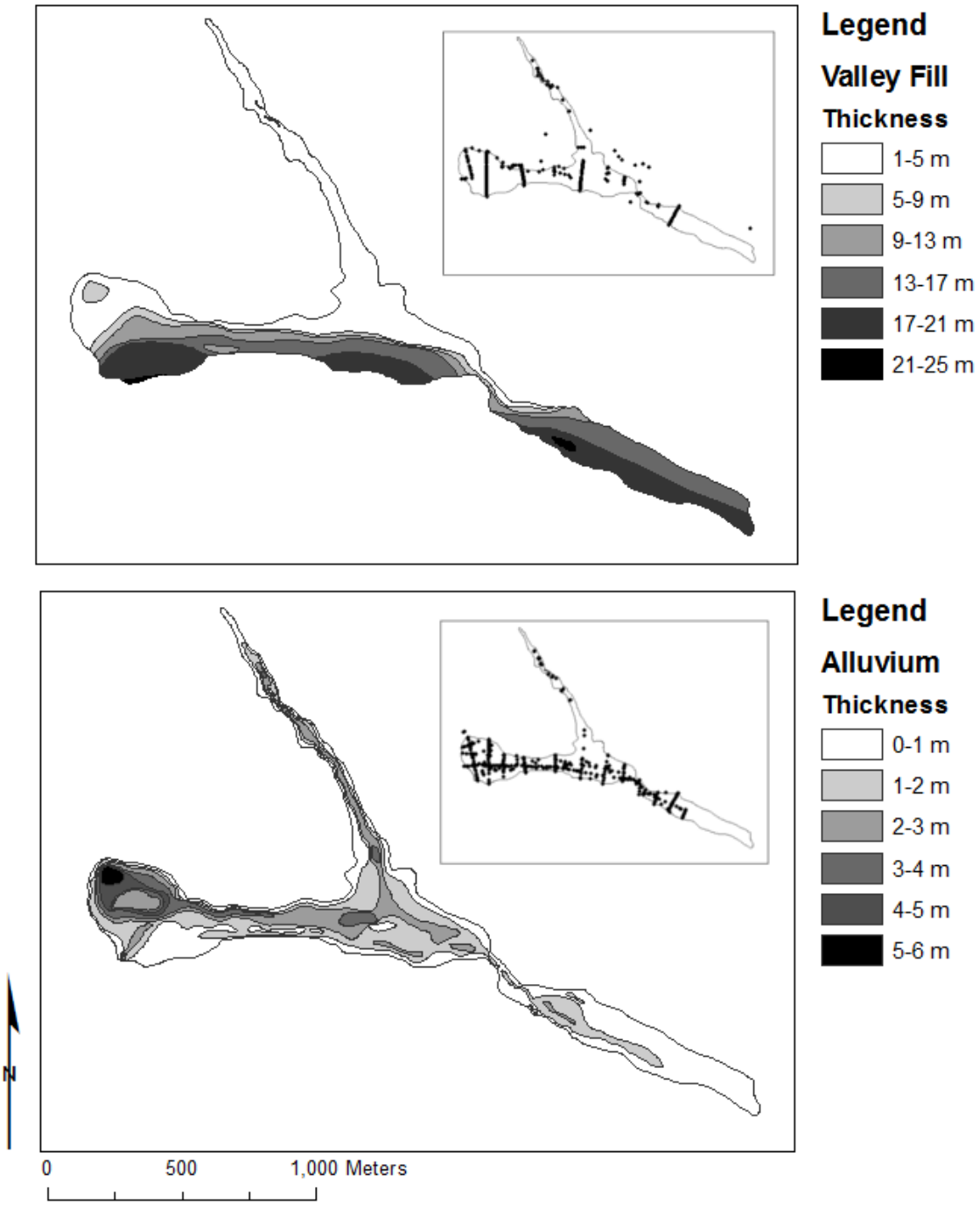

Figure 3.7: Isopach maps of valley fill and alluvium. The inset maps show spatial distribution of contoured points. Note that the contour interval differs between the two maps.

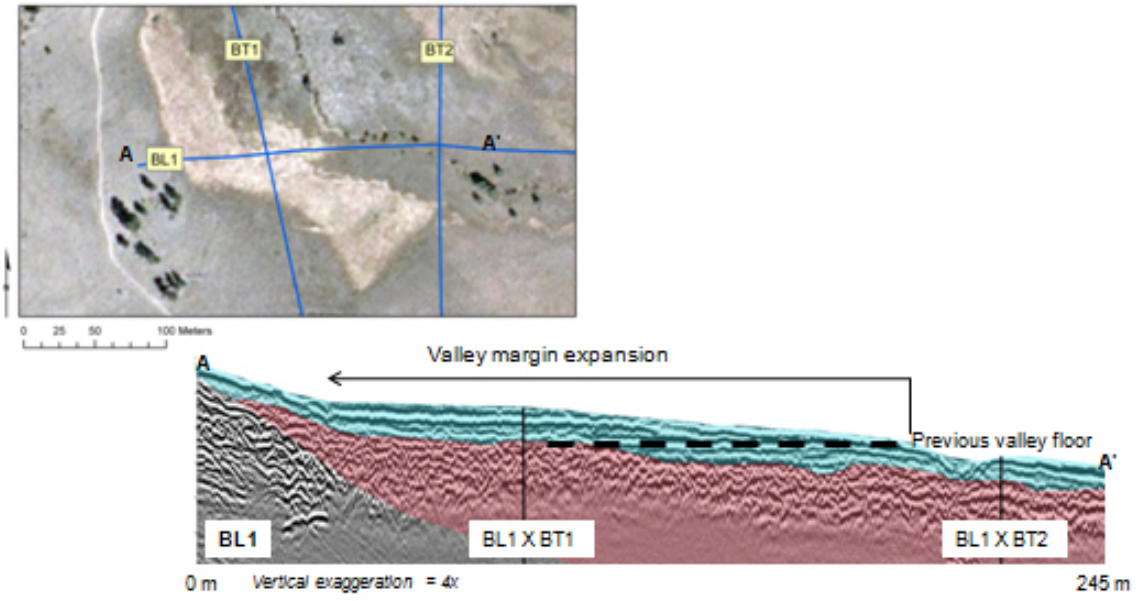

Figure 3.8: Evidence for meadow margin expansion by beaver.

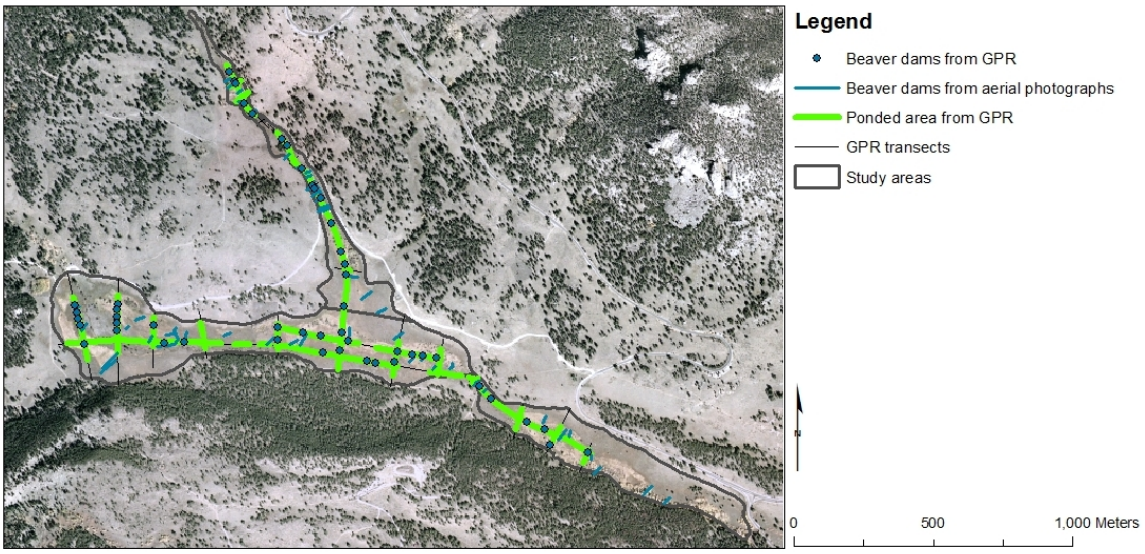

Figure 3.9: Spatial distribution of buried beaver dams and ponding. Buried beaver dams are pictured in relation to recognized dams on aerial photographs. Compilation of dams located on aerial photographs by Polvi (in prep) for 1938, 1947, 1964, 1969, 1987 and 2001. No active dams were noted post 1947. Aerial photograph in background is 2001. The analyses of historical aerial photographs was done independently of the GPR analysis.

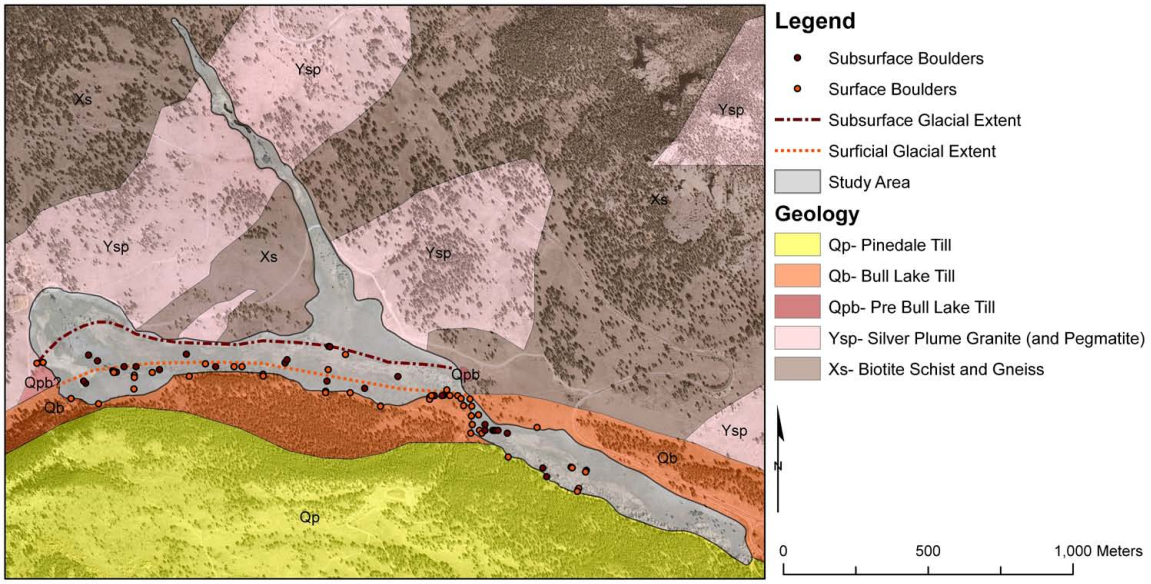

Figure 3.10: Maximum subsurface glacial extent.

4 DISCUSSION

In Beaver Meadows, beaver-induced sedimentation is unquestionably an important process for aggradation during the Holocene. Beaver-induced sedimentation constituted a substantial portion of the cross section of alluvium in all of the study areas (>40%). The proportion of beaver-induced sedimentation was higher in EBM, which may be due to the spatial arrangement of GPR survey transects. However, this higher proportion of beaver-induced sedimentation could reflect reality since there may be lesser amounts of fluvial and colluvial related aggradation in this location. The hillslopes are less steep and most bedload transported in the steeper gradient of the upper catchments would have been deposited in WBM and NBM.

Even though beavers were important agents contributing to aggradation, the question remains whether they contributed a magnitude of aggradation capable of altering the physiographic appearance of valley bottoms, as suggested by Ives (1942) and Ruedemann and Schoonmaker (1938). This study has found that, they did and did not, depending on scale. In the main meadows (WBM and EBM), the broad valley floor (width $\approx$ 200 m) was set by deposition of glacial deposits and it is unlikely that subsequent Holocene alluviation greatly altered its form. The alluvium did not constitute a substantial portion of the valley fill ($\sim$15%) and had a net aggradation of only $\sim$1.3 m, with the thickest deposition ($\sim$2.5-6 m) occurring in pockets of natural deposition zones. In addition, the ratio of alluvium thickness over valley bottom width is only on the order of 1×10^{-3}. Although I noted evidence for some meadow valley margin expansion by beavers during the Holocene (Figure 3.8), it appeared only to enhance a pre-existing template set by glacial deposits.

Contrary to the main meadows, in NBM there is evidence that Holocene alluviation created a broader and flatter valley bottom (width $\approx$ 50 m). NBM was never glaciated, alluvium constitutes 100% of the valley fill and C^{14} dating suggests all of the alluvium is of Holocene age (Polvi, in prep). However, just because the alluvium comprised 100% of the valley fill (accept H1), I did not automatically assume that alluviation significantly widened the valley bottom since a thin thickness compared to valley bottom width would imply an insufficient amount of sediment to alter form. The ratio of alluvium thickness over valley bottom width in NBM is $\sim 1 \times 10^{-2}$, which is one order of magnitude larger than in the main meadows. In addition, the alluvium was not just a drape over

bedrock, but a wedge, which infilled and broadened the valley bottom, giving it a u-shaped profile in a valley which would otherwise be v-shaped. These two observations led me to conclude that a thin cover of alluvium was great enough to alter the physiographic appearance in NBM (drainage area <1 km^2) but was insufficient in the main meadows.

It is notable that the mean thickness and the number of dams per cross-sectinal area in NBM are comparable to the main meadows (Table 3.4) even though the basin area is 76% smaller and the stream gradient is 150% greater. Similar aggradation thicknesses for such different drainage basin sizes and stream gradients suggests that aggradation was not only due to fluvial processes. The rejection of $H2_o$ for the entire study area demonstrates the importance of beavers in causing sediment aggradation, and the consistency in alluvial thicknesses strongly supports this conclusion. Although maximum thickness of alluvium was ~6 m, beaver-related deposition was generally <3 m. This value is remarkably consistent with work done in Yellowstone, where Persico and Meyer (2009) found that beaver-related sedimentation was generally <2 m. The consistency in thickness of beaver-related aggradation between Yellowstone and this study suggests that the thickness of Holocene beaver-related aggradation may be similar throughout the mountainous regions of the western United States and perhaps in mountainous regions elsewhere. The relative importance of these deposits then depends on total sediment thickness and valley geometry.

What is most surprising about these results is that the alluvial deposition post glacial retreat, ~14000 BP, averages only 1.3 m across all study areas. This thin veneer of sedimentation raises questions pertaining to sediment supply and removal dynamics in the valley. Is sediment accumulation thin because supply is minimal, or is sediment being stored and removed episodically so that over time it does not accumulate great thicknesses? I think that it is a combination of the two.

Sediment supply is minimal in Beaver Meadows. Most of the fine grained sediments in the Front Range are non-native and are blown in from the semiarid North Park and Middle Park basins on the west side of the continental divide (Muhs and Benedict, 2006). The GPR data support a non-native source for fine silts and clay sized particles. GPR surveys in the meadow had good penetration (~7 m), indicating an absence of clay minerals, which, when present, rapidly attenuate radar signals due to absorption of energy. If the clays were locally derived from the weathering of feldspars within the bedrock, the radar waves would have been attenuated so rapidly as to render GPR surveying useless. Furthermore, there is a noticeable lack of suspended sediment in Beaver Brook, which supports conclusions by Caine (1986) that sediment delivery of fine grained material to the stream

channels from the hillslopes is minimal. There is also a lack of evidence of hillslope failures on the surface and minimal evidence of colluvial input in the subsurface. Thus, the delivery of exotic fines to sediment accumulation sites is slowed by long residence times on hillslopes.

In a setting where most of the fine sediment supply may be eolian and the hillslopes are decoupled from valley bottoms, the efficiency of beavers at trapping sediment and likewise the absence of beaver may have a great impact on rates of sedimentation throughout the Holocene. Persico and Meyer (2009) have shown that there are consistent episodes of beaver-related aggradation marked by periods of no aggradation relating to fluctuations in climate and predator-prey relationships. In the absence of beaver, previous sites of aggradation become sites of incision and sediment removal. Considering this, it may not be a coincidence that the mean thickness of alluvium, ~1.3 m, is approximately the same height as a beaver dam, which is generally <2 m (Gurnell, 1998; Bigler et al., 2001; Westbrook et al., 2006; Persico and Meyer, 2009; Butler and Malanson, 1995). I suggest that these low gradient valleys are not sites of continued sediment deposition through the Holocene, but that a thickness of alluvium approximately equal to the height of a beaver dam is maintained by beavers. When dams are present, sediment aggrades up to the height of the dam, and when they are absent, the sediment is exhumed and re-distributed down valley. I did find examples in the GPR profiles of stacked sequences of beaver pond sediments, but there were never more than three and they never reached thicknesses >3 m.

As in Yellowstone (Persico and Meyer, 2009), there is no evidence in Beaver Meadows of continual stacking of sediments throughout the Holocene, as Ives (1942) and Ruedemann and Schoonmaker (1938) suggest. If there was continued stacking, I would expect beaver-induced sedimentation to be much greater than the height of a single dam. I also maintain that there is evidence that beavers maintain a beaver meadow as described by Westbrook et al. (2010) by creating spatially heterogeneous patches of sediment which overlap with other patches in time and space. Westbrook's assertion: "...the cycle of beaver colonization and abandonment of dams over time would... vertically layer [sediment] patches on top of one another throughout the floodplain", is only true up to a point. Beavers do cause sedimentation and expand the valley margin, but only to the height of one to two or at most three beaver dams.

There is evidence that when beavers are present in Beaver Meadows they create a multi-thread channel network, and when they are absent, the system naturally resorts to a straight single thread channel (Polvi, in prep). In the hypothetical situation in which beavers never occupied this site, I

hypothesize that sediment storage of fines would be very minimal and confined near the channel. So, although I concluded that beavers did not cause sediment to aggrade to such a degree as to significantly alter valley bottom form, the aggradation of sediment that they did achieve significantly altered the sediment-vegetation dynamics of the meadow by depositing and episodically replenishing fertile substrate for new plant growth much further from the channel than would otherwise likely occur.

5 CONCLUSION

5.1 On Beaver-induced Sedimentation ...

This thesis investigated the relative magnitude and extent of beaver-induced sedimentation throughout the Holocene in Beaver Meadows with the main hypotheses (H1 and H2) being:

- $H1_o$: Alluvium does not constitute a substantial portion of valley fill (<25%).
- $H1_a$: Alluvium constitutes a substantial portion of valley fill (>25%).

and

- $H2_o$: Beaver-induced sedimentation does not constitute a substantial portion of alluvium (<25%).
- $H2_a$: Beaver-induced sedimentation constitutes a substantial portion of alluvium (>25%).

In the main meadows (EBM and WBM), $H1_o$ was not rejected and $H2_o$ was rejected. Although beaver-related sediments make up at least ~32% of the volume of alluvium in the main meadow (46% of the cross-sectional area along GPR lines), the alluvium comprises only ~13% of the valley fill with a mean thickness of 1.5 m. For the northern tributary (NBM), both $H1_o$ and $H2_o$ were accepted. In NBM, beaver sediments make up ~38% of the volume of alluvium, which is 100% of the valley fill. However, the thickness of alluvium was small, 1.3 m.

Thus I conclude that:

- **Beaver damming is an important aggradational process trapping sediments within the Holocene, but did not cause significant amounts of aggradation.**

The thin veneer of Holocene sedimentation (~1.3 m) implies that Beaver Meadows is not a site of continuous sediment deposition, but rather one characterized by episodic temporal and spatial aggradation, punctuated by incision. Furthermore, I suggest that a thickness of alluvium approximately equal to the height of a beaver dam (<2 m) is maintained by the fluctuation between the

presence and absence of beavers both spatially and temporally. When dams are present, sediment aggrades up to the height of the dam, and when they are absent, the sediment is exhumed and re-distributed down valley.

The consistency in thickness of beaver-related aggradation between Yellowstone (Persico and Meyer, 2009) and this study suggests that the thickness of Holocene beaver-related aggradation may be consistent throughout the mountainous regions of the western United States and perhaps in mountainous regions elsewhere. This claim should be investigated further. If the thickness of beaver-related aggradation is consistent in many places, it could be used to quickly estimate volumes of beaver-related sedimentation regionally. In addition, the relative importance of beaver aggradation compared to total sediment thickness and valley geometry should be investigated more thoroughly.

More data regarding the input of sediment is needed in order to more fully understand sedimentation dynamics relating to the presence of beaver dams throughout the Holocene. There remain significant gaps in background data (not related to disturbances such as fire) concerning the modern rates and quantity of sediment delivery to basins in the Colorado Front Range. Some interesting questions to ask, are: What is the background rate of hillslope creep? How well are the hillslopes connected to the valley bottoms and stream channels? How much fine sediment is brought in via streams, hillslopes, and the atmosphere? Is sediment delivery episodic throughout the Holocene? And, how might periods of increased sediment supply (perhaps associated with periods of drought and thus an increase in windblown fines) relate to periods of beaver presence and absence?

5.2 On Ground Penetrating Radar ...

I conclude that:

- **GPR is a non-invasive, inexpensive and effective technique for (1) differentiating between subsurface strata of glacial and non-glacial origin and (2) identifying beaver dams and associated sedimentation, both modern and buried (as long as deposition of fines behind beaver dams include clay particles rather than clay minerals).**

Furthermore, I suggest that the type radar stratigraphy developed in this thesis provides a useful guideline for future GPR studies in similar valleys throughout the Rockies. A short summary of the three type radar packages identified in section 3.1.2 follows:

- The radar package relating to **glacial** deposition was wedge-shaped and predominantly composed of a diffraction-rich, chaotic facie.

- The radar package relating to **alluvium** was draped over the glacial deposits and was characterized by multiple facies, but in general contained complex, slightly continuous reflectors interfingered with continuous, horizontal to subhorizontal reflectors.

- The radar package related to **beaver-related** sedimentation was characterized by a laterally continuous parallel facie, interpreted to be ponded sediment, that abruptly truncated into a zone of chaotic reflectors, interpreted to be a beaver dam.

In addition to testing the hypotheses, I used the radar stratigraphy described above to map the maximum extent of subsurface glacial deposits, which extend (mostly) the width of the main valley floor (Figure 3.10). Subsurface extent, thickness, and anomalous surficial deposits suggest that a pre-Bull Lake till underlies the valley. Although not fully explored within the scope of this thesis, there is potential for further glacial subsurface interpretation and mapping using GPR.

REFERENCES

Anderson, R., Riihimaki, C., Safran, E., MacGregor, K., 2006. Facing Reality: Late Cenozoic evolution of smooth peaks, glacially ornamented valleys, and deep river gorges of Colorado's Front Range. In: Willet, S., Hovius, N., Brandon, M., Fisher, D. (Eds.), Tectonics, climate, and landscape evolution. Geological Society of America Special Paper 398, pp. 397–418.

Andrews, J., Birkeland, P., Harbor, J., Dellamonte, N., Litaor, M., Kihl, R., 1985. Holocene sediment record, Blue Lake, Colorado Front Range. Zeitschrift fur Gletscherkunde and Glazialeologie 21, 25–34.

Annan, A., 1999. Practical processing of GPR data. In: Proceedings of the Second Government Workshop on Ground Penetrating Radar. Sensors and Software, Inc.

Baker, G., Jordan, T., Pardy, J., 2007. An introduction to ground penetrating radar (GPR). In: Baker, G., Jol, H. (Eds.), Proceedings of the Second Government Workshop on Ground Penetrating Radar. Geological Society of America Special Paper 432, pp. 1–18.

Barton, N., 2007. Rock Quality, Seismic Velocity, Attenuation and Anisotropy. Taylor and Francis Goup.

Benedict, J. B., 1979. Fossil ice-wedge polygons in the Colorado Front Range: Origin and significance. Geological Society of America Bulletin, Part I 90, 173–180.

Benedict, J. B., 1999. Effects of changing climate on game-animal and human use of the Colorado high country (U.S.A) since 1000 BC. Arctic, Antarctic and Alpine Research 31 (1), 1–15.

Benedict, J. B., J., B. R., Lee, C. M., Staley, D. M., 2008. Spruce trees from a melting ice patch: evidence for Holocene climate change in the Colorado Rocky Mountaints, USA. The Holocene 18 (7), 1067–1076.

Beres, M., Huggenberger, P., Green, A., Horstmeyer, H., 1999. Using two- and three-dimensional georadar methods to characterize glaciofluvial architecture. Sedimentary Geology 129, 1–24.

Bersezio, R., Giudici, M., Mele, M., 2007. Combining sedimentological and geophysical data for high-resolution 3-D mapping of fluvial architectural elements in the Quaternary Po plain (Italy). Sedimentary Geology 202, 230–248.

Bigler, W., Butler, D. R., Dixon, R. W., 2001. Beaver-pond sequence morphology and sedimentation in northwestern Montana. Physical Geography 22 (6), 531–540.

Braddock, W. A., Cole, J. C., 1990. Geologic map of Rocky Mountain National Park and vicinity, Colorado. U.S. Geological Survey, miscellaneous investigations series I-1973, 1:50,000 scale map.

Buchholtz, C., 1983. Rocky Mountain National Park: A history. Colorado Associated University Press.

Butler, D. R., Malanson, G. P., 1995. Sedimentation rates and patterns in beaver ponds in a mountain environment. Geomorphology 13 (1-4), 255–269.

Caine, T., 1986. Sediment movement and storage on alpine slopes in the Colorado Rocky Mountains. In: Abrahams, A. (Ed.), Hillslope Processes. Allen and Unwin, pp. 115–137.

Cooper, D. J., Dickens, J., Hobbs, N. T., Christensen, L., Landrum, L., 2006. Hydrologic, geomorphic and climatic processes controlling willow establishment in a montane ecosystem. Hydrological Processes 20, 1845–1864.

Dethier, D., Birkeland, P., Shroba, R., 2003. Quaternary stratigraphy, geomorphology, soils and alpine archaelogy in an alpine-to-plains transect, Colorado Front Range. In: Eeasterbrook, D. (Ed.), Quaternary Geology of the United States, INQUA 2003 Field Guide Volume. Desert Research Institute, Reno, NV, pp. 81–104.

Dillon, G. K., Knight, D. H., Meyer, C. B., 2005. Historic range of variability for upland vegetation in the Medicine Bow National Forest, Wyoming. General technical report rmrs-gtr-139, US Department of Agriculture, US Forest Service, Rocky Mountain Research Station, Fort Collins.

Elias, S., Short, S., Clark, P., 1986. Paleoenvironmental interpretations of the late Holocene, Rocky Mountain National Park, Colorado. Revue de Paleobiologie 5, 127–142.

Fall, P., 1985. Holocene dynamics of the subalpine forest in central Colorado. In: Jacobs, B. F., L., F. P., K., D. O. (Eds.), Late Quaternary vegetation and climates of the American Southwest. American Association of Stratigraphic Palynolologists Foundation, pp. 31–46.

Fall, P., 1997. Timberline fluctuations and late Quaternary paleoclimates in the Southern Rocky Mountains, Colorado. Bulletin of the Geological Society of America 109, 1306–1320.

Graf, D. D., 1997. Effects of water diversion in Upper Beaver Meadow Rocky Mountain National Park. Ms thesis, Colorado State University, Fort Collins, CO.

Groshong, R., 2006. 3-D structural geology a practical guide for surface and subsurfaces map interpretation, 2nd Edition. Springer.

Gurnell, A. M., 1998. The hydrogeomorphological effects of beaver dam-building activity. Progress in Physical Geography 22 (2), 167–189.

Harbor, J., 1984. Terrestrial and lacustrine evidence for Holocene climatic/geomorphic change in the Blue Lake and Green Lakes valeys of the Colorado Front Range. Ms thesis, University of Colorado, Boulder, CO.

Hay, K., 1955. Development of a beaver census method applicable to mountain terrain in Colorado. Ms thesis, Colorado A and M College, now Colorado State University, Fort Collins, CO.

Hess, K. J., 1993. Rocky times in Rocky Mountain National Park: An unnatural history. University Press of Colorado.

Ives, R. L., 1942. The beaver-meadow complex. Geomorphology 5 (3), 191–203.

Jarrett, R., 1990. Hydrologic and hydraulic research in mountain rivers. Water Resources Bulletin 26, 419–429.

Jol, H., 1995. Ground-penetrating radar antennae frequencies and transmitter powers compared for depth, resolution and reflection continuity. Geophysical Prospecting 43 (5), 693–709.

Jol, H., 2009. Ground penetrating radar theory and applications. Elsevier, ISBN 978-0-444-53348-7.

Kostic, B., Aigner, T., 2007. Sedimentary architecture and 3D ground-penetrating radar analysis of gravelly meandering river deposits: Neckar Valley, SW Germany. Sedimentology 54 (4), 789–808.

Lee, W., 1917. The geologic story of the Rocky Mountain National Park, Colorado. USGS.

Lennox, D. H., 1967. Geophysical exploration for buried valleys in an area north of Two Hills, Alberta. Geophysics 32 (2), 331 – 362.

Leopold, M., 2008. Using geophysical methods to study the shallow subsurface of a sensitive alpine environment, Niwot Ridge, Colorado Front Range, U.S.A. Arctic, Antarctic, and Alpine Research 40 (3), 519 – 530.

Locke, W., 1987. Low-energy seismic survey of Quaternary materials, Rocky Mountain National Park, Colorado. The Mountain Geologist 24 (2), 45–49.

Madole, R. F., 1980. Time of Pinedale de-glaciation in north-central Colorado: further considerations. Geology 8 (3), 118–122.

Madole, R. F., Honke, J. S., Langdon, P., 2010. Evidence from the Front Range, Colorado, indicates that Pinedale glaciation began prior to 31,000 yr ago. In: Abstracts and Programs. Geological Society of America.

Madole, R. F., VanSistine, D. P., Michael, J. A., 1998. Pleistocene glaciation in the upper Platte River drainage basin, Colorado. U.S. Geological Survey, 99-0017-S, 1:50,000 scale map and text.

Mann, M., Zhang, Z., Rutherford, S., Bradley, R., Hughes, M., Shindell, D., Ammann, C., Faluvegi, G., 2009. Global signatures and dynamical origins of the Little Ice Age and Medieval Climate Anomaly. Science 326 (5957), 1256–1260.

McKinstry, M. C., Caffrey, P., Anderson, S. H., 2001. The importance of beaver to wetland habitats and waterfowl in Wyoming. Journal of teh American Water Resources Association 37 (6), 1571–1577.

McMillan, M. E., 1984. Soil development on a Pinedale moraine and erosion ten years after a burn, Rocky Mountain National Park, Colorado. Ms thesis, University of Colorado, Boulder, CO.

Millar, C. I., Woolfenden, W. B., 1999. The role of climate change in interpreting historical variability. Ecological Applications 9, 1207–1216.

Mills, E., 1905. The Story of Estes Park. Longs Peak, Estes Park, CO.

Mills, E., 1913. In beaver world. Houghton Mifflin Company, the Riverside Press.

Mitchell, D., Tjornehoj, J., Baker, B., 1999. Beaver populations and possible limiting factors in Rocky Mountain National Park, 1999. Tech. rep., U.S. Geological Survey, midcontinent Ecological Science Center.

Mitchell, S. C., Cunjak, R. A., 2007. Stream flow, salmon and beaver dams: roles in the structuring of stream fish communities within an anadromous salmon dominated system. Journal of Animal Ecology 76, 1062–1074.

Muhs, D. R., Benedict, J. B., 2006. Eolian additions to late Quaternary alpine soils, Indian Peaks Wilderness Area, Colorado Front Range. Arctic, Antarctic and Alpine Research 38 (1), 120–130.

Naiman, R. J., Johnston, C. A., Kelley, J. C., 1988. Alteration of North-American streams by beaver. Bioscience 38 (11), 753–762, 32.

National Park Service, 1939. Hondius-Beaver pipeline testimony. District Court, case no. 10077 June 23.

Neal, A., 2004. Ground-penetrating radar and its use in sedimentology: principles, problems and progress. Earth-Science Reviews 66 (3-4), 261–330.

Nilsson, C., 2002. Basic principles and ecological consequences of changing water regimes: Riparian plant communities. Environmental Management 30 (4), 468–480.

Olson, R., Hubert, W. A., 1994. Beaver: Water resources and riparian habitat engineer. University of Wyoming, Laramie, WY.

Packard, F., 1947. A survey of the beaver population of Rocky Mountain National Park, Colorado. Journal of Mammalogy 28 (3), 219–227.

Peirson, M. E., 1991. Cross section models of buried valleys, Wallenpaupack drainage basin, northeastern Pennsylvania. Master's thesis, Bowling Green State University, Bowling Green, OH.

Persico, L., Meyer, G., 2009. Holocene beaver damming, fluvial geomorphology, and climate in Yellowstone National Park, Wyoming. Quaternary Research 71, 340–353.

Polvi, L., in prep. Post-glacial floodplain dynamics in the Colorado Front Range. Phd dissertation, Colorado State University, Fort Collins, CO, expected completion: Summer 2011.

Press, F., 1966. Seismic velocities. In: Handbook of physical constants. Geological Society of America Memoir 97, pp. 195–218.

Rainey, E., 1987. Sedimentary record of Pinedale ice recession in Horseshoe Park, Rocky Mountain National Park, Colorado. Phd dissertation, University of Northern Colorado, Greeley, CO.

Rensch, H., 1935. Historical background for the Rocky Mountain National Park. U.S. Dept of the Interior National Park Service Field Division of Education, Berkeley, CA.

Reynolds, J., 1997. An Introduction to applied and environmental geophysics. John Wiley and Sons, Ltd., West Sussex, England.

Richmond, G. M., 1960. Glaciation of the east slope of Rocky Mountain National Park, Colorado. Bulletin of the Geological Society of America 71, 1371–1382.

Richmond, G. M., 1986. Stratigraphy and correlation of glacial deposits of the Rocky Mountains, the Colorado Plateau and the ranges of the Great Basin. Quaternary Science Reviews 5, 99–127.

Rosell, F., Bozser, O., Collen, P., Parker, H., 2005. Ecological impact of beavers *Castor fiber* and *Castor canadensis* and their ability to modify ecosystems. Mammal Review 35 (3-4), 248–276.

Rubin, Z., 2010. Channel response as a context for restoration, upper Colorado river, Rocky Mountain National Park. Ms thesis, Colorado State University, Fort Collins, CO.

Ruedemann, R., Schoonmaker, W., 1938. Beavers as geologic agents. Science 88 (2292), 523–525.

Rutherford, W. H., 1964. The beaver in Colorado: Its biology, ecology, management and economics. Colorado Game, Fish and Parks Department, game research division, technical publication 17.

Salas, D., Stevens, J., Schulz, K., 2005. Rocky Mountain National Park, Colorado: USGS-NPS vegetation mapping program. Technical Memorandum 8260-05-02, U.S. Bureau of Reclamation, prepared for U.S. National Park Service and U.S. Geological Survey.

Schrott, L., Sass, O., 2008. Application of field geophysics in geomorphology: Advances and limitations exemplified by case studies. Geomorphology 93 (1-2), 55–73.

Sensors and Software, 2003. EKKO View Enhanced and EKKO View Deluxe users guide. Tech. rep., Sensors and Software, Inc.

Short, S. K., 1985. Palynology of Holocene sediments, Colorado Front Range: vegetation and treeline changes in the subalpine forest. Aasp contribution series, Institute of Arctic and Alpine Research, Boulder Colorado, no. 16.

Stevens, D., Christianson, S., 1980. Beaver populations on east slope of Rocky Mountain National Park . Special report, National Park Service, Estes Park, call no. VF599.3232 STE.

Tearpock, D., Bischke, R., 1991. Applied subsurface geological mapping. Prentice Hall.

Tsimba, R., Hussein, J., Ndlovu, L. R., 1999. Relationships between depth of tillage and soil physical characteristics of sites farmed by smallholders in Mutoko and Chinyika in Zimbabwe. In: Kaumbutho, P. G., Simalenga, T. E. (Eds.), Conservation tillage with animal traction. Animal Traction Network for Eastern and Southern Africa, pp. 84–88.
URL http://www.atnesa.org

USGS, Sept 2010. StreamStats for Colorado: Interactive Map.
URL http://streamstats09.cr.usgs.gov

USGS-NPS, Oct 2010. Vegetation mapping program.
URL http://biology.usgs.gov/npsveg/romo/index.html

Vandenberghe, J., van Overmeeren, R., 1999. Ground penetrating radar images of selected fluvial deposits in the netherlands. Sedimentary Geology 128, 245–270.

Veblen, T. T., Donnegan, J. A., 2005. Historical range of variability for forest vegetation of the national forests of the Colorado Front Range. Final report, USDA Forest Service, Agreement No. 1102-0001-99-033 with University of Colorado, Boulder.

Welder, F. A., 1971. Ground-water reconnaissance study of selected sites in Rocky Mountain National Park and Shadow Mountain National Recreation Area. U.S. Dept. of the Interior, Geological Survey, Water Resources Division, Colorado District, Denver, CO, open-file report 71001.

Westbrook, C. J., 2005. Beaver as drivers of hydrogeomorphic and ecological processes in a mountain valley. Phd dissertation, Colorado State University, Fort Collins, CO.

Westbrook, C. J., Cooper, D. J., Baker, B. W., 2006. Beaver dams and overbank floods influence groundwater-surface water interactions of a Rocky Mountain riparian area. Water Resources Research 42 (6), 42.

Westbrook, C. J., Cooper, D. J., Baker, B. W., 2010. Beaver assisted river valley formation. Wiley InterScience.
URL www.interscience.wiley.com

Wohl, E. E., 2001. Virtual rivers: lessons from the mountain rivers of teh Colorado Front Range. Yale University Press, New Haven and London.

Woodhouse, C., Lukas, J., 2006. Multi-century tree-ring reconstructions of Colorado streamflow for water resource planning. Climate Change 78, 293–315.

A Supplemental Data

Substrate at deepest penetration of core or rebar probe, data from this study. bgs= meters below ground surface. Coordinates taken from handheld GPS unit with 3-4 m accuracy and are recorded in UTM NAD83 Zone 13N.

ID	type	bgs	substrate	interp	E	N	
C1	core	1.60	silt/clay	post-glacial	448343	4469146	GPS
C2	core	1.50	unpenetrable	glacial	448351	4469103	GPS
C3	core	1.20	gravels	post-glacial	448357	4469054	GPS
C4	core	1.60	clay	post-glacial	448437	4470060	GPS
C5	core	1.50	unpenetrable	glacial	448837	4469010	GPS
C6	core	1.55	unpenetrable	pre-glacial	449077	4469120	GPS
C7	core	1.50	unpenetrable	pre-glacial,glacial?	449188	4469021	GPS
C8	incised channel	1.40	clay	post-glacial	448883	4469115	GPS
R1	rebar	1.05	unpenetrable	pre-glacial	448483	4469970	GPS
R2	rebar	0.65	unpenetrable	pre-glacial	448488	4469950	GPS
R3	rebar	0.35	unpenetrable	pre-glacial	448501	4469940	GPS
R4	rebar	0.30	unpenetrable	pre-glacial	448523	4469900	GPS
R5	rebar	0.25	unpenetrable	pre-glacial	448557	4469890	GPS
R6	rebar	1.80	unpenetrable	pre-glacial	448582	4469850	GPS
R7	rebar	1.60	silt clay	post-glacial	448623	4469830	GPS
R8	rebar	1.20	clay	post-glacial	448678	4469730	GPS
R9	rebar	0.90	clay	post-glacial	448669	4469720	GPS
R10	rebar	0.70	unpenetrable	pre-glacial	448821	4469340	GPS
R11	rebar	0.65	unpenetrable	pre-glacial	448842	4469340	GPS
R12	rebar	1.70	unpenetrable	glacial	448843	4469130	GPS
R13	rebar	1.80	sand	post-glacial	449073	4469050	GPS
R14	rebar	1.40	sand	post-glacial	449038	4469051	GPS
R15	rebar	1.30	sand	post-glacial	448964	4469079	GPS
R16	rebar	0.90	unpenetrable	glacial	448901	4469102	GPS

Substrate at deepest penetration of core, data from Polvi (2011). bgs= meters below ground surface. Coordinates taken from handheld GPS unit with 3-4 m accuracy and are recorded in UTM NAD83 Zone 13N.

ID	type	bgs	substrate	interp	E	N	
BC-1	core	0.47	large clasts	glacial, pre-glacial?	448450	4469104	GPS
BC-2	core	1.04	unpenetrable	glacial	448452	4469060	GPS
BC-3	core	1.07	coarse gvl	pre-glacial	448487	4469134	GPS
BC-4	core	1.56	clay	post-glacial	447905	4469150	GPS
BC-5	core	2.66	clay	post-glacial	447910	4469173	GPS
BC-6	core	2.65	clay/silt	post-glacial	448058	4469162	GPS
BC-8	core	2.07	unpenetrable	glacial	448692	4469074	GPS
BC-8,R	rebar	1.99	unpenetrable	glacial	448692	4469073	GPS
BC-9	core	2.67	gravels?	post glacial?	448692	4469064	GPS
BC-10	core	2.66	gravels?	post glacial?	448716	4469085	GPS
BC-11	core	2.64	sands/gravels	post-glacial	447933	4469183	GPS
BC-12	core	1.90	unpenetrable	glacial	448097	4469046	GPS
BC-13,R	rebar	1.50	unpenetrable	glacial	448109	4469041	GPS
BC-12,R	rebar	0.36	unpenetrable	glacial	448099	4469042	GPS
BC-13	core	1.12	unpenetrable	glacial	448099	4469045	GPS
BC-14	core	2.47	unpenetrable	glacial	449082	4469026	GPS
BC-15	core	2.50	unpenetrable	glacial	448967	4468985	GPS
BC-16	core	2.70	clay	post-glacial	448698	4469096	GPS
NC-2	core	1.60	clay	post-glacial	448483	4470006	GPS
NC-3	core	2.00	clay to grit, bedrock?	pre-glacial	448475	4469993	GPS
NC-5	core	2.50	gravels	pre-glacial	448478	4469941	GPS
NC-6	core	2.50	hard easy hard	pre-glacial	448515	4469919	GPS
BC-101	core	1.72	sand gravel	post-glacial	448478	4469983	GPS
BC-102	core	1.83	sandy gravel	post-glacial	448478	4469989	GPS
BC-103	core	1.82	gravelly clay	post-glacial	448475	4469993	GPS
BC-104	core	1.78	sandy gravel with some clay	post-glacial	448702	4469080	GPS
BC-105	core	1.82	sand	post-glacial	448704	4469080	GPS
BC-106	core	1.83	sandy gravel	post-glacial	448704	4469079	GPS
BC-107	core	1.83	med-coarse sand	post-glacial	448696	4469083	GPS
BC-107	core	1.83	sand	post-glacial	448696	4469083	GPS
BC-108	core	0.43	unpenetrable	pre-glacial?	448495	4469950	GPS
BC-109	core	1.79	sandy gravel	post-glacial	448498	4469950	GPS
BC-110	core	1.80	sandy gravel	post-glacial	448493	4469950	GPS
BC-111	core	0.30	unpenetrable	pre-glacial?	448521	4469914	GPS
BC-112	core	0.30	unpenetrable	pre-glacial?	448521	4469914	GPS
BC-113	core	1.20	unpenetrable	glacial	448003	4469003	GPS
BC-114	core	1.30	unpenetrable	glacial	447996	4469010	GPS
BC-116	core	1.50	unpenetrable	glacial	448847	4469129	GPS
BC-117	core	1.50	unpenetrable	glacial	448699	4469084	GPS
BC-118	core	1.00	sandy gravel	post-glacial	448699	4469084	GPS
BC-119	core	1.70	gravelly clay	post-glacial	448475	4469993	GPS
BC-120	core	1.80	gravelly clay	post-glacial	448493	4469950	GPS

Miscellaneous surface observations, data from this study. bgs= meters below ground surface. Coordinates are recorded in UTM NAD83 Zone 13N. Some coordinates correspond to locations along GPR lines and were surveyed in with a total station, they are marked GPR-TS. Most coordinates were taken with GPS, accuracy=4m

ID	type	bgs	substrate	interp	E	N	
78	surface	0.00	old beaver pond	post-glacial	448065	4469060	GPS
79	surface	0.00	old beaver pond	post-glacial	448167	4469100	GPS
82	surface	0.00	schist	pre-glacial	448243	4469160	GPS
83	surface	0.00	schist	pre-glacial	448269	4469180	GPS
84	surface	0.00	granite	pre-glacial	448288	4469190	GPS
85	surface	0.00	granite	pre-glacial	448340	4469160	GPS
86	surface	0.00	granite	pre-glacial	448394	4469140	GPS
87	surface	0.00	old beaver pond	post-glacial	448422	4469120	GPS
CBC1	cutbank	1.30	boulder	glacial	448258	4469050	GPS
1097	surface	0.00	boulder	glacial	447953	4468950	GPR-TS
2102	surface	0.00	boulder	glacial	448047	4468932	GPR-TS
3046	surface	0.00	boulder	glacial	448171	4469031	GPR-TS
3047	surface	0.00	boulder	glacial	448171	4469023	GPR-TS
3055	surface	0.00	boulder	glacial	448170	4468983	GPR-TS
4004	surface	0.00	granite	pre-glacial	448340	4469170	GPR-TS
4035	surface	0.00	boulder	glacial	448361	4469027	GPR-TS
513	surface	0.00	boulder	glacial	449240	4468962	GPR-TS
88	surface	0.00	granite	pre-glacial	448521	4469150	GPS
89	surface	0.00	granite/schist contact	pre-glacial	448505	4469220	GPS
90	surface	0.00	schist	pre-glacial	448315	4469190	GPS
91	surface	0.00	schist	pre-glacial	448265	4469190	GPS
92	surface	0.00	schist	pre-glacial	448233	4469170	GPS
93	surface	0.00	granite	pre-glacial	448181	4469180	GPS
5052	surface	0.00	boulder	glacial	448616	4469034	GPR-TS
5054	surface	0.00	boulder	glacial	448616	4469028	GPR-TS
6066	surface	0.00	boulder	glacial	448832	4468975	GPR-TS
6067	surface	0.00	boulder	glacial	448832	4468970	GPR-TS
7083	surface	0.00	boulder	glacial	449022	4468924	GPR-TS
7084	surface	0.00	boulder	glacial	449022	4468923	GPR-TS
8054	surface	0.00	boulder	glacial	449192	4468955	GPR-TS
8056	surface	0.00	boulder	glacial	449192	4468953	GPR-TS
8059	surface	0.00	boulder	glacial	449192	4468947	GPR-TS
517	surface	0.00	boulder	glacial	449262	4468960	GPR-TS
580	surface	0.00	boulder	glacial	449338	4468923	GPR-TS
594	surface	0.00	boulder	glacial	449361	4468894	GPR-TS
9010	surface	0.00	boulder	glacial	449331	4468949	GPR-TS
9040	surface	0.00	boulder	glacial	449309	4468925	GPR-TS
670	surface	0.00	boulder	glacial	449681	4468713	GPR-TS
671	surface	0.00	boulder	glacial	449684	4468711	GPR-TS
10046	surface	0.00	boulder	glacial	449463	4468748	GPR-TS
12010	surface	0.00	boulder	glacial	449733	4468702	GPR-TS
12013	surface	0.00	boulder	glacial	449731	4468697	GPR-TS

12016	surface	0.00	boulder	glacial	449731	4468696	GPR-TS
12033	surface	0.00	boulder	glacial	449707	4468640	GPR-TS
12048	surface	0.00	boulder	glacial	449703	4468630	GPR-TS
12049	surface	0.00	boulder	glacial	449702	4468629	GPR-TS
12050	surface	0.00	boulder	glacial	449702	4468629	GPR-TS
A104	surface	0.00	boulder	glacial	447834	4469072	GPR-TS
A116	surface	0.00	boulder	glacial	447854	4469074	GPR-TS
A117	surface	0.00	boulder	glacial	447855	4469074	GPR-TS
A118	surface	0.00	boulder	glacial	447856	4469074	GPR-TS
94	surface	0.00	old beaver pond	post-glacial	448171	4469170	GPS
100	surface	0.00	old beaver pond	post-glacial	448066	4469210	GPS
106	surface	0.00	granite	pre-glacial	447923	4469330	GPS
107	surface	0.00	granite	pre-glacial	447985	4469310	GPS
108	surface	0.00	granite	pre-glacial	448059	4469300	GPS
109	surface	0.00	schist, granite underneath?	pre-glacial	448132	4469250	GPS
110	surface	0.00	schist, granite underneath?	pre-glacial	448181	4469210	GPS
111	surface	0.00	bedrock	pre-glacial	449333	4469050	GPS
112	incised channel	2.00	boulders	glacial	449202	4468960	GPS
113	incised channel	2.00	boulders	glacial	449208	4468960	GPS
114	incised channel	2.00	boulders	glacial	449235	4468960	GPS
115	surface	0.00	boulders	glacial	449251	4468980	GPS
116	surface	0.00	boulders	glacial	449289	4468960	GPS
118	surface	0.00	boulders	glacial	449300	4468950	GPS
119	incised channel	1.00	sand	post-glacial	449313	4468940	GPS
120	surface	0.00	boulders	glacial	449336	4468890	GPS
121	surface	0.00	boulders	glacial	449339	4468860	GPS
122	surface	0.00	boulders	glacial	449334	4468830	GPS
123	surface	0.00	boulders	glacial	449364	4468840	GPS
124	surface	0.00	boulders	glacial	449372	4468830	GPS
125	channel	0.50	boulders	glacial	449383	4468840	GPS
126	channel	0.50	boulders	glacial	449383	4468860	GPS
127	channel	0.00	bedrock	pre-glacial	449391	4468880	GPS
128	channel	0.50	boulders	glacial	449410	4468840	GPS
129	channel	0.50	boulders	glacial	449416	4468840	GPS
130	channel	0.50	boulders	glacial	449420	4468840	GPS
131	channel	0.50	boulders	glacial	449428	4468840	GPS
132	channel	0.50	boulders	glacial	449460	4468830	GPS
133	channel	1.00	mud/sand	post-glacial	449480	4468810	GPS
134	surface	0.00	old beaver pond	post-glacial	449522	4468750	GPS
135	incised channel	1.20	sand	post-glacial	449579	4468710	GPS
136	channel	0.50	boulders	glacial	449583	4468710	GPS
137	channel	0.00	boulders	glacial	449596	4468680	GPS

54	surface	1.45	boulder	glacial	447899	4469280	GPS
55	channel	2.00	sand and gravel	post-glacial	447934	4469180	GPS
56	channel	1.25	sand and gravel	post-glacial	447966	4469100	GPS
57	channel	1.30	boulder	glacial	448013	4469100	GPS
58	channel	1.15	boulder	glacial	448044	4469080	GPS
59	surface	0.00	schist boulder	glacial	448100	4469040	GPS
60	channel	0.70	boulder	glacial	448136	4469060	GPS
61	channel	0.00	boulder	glacial	448177	4469060	GPS
62	surface	1.05	boulder	glacial	448233	4469040	GPS
63	surface	0.00	boulder	glacial	448417	4469070	GPS
64	surface	0.50	boulder	glacial	448516	4469060	GPS
65	surface	0.65	boulder	glacial	448543	4469060	GPS
66	surface	0.60	sand and gravel	post-glacial	448631	4469070	GPS
67	surface	0.00	schist	pre-glacial	448699	4469160	GPS
68	surface	0.00	schist	pre-glacial	448652	4469180	GPS
69	surface	0.00	granite/schist contact	pre-glacial	448541	4469450	GPS
138	surface	0.00	schist	pre-glacial	449411	4469170	GPS
139	surface	0.00	granite	pre-glacial	449362	4469200	GPS
140	surface	0.00	schist	pre-glacial	449297	4469190	GPS
141	surface	0.00	granite/schist contact	pre-glacial	449188	4469230	GPS
142	surface	0.00	schist	pre-glacial	449160	4469260	GPS
143	surface	0.00	granite	pre-glacial	449122	4469310	GPS
144	surface	0.00	pegmatite	pre-glacial	448917	4469480	GPS
145	surface	0.00	schist with granite just upslope	pre-glacial	448640	4469840	GPS
146	surface	0.00	granite	pre-glacial	448599	4469860	GPS
155	surface	0.00	fan	post-glacial	448681	4469730	GPS
161	surface	0.00	boulder	glacial	448841	4469050	GPS
163	surface	0.00	boulder	glacial	448917	4468970	GPS
165	surface	0.00	silt	post-glacial	449080	4469080	GPS
167	surface	0.00	boulder	glacial	449198	4468960	GPS
168	surface	0.00	granite	pre-glacial	449392	4468880	GPS
169	surface	0.00	granite	pre-glacial	449403	4468870	GPS
170	surface	0.00	granite/Bull Lake contact	glacial	449563	4468850	GPS
180	surface	0.00	boulder	glacial	448901	4469102	GPS

Core descriptions. Intervals in meters below ground surface. Coordinates given in previous table within this appendix

C1	core along BT4	
	0.00-0.35	Dark brown organic rich soil with some gruss
	0.35-1.30	Greyish brown gritty silt, clay content increases with depth
	1.30-1.60	Gritty grey clay with some orange streaks of oxidized iron
C2	BC2- core along BT4	
	0.00-0.75	Light brown fluffy silt
	0.75-1.50	Dark brown gravelly silt with increased clay with depth
	1.5	unpenetrable, boulder?
C3	core along BT4	
	0.00-0.30	silt
	0.30-0.80	washed fluvial gravels and sands
	0.75-1.20	organic rich clay
	1.20-1.60	washed fluvial gravels and sands
C4	core in upper arm	
	0.00-0.25	silty soil
	0.25-0.40	increase in grit from gravels (gruss?)
	0.40-0.80	increase in clay content
	0.80-1.6	clay
C5	core south end of BT6	
	0.00-0.60	silt gruss, slopewash
	0.60-0.80	black clay with mica
	0.80-1.4	clay and silt with lenses of fluvial sands
	1.4-1.5	sandy and gravelly
	1.5	unpenetrable boulder
C6	Core near north end of BT7	
	0.00-0.70	silt with gruss slopewash
	0.70-1.35	sandy clay oxidized at top light tan at bottom
	1.35-1.45	fluvial qtz sand
	1.45-1.55	increase in clay content gritty with gravels
	1.55	unpenetrable
C7	core near BL2 and BT8	
	0.00-0.15	silty overburden
	0.15-0.35	sandy silt
	0.35-0.40	sand with mica
	0.40-0.50	clay lens
	0.50-0.75	fluvial sand
	0.75-0.8	black clay
	0.80-1.4	sandy black clay with mica
	1.40-1.50	gravelly oxidized sand
	1.5	unpenetrable
C8	nice exposure in stream	
	0-0.10	soil
	0.10-0.20	silt
	0.20-0.30	sand lens
	0.30-0.40	silt
	0.40-0.50	sand lens
	0.50-0.80	thick massive black clay
	0.80-1.20	sand lens in clay
	1.20-1.40	clay
	1.4	unpenetrable

Rebar probe descriptions. Intervals in meters below ground surface. Coordinates given in previous table within this appendix.

R1	rebar probe in upper arm	
	0.00-0.45	wet black muck
	0.45-0.55	gritty layer, probably sand
	0.55-0.90	wet black muck
	0.90-1.05	gritty layer, probably sand or gruss
	1.05	unpenetrable, bedrock
R2	rebar probe in incised channel in upper arm	
	0.00-0.65	wet black muck
	0.65	unpenetrable, bedrock
R3	rebar probe in incised channel in upper arm	
	0.00-0.30	wet black muck
	0.3	unpenetrable, bedrock
R4	rebar probe in incised channel in upper arm	
	0.00-0.30	wet black muck
	0.3	unpenetrable, bedrock
R5	rebar probe in incised channel in upper arm	
	0.00-0.25	wet black muck
	0.25	unpenetrable bedrock
R6	rebar probe in incised channel in upper arm near AT3	
	0-1.8	unpenetrable at 1.8 m below the level of the terrace
R7	rebar probe near north end of AL1	
	0.00-1.6	gritty
R8	rebar probe near AT4 lower arm	
	0.00-0.25	silty soil
	0.25-1.1	gritty silt
	1.1-1.2	clay difficult to penetrate some grit present
R9	rebar probe near AT4 lower arm	
	0.00-0.55	soft silt with some clay
	0.55-0.90	increase in grit
	0.9	clay, difficult to penetrate
R10	rebar probe near AT6	
	0.00-0.60	silt with some grit
	0.60-0.70	increase in girt, slopewash?, gruss
	0.7	unpenetrable, bedrock
R11	rebar probe near AT6	
	0-0.65	Black clay
	0.65	unpenetrable, bedrock
R12	rebar probe near BT6 in inset stream	
	0-1.7	unpenetrable at 1.7 m below the level of the terrace
R13	rebar probe in inset channel	
	0-1.8	unpenetrable at 1.8 m below the level of the terrace
R14	rebar probe near BT7	
	0-1.4	sand at 1.4 m below the level of the terrace
R15	rebar probe in inset channel	
	0-1.3	sand at 1.3 m below the level of the terrace
R16	rebar probe in inset channel	
	0-0.9	unpenetrable at 0.9 m below the level of the terrace

B GPR Profiles

The GPR profiles presented in this Appendix are located on the figure below. Each profile is shown with no vertical exaggeration (top) and 4x vertical exaggeration (bottom). Note that the air wave and direct ground wave for each profile were edited out of the image. Radar packages are identified as different color shading: **no shading** = bedrock (contact inferred at depth from seismic data), **red shading** = P1, which is interpreted to be glacial deposits. **Blue shading** = P2, which is interpreted to be alluvium, and **green shading** (only drawn on the lower profile) = sub package P2a, which is interpreted to be beaver-related sedimentation.

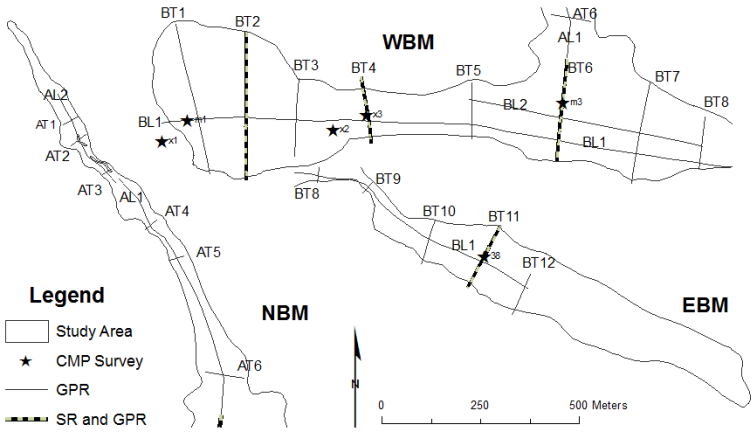

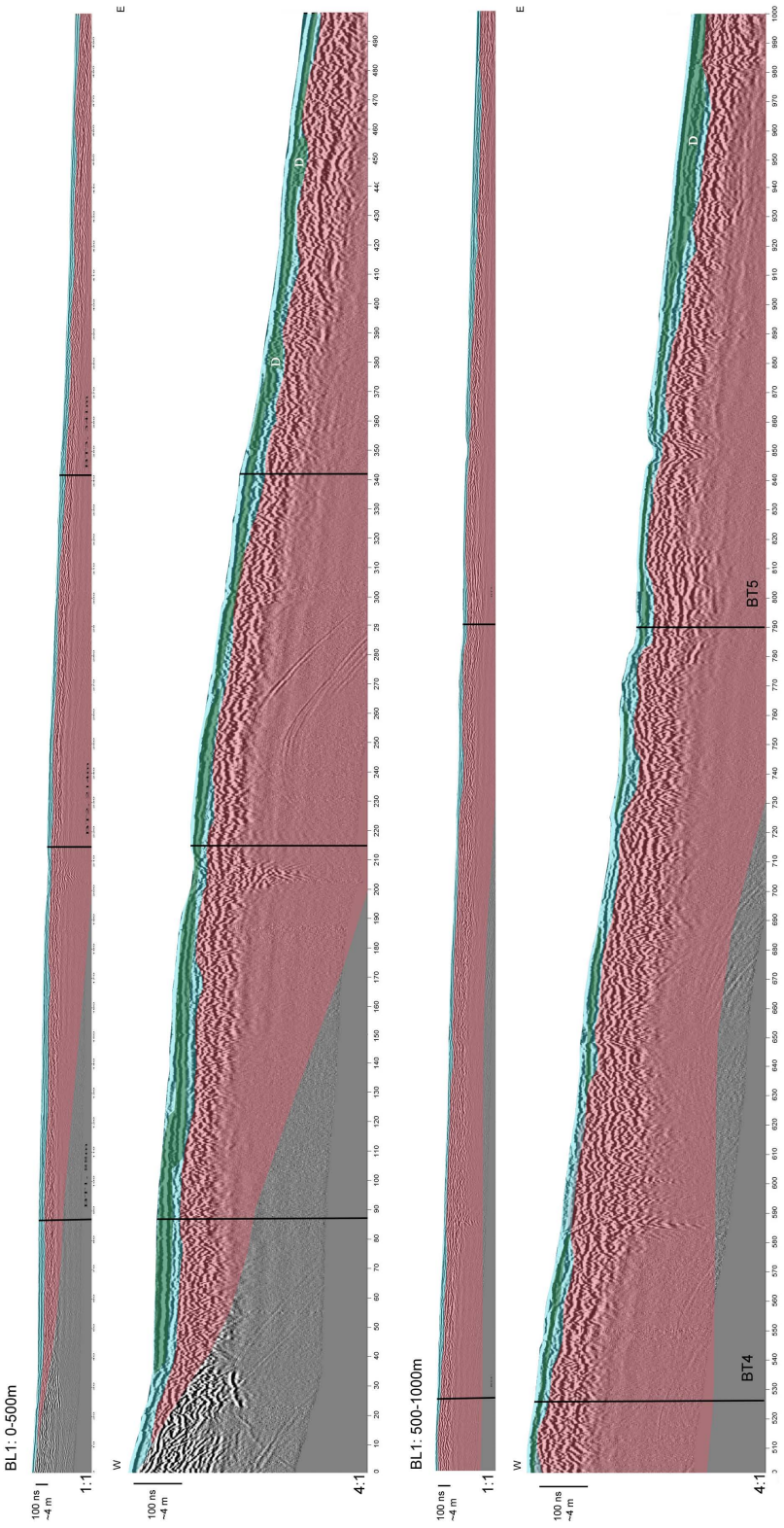
BL1: 0-500m
100 ns
~4 m
1:1
W
E
D
100 ns
~4 m
4:1
BL1: 500-1000m
100 ns
~4 m
1:1
W
E
BT4
BT5
D
100 ns
~4 m
4:1

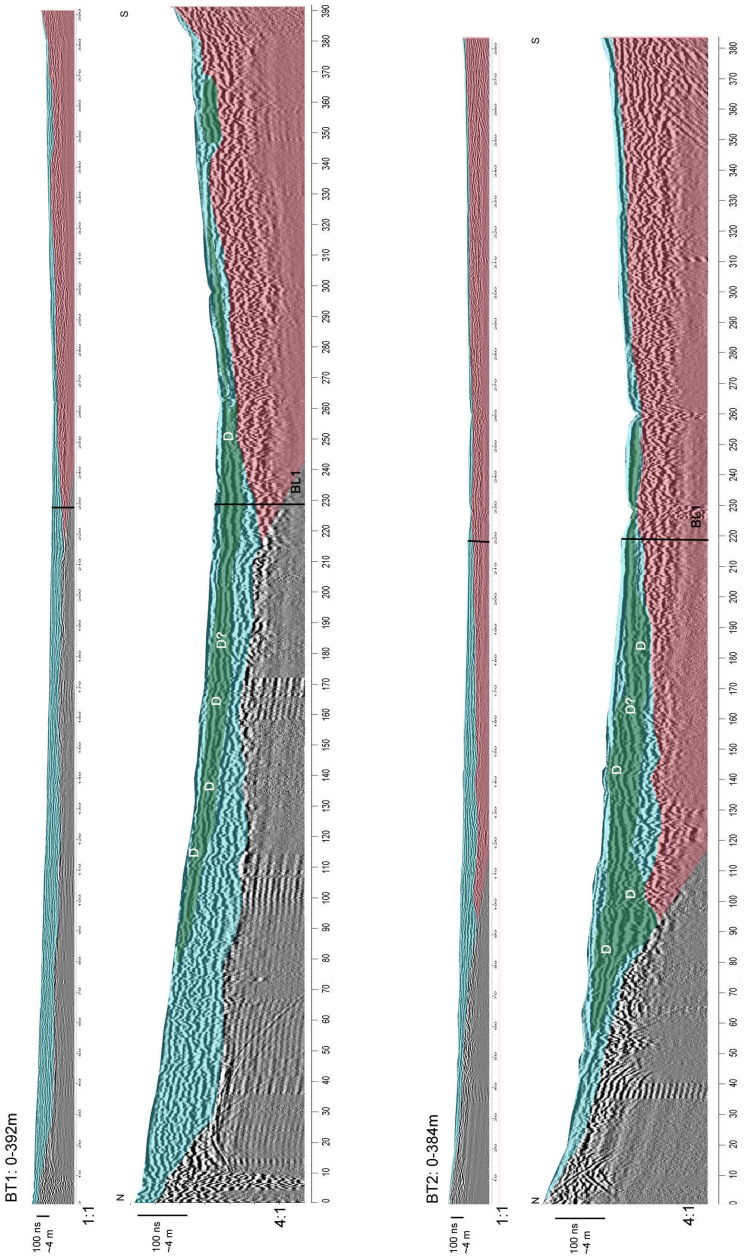
BT1: 0-392m
100 ns
~4 m
1:1
N
S
D
D
D
D?
D
BL1
100 ns
~4 m
4:1
BT2: 0-384m
100 ns
~4 m
1:1
N
S
D
D
D
D?
D
BG1
100 ns
~4 m
4:1

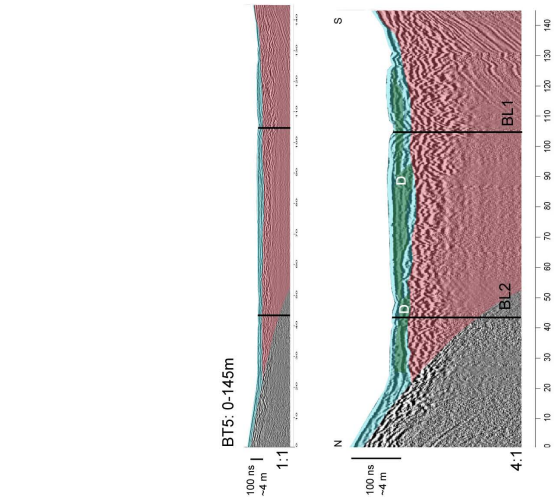
BT5: 0-145m
100 ns
~4 m
1:1
N
S
D
BL2
BL1
4:1

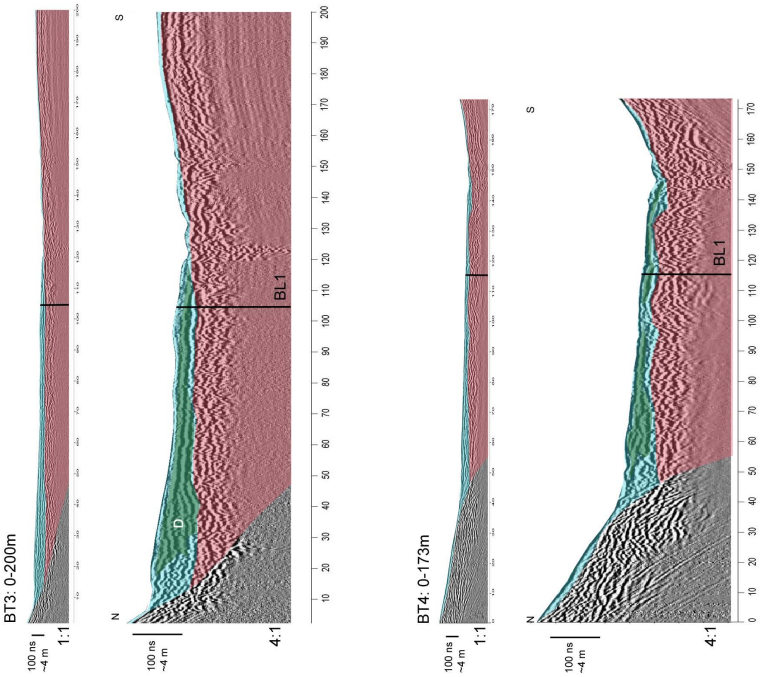
BT3: 0-200m
BT4: 0-173m
100 ns
~4 m
1:1
4:1
N
S
D
BL1

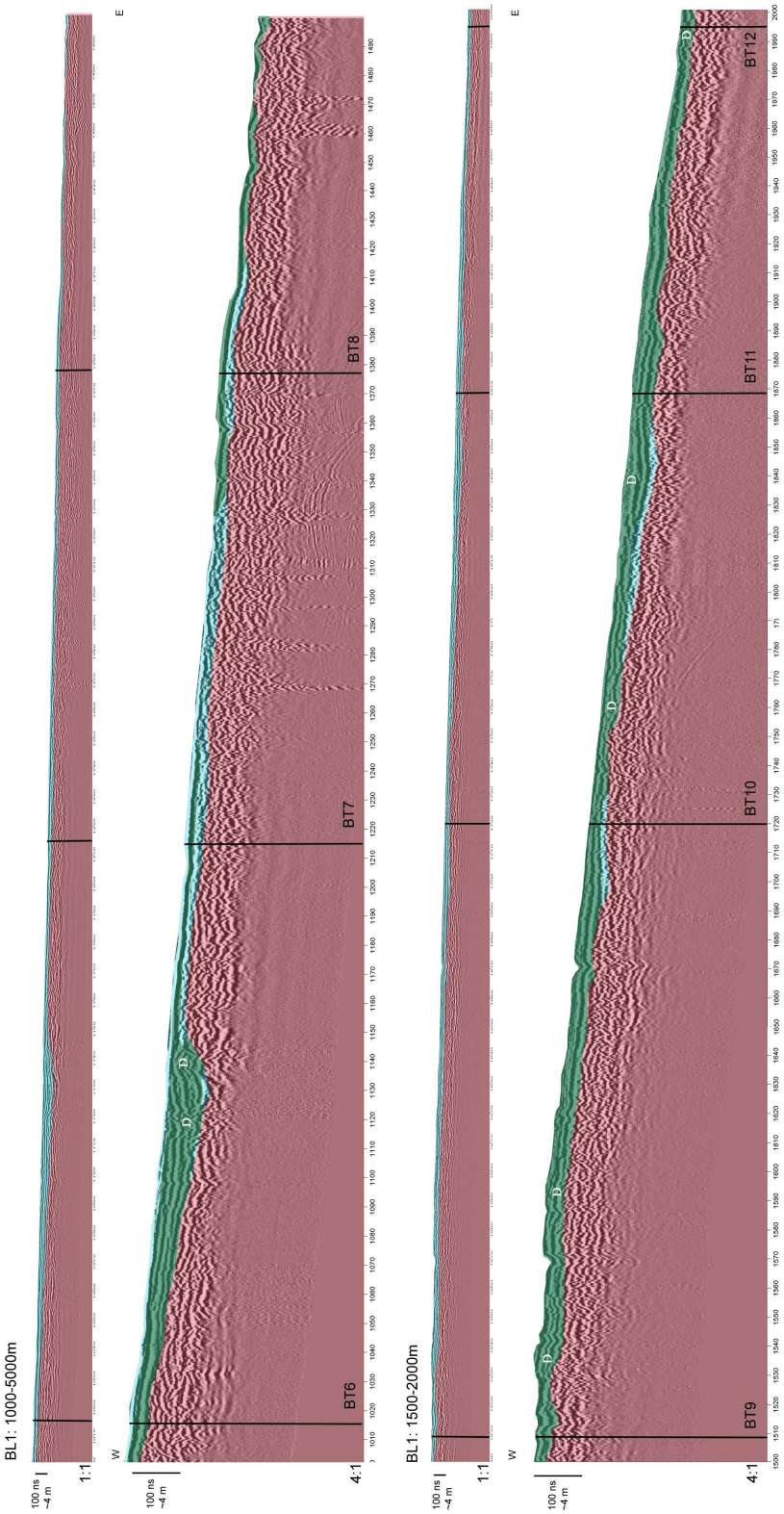
BL1: 1000-5000m
100 ns
~4 m
1:1
W
E
BT6
BT7
BT8
D
4:1
BL1: 1500-2000m
BT9
BT10
BT11
BT12

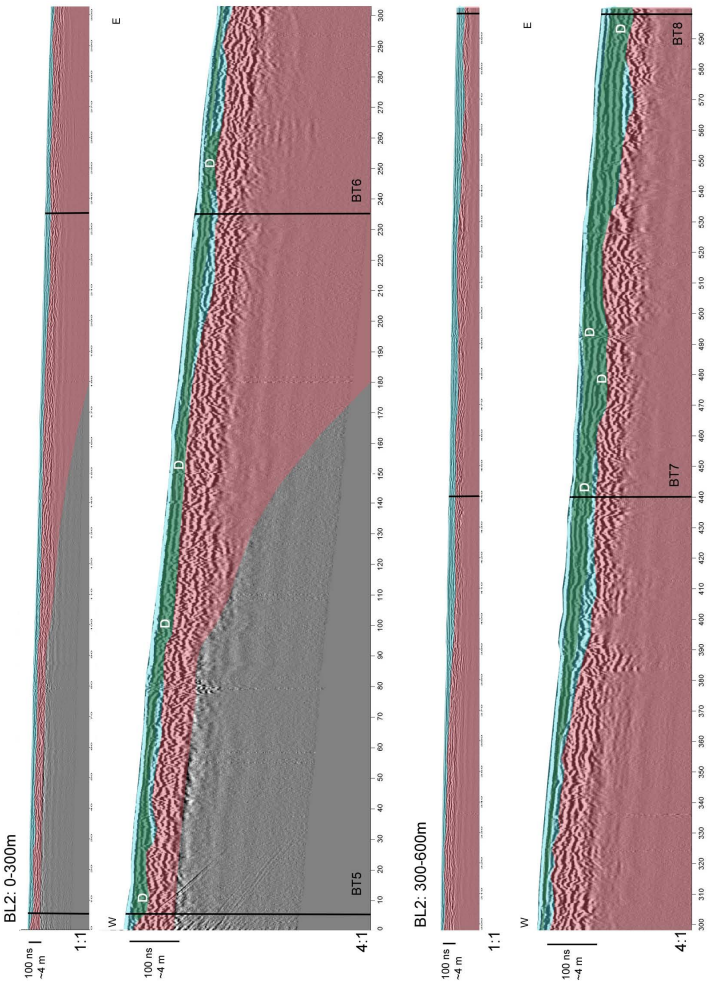
BL2: 0-300m
1:1
100 ns
~4 m
W
E
D
BT5
BT6
4:1
BL2: 300-600m
BT7
BT8

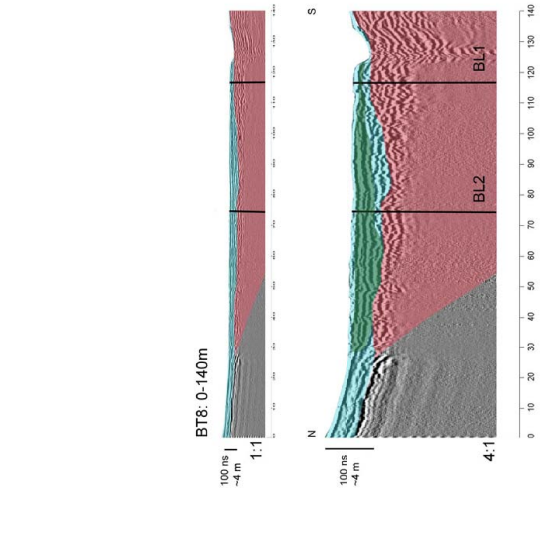
BT8: 0-140m
100 ns
~4 m
1:1
N
S
BL1
BL2
4:1
BT6: 0-270m
BT7: 0-268m
D

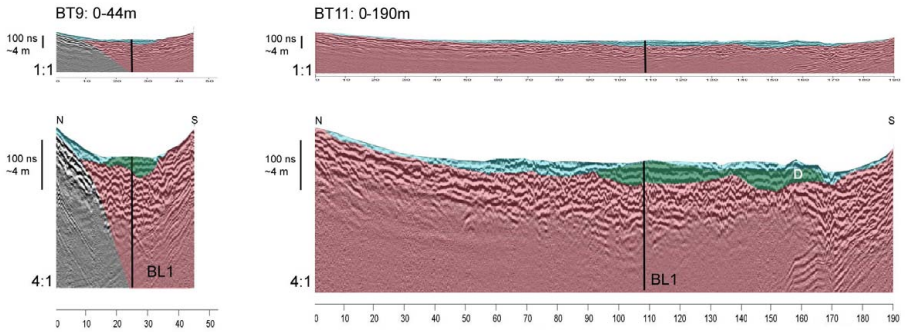
BT9: 0-44m
BT11: 0-190m
100 ns
~4 m
1:1
4:1
N
S
BL1
D

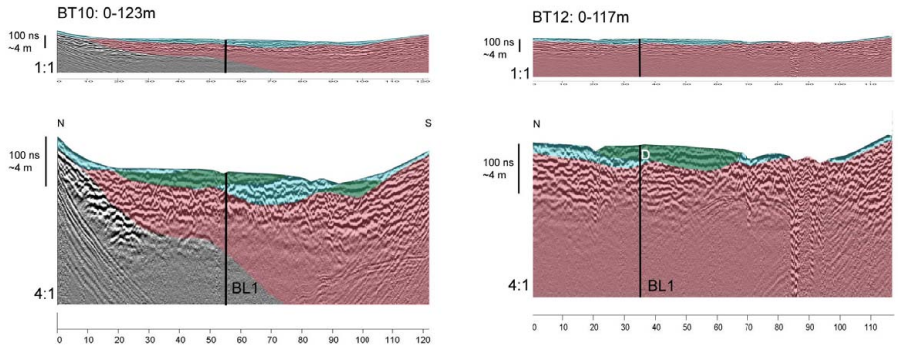
BT10: 0-123m
BT12: 0-117m
100 ns
~4 m
1:1
4:1
N
S
BL1
D

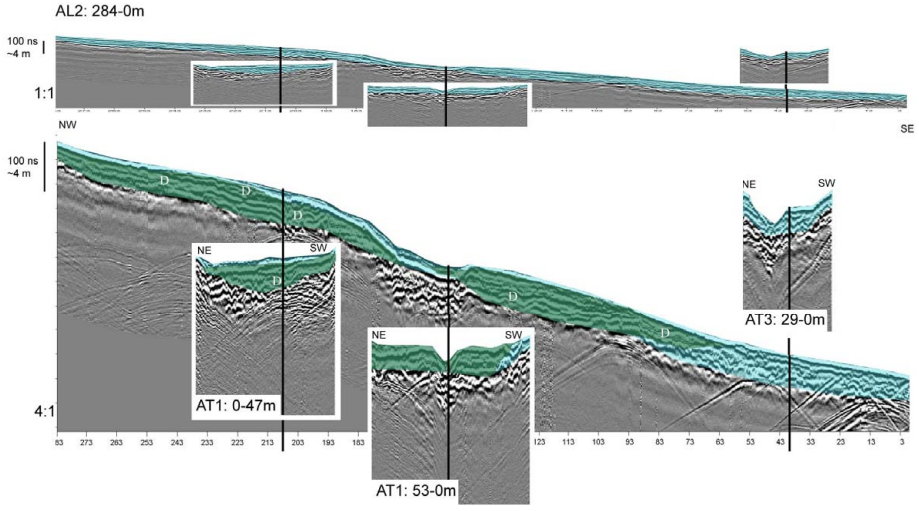
AL2: 284-0m
100 ns
~4 m
1:1
4:1
NW
SE
NE
SW
D
AT1: 0-47m
AT1: 53-0m
AT3: 29-0m

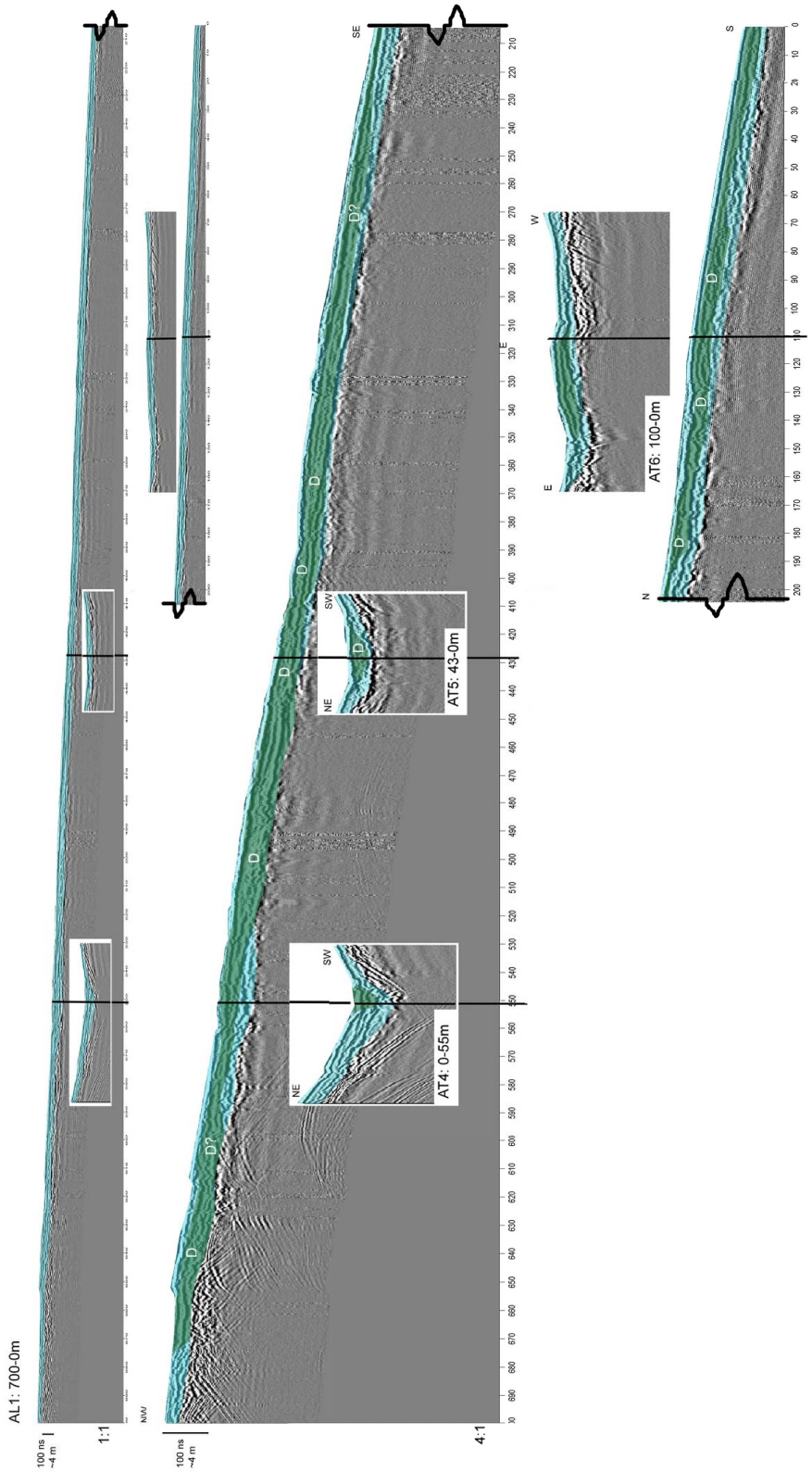
AL1: 700-0m
1:1
100 ns
~4 m
NW
SE
4:1
D
D?
AT4: 0-55m
AT5: 43-0m
AT6: 100-0m
SW
NE
W
E
S
N

C SSR Profiles

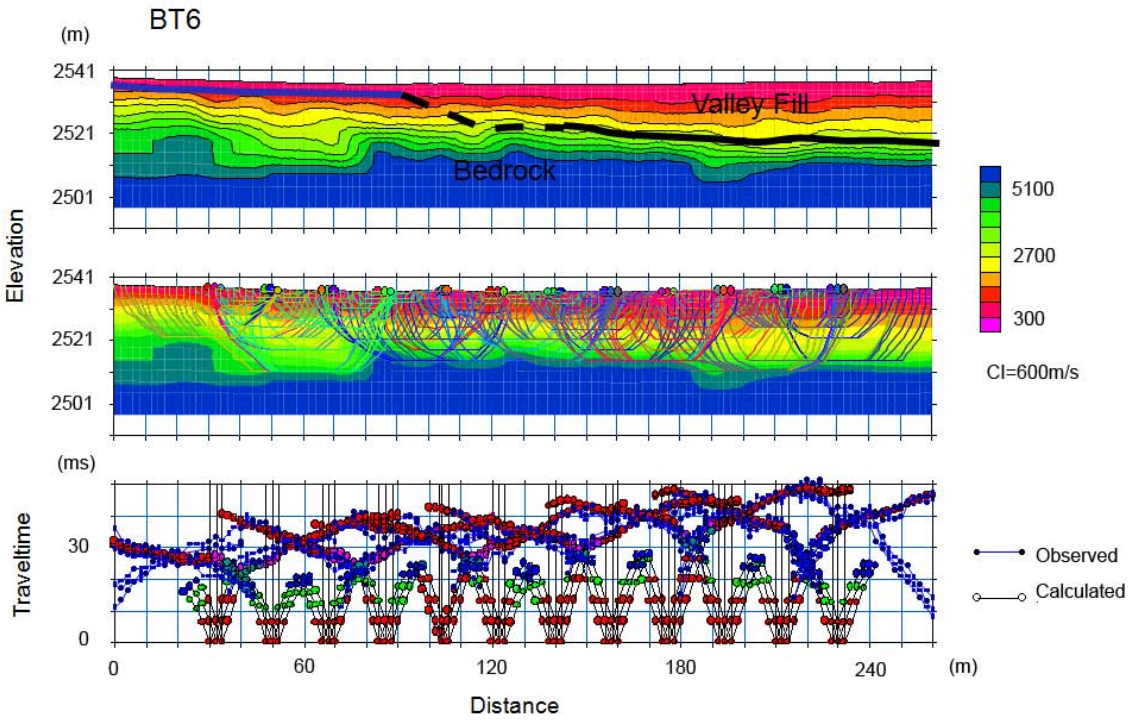

Top. Contoured velocity profile with depth to bedrock interpretation, blue line indicates interpretation from GPR profiles. **Middle.** Velocity profile with ray traces. **Bottom.** Fitted and observed first arrival picks, RMSE=3 ms.

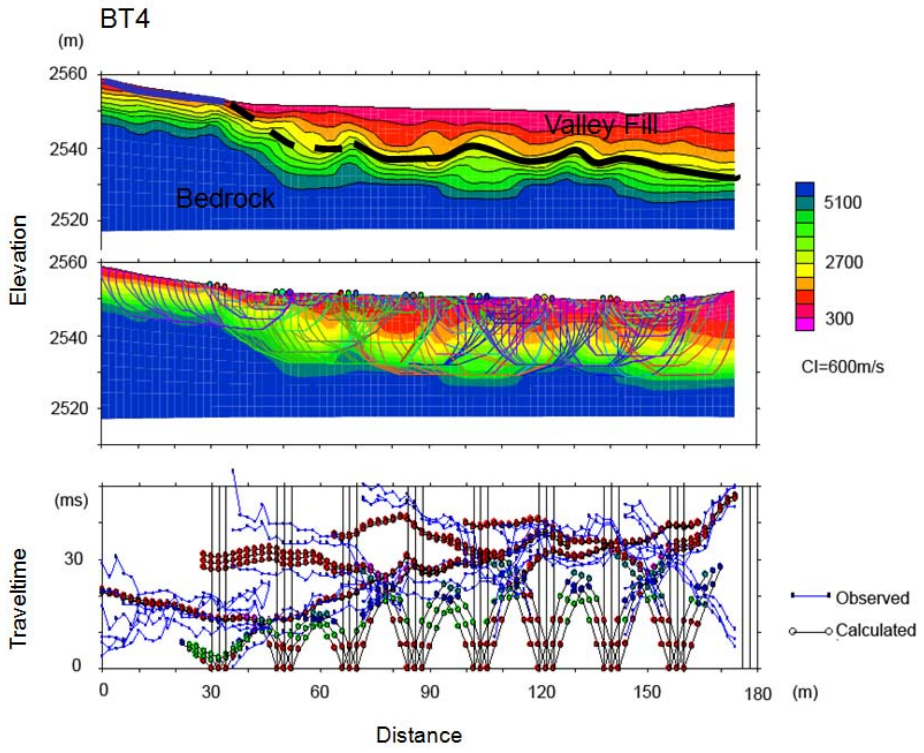

Top. Contoured velocity profile with depth to bedrock interpretation, blue line indicates interpretation from GPR profiles. **Middle.** Velocity profile with ray traces. **Bottom.** Fitted and observed first arrival picks, RMSE=4 ms.

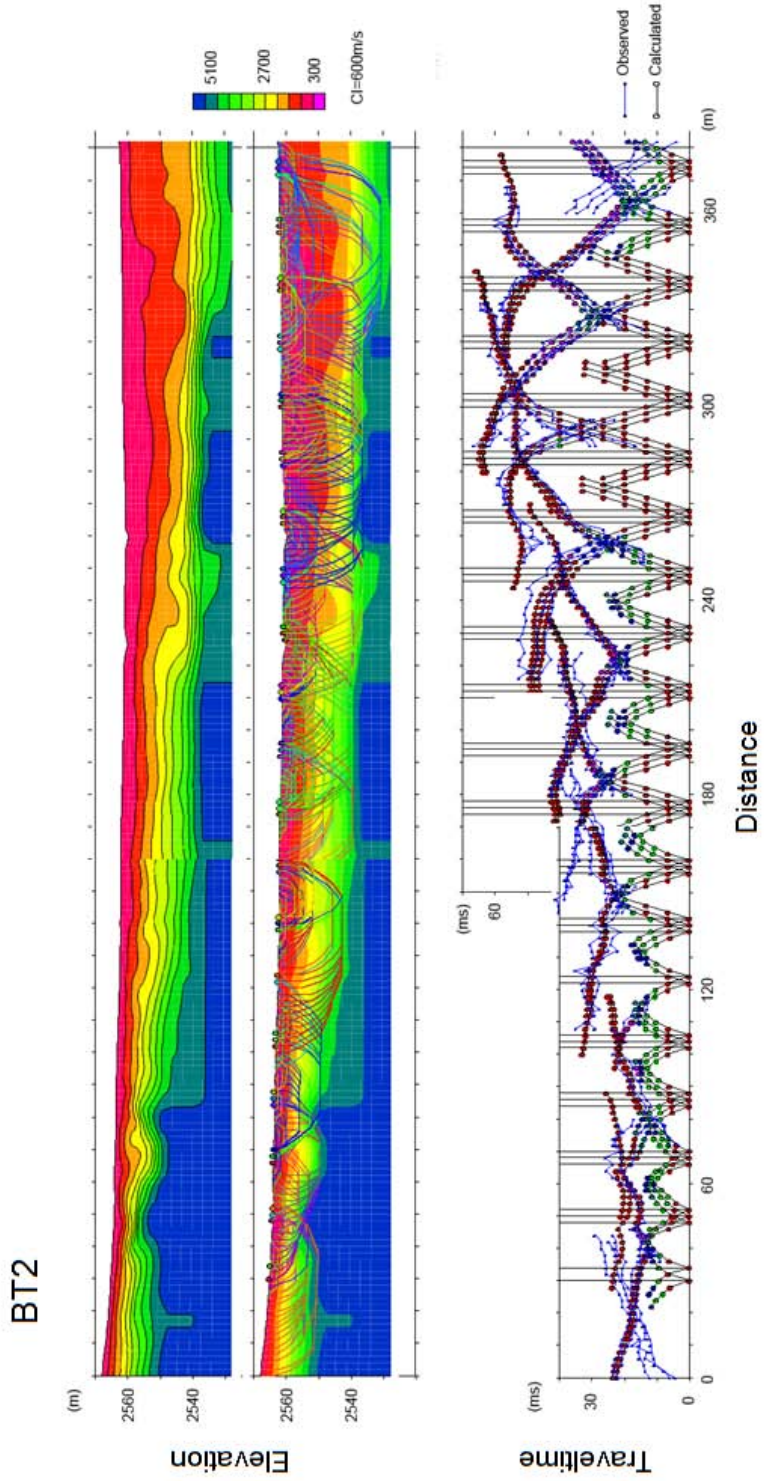

Top. Contoured velocity profile with depth to bedrock interpretation, blue line indicates interpretation from GPR profiles. **Middle.** Velocity profile with ray traces. **Bottom.** Fitted and observed first arrival picks, RMSE=3 ms. This transect was modeled in two segments due to software constraints and then stitched together at 160m.

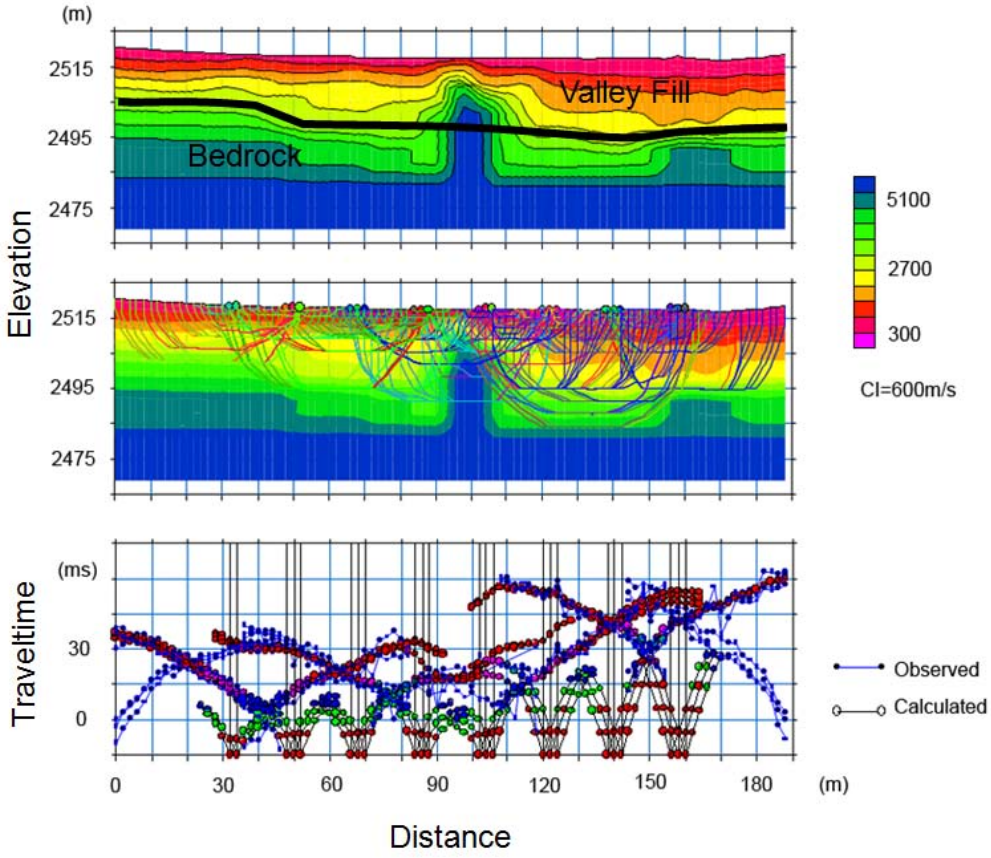

Top. Contoured velocity profile with depth to bedrock interpretation, blue line indicates interpretation from GPR profiles. **Middle.** Velocity profile with ray traces. **Bottom.** Fitted and observed first arrival picks, RMSE=3 ms. The bedrock high in the middle of the transect was ignored due to noisy and incomplete data.